Control of Wind Turbines for Power Regulation and Load Reduction

Juan Jose Garcia Quirante

Kongens Lyngby 2007
IMM – MSc. 2007 - 98

Technical University of Denmark
Informatics and Mathematical Modelling
Building 321, DK-2800 Kongens Lyngby, Denmark
Phone +45 45253351, Fax +45 45882673
reception@imm.dtu.dk
www.imm.dtu.dk

Abstract

This thesis describes the design of controllers for power regulation and load reduction and their ensemble in a variable-speed wind turbine.

The power regulation is carried out by manipulating the generator torque and/or the pitch angle of all blades, namely collective pitch angle, conveniently for a given wind speed. The model predictive control theory is used for the design of this controller.

The load reduction problem is achieved by modifying the collective pitch angle derived from the power regulation problem, by a fine individual component. Two methods for calculating this individual component are presented: cyclic and individual pitch control.

Preface

This thesis was prepared at Informatics Mathematical Modelling, the Technical University of Denmark in partial fulfilment of the requirements for acquiring the M.Sc. degree in engineering.

The thesis deals with different aspects of mathematical modelling of wind turbines, and especially the control methods suited for power regulation and load reduction.

For power regulation, model predictive control with and without constraints has been investigated. For load reduction, cyclic and individual pitch controllers have been implemented.

Lyngby, October 2007

Juan Jose Garcia Quirante

Acknowledgements

First, I would like to thank my supervisor Professor Henrik Madsen (IMM, DTU) and Senior Scientist Peter Hauge Madsen (Siemens Wind Power A/S) for their interest and work for defining such a project and the framework involving both IMM and Siemens Wind Power A/S.

I would like to thank my supervisor Assoc. Prof. Niels Kjølstad Poulsen (IMM, DTU) for his guidance, patience and full-time availability. I would also like to thank Senior Scientist Kenneth Thomsen (Siemens Wind Power A/S) for his interest and experience, and the Ph.D students Sven Creutz Thomsen and Lars Christian Henriksen for their selfless help any time I needed.

Finally, I would like to thank my girlfriend Zhang Yuqi for her permanent support, patience, and many other things.

Contents

CHAPTER 1

Introduction

Renewable energies in general, and wind energy in particular, have become an essential part of the energy programmes for most of governments all over the world. The need of reducing the emission of greenhouse gases as a commitment under the Kyoto protocol for preventing the global warming, or the political and economical uncertainty derived from the dependency of foreign sources of energy are just some of the reasons.

An increase in the importance of wind energy has necessarily yielded a research for improving the techniques involved. In particular, the power regulation is the crux of most of efforts in the control area.

Traditionally, the controllers for power regulation were implemented as PID with a simple system identification and gain scheduling. They worked acceptably well, but better results are possible with more sophisticated system identification and some optimization of a cost function.

In this project, model predictive control theory has been used for implementing such a power regulator, yielding excellent results.

Moreover, the increase of the cost of wind turbines derived from either their size or the off-shore implementation makes especially interesting the attempt to extend their lifespan. In order to achieve this goal, load reduction of wind turbines has been included.

To summary, the present project deals with the design and implementation of two *nearly* independent controllers so that the generated power is optimized while the loads in the wind turbine are reduced.

The report has been divided into 4 parts as follows:

Part I. Modelling presents the FAST model of the variable-speed wind turbine, with its operation modes as a function of the wind speed. A linear model has been obtained from the linearization tool for each of them. Moreover, a generator and a pitch actuator models have been included.

Next, an unsteady BEM code has been developed for modelling the aerodynamics. This is of special interest in Part III, where rotor flow measurements are necessary for the design of a controller for load reduction.

Part II. Power regulation describes a controller based on the separation of control objectives according to the operation modes. For those which have a steady reference set point, a model predictive controller has been implemented. The manipulated variables to accomplish the optimization of the generated power are the generator torque and the collective pitch angle.

Remark: The collective pitch angle is defined as the common component in all 3 blades for regulating the power.

Part III. Load reduction introduces the so called Cyclic and Individual pitch controllers, which require either measurements of the yaw and tilt moments, or the wind speed and direction seen by the blades, respectively. In order to achieve this control, the pitch angles are deviated individually from the collective component.

Part IV. Conclusions and Perspectives summarizes the issues dealt with throughout the project, and discusses the results obtained. Last, it suggests the new steps in order to achieve a state-of-the-art controller with real possibilities to be applied in industry.

In order to develop this project, a number of tools have been used:

1. **Matlab/Simulink** is the interface where most of calculations are done, especially the controller design and simulations.

2. The **FAST** code has provided the non-linear model of the wind turbine, and has been used for:

> (a) Obtaining a linear model of the wind turbine at different wind speeds, which has been used for the design of the power regulation controller
>
> (b) Simulating the response of the wind turbine in a setup with both power regulation and load reduction controllers implemented.

The FAST code has been implemented as an S-Function of Simulink, introducing a tremendous flexibility in control design and simulation.

3. The **AeroDyn** code has been used for aerodynamic calculations based on the specifications in the input file. AeroDyn is based on a steady BEM code, to which some corrections have been included in order to model the transients resulting from varying loads. These variations will be due to some skew inflow, wind shears or turbulences in a wind field.

4. The **TurbSim** code is used for creating realistic wind data files according to the standards IEC-61400, introducing different models of turbulences. The wind data files used in this project are essentially modelled by a grid of time-varying wind speeds, so that the wind speed at a certain spatial point is determined by interpolation. The resulting wind data files are inputs for the code AeroDyn.

FAST, AeroDyn and TurbSim have all been developed by the NREL (National Renewable Energy Laboratory) of United States, and can be downloaded free of charge from the website http://wind.nrel.gov/designcodes/simulators/.

Part I

Modelling

CHAPTER 2

Wind Turbine Model

The wind turbine has been modelled by means of the FAST (Fatigue, Aerodynamics, Structures, and Turbulence) code.

The FAST code can model a three-bladed HAWT with 24 degrees of freedom (DOFs), distributed as follows:

1. Translational (surge, sway, and heave) and rotational (roll, pitch, and yaw) motions of the support platform relative to the inertia frame (6 DOFs).

2. Tower motion (4 DOFs): longitudinal modes (2 DOFs), and lateral modes (2 DOFs).

3. Yawing motion of the nacelle (1 DOF).

4. Rotor azimuth angle, for variable rotor speed (1 DOF).

5. Compliance in the drivetrain between the generator and hub/rotor, for drive-shaft flexibility (1 DOF).

6. For each blade, flapwise tip motion for the first and second modes, and the blade edgewise tip displacement for the first edgewise mode (3 DOFs/blade · 3 blades = 9 DOFs).

7. Rotor-furl (1 DOF) and tail-furl (1 DOF).

Due to the constraint in time, it has not been included the flexibility or deflection in any component, except for the rotor azimuth rotation. Further work may yield to an extension for a more accurate model of a wind turbine by simply enabling the corresponding flags in the FAST primary input file, and updating afterwards the matrices of the linear model for the design of the controllers.

2.1 Technical specifications of the FAST model of the wind turbine

Operational data	
Cut-in wind speed	3 m/s
Rated wind speed	12 m/s
Cut-out wind speed	25 m/s
Rated power	1.5 MW (1544 kW)
Rated rotor speed	20 rpm
Model features	
Flexibility in blades	Disabled
Flexibility in tower	Disabled
Flexibility in drivetrain	Disabled
Yaw system	Disabled
Aerodynamic brakes	Disabled
Mechanical brake	Disabled
Mass and inertia	
Turbine mass	201.054 Tn
Tower-top mass	78.054 Tn
Nacelle mass	51.170 Tn
Hub mass	15.148 Tn
Blade mass	3.912 Tn
Tower mass	123.000 Tn
Generator inertia about high speed shaft (HSS)	53.036 $kg \cdot m^2$
Hub inertia about low speed shaft (LSS)	$34.600 \cdot 10^3$ $kg \cdot m^2$
Rotor Inertia about low speed shaft (LSS)	$2962.444 \cdot 10^3$ $kg \cdot m^2$
Rotor	
Hub radius	1.75 m
Blade length	35 m
Swept area	3167 m^2

Drivetrain	
Gearbox efficiency	100 %
Gearbox ratio	1:87.965
Overall distances	
Hub-Height	84.00 m
Rotor shaft length	3.3 m

Table 2.1 Technical specification of the wind turbine

Further information about the model is available in the primary input file of FAST, in appendix A.

2.2 Description of the operation modes

The range of wind speeds at which the wind turbine is operative is [3, 25] m/s. Below the cut-in wind speed, the power generation is not possible, and above the cut-out the wind turbine must be stopped in order to preserve its integrity.

A variable-speed wind turbine has 4 operation modes depending on the wind speed; therefore, the rotor speed is adjusted in such a way that the generated power is as close as possible to the rated one, either by optimizing it for wind speeds below rated, or limiting it to constant for higher wind speeds.

Operation modes I, II and III are located below rated wind speed, and therefore characterized by the maximization of the power efficiency C_p, defined in terms of the generated power over the available power from the wind in a circular cross section with the same area as the rotor disc, given the wind speed:

$$C_p = \frac{P_{el}}{\frac{1}{2} \cdot \rho \cdot \pi \cdot R^2 \cdot v^3} \tag{2.1}$$

The C_p coefficient is a function of the so called tip speed ratio (λ) and the pitch angle of the blades (θ_{Bi}). The tip speed ratio is defined as:

$$\lambda = \frac{\omega_r \cdot R}{v} \tag{2.2}$$

Remark: Unless specified the opposite, the pitch angle of every blade is considered to be the same, in other words:

$$\theta_{Bi} = \theta_{collective} \tag{2.3}$$

2.2.1 Mode I

Mode I is an intermediate operation mode between the start-up and mode II. The wind speed is not high enough for achieving the optimal C_p coefficient (C_p^{max}), as the maximum power subjected to this mode is obtained for larger values of the tip speed ratio and pitch angle than the optimal ones. In other words, optimal speed ratio and pitch angle are not feasible.

By keeping the rotor speed constant at its minimum value, $\omega_{r,min}$, as the wind speed increases, the tip speed ratio decreases approaching to the optimal. Once achieved this point, the generated power is the maximum available (P_L), and the operation mode turns into mode II.

On the other hand, it is well known that the pitch angle is non-zero, and decreases with wind speed towards its optimal value. However, for simplicity it has been neglected.

Mode I	Operation range	Linearization point
Wind speed (m/s)	3 – 4	3
Rotor speed (rpm)	$\omega_{r,min}$	$\omega_{r,min}$
Generated power (kW)	30 - P_L	30
Pitch angle (deg)	0	0

Table 2.2 Description of operation mode I

2.2.2 Mode II

Mode II is characterized by the full maximization of the power efficiency C_p, as the optimal tip speed ratio and pitch angles are feasible in the wind speed range, and therefore, they are kept constant.

The C_p-curve calculated by means of the BEM code described in Chapter 3, for a range of values of λ and θ_{Bi} and a wind speed of 7m/s is depicted in figure 2.1.

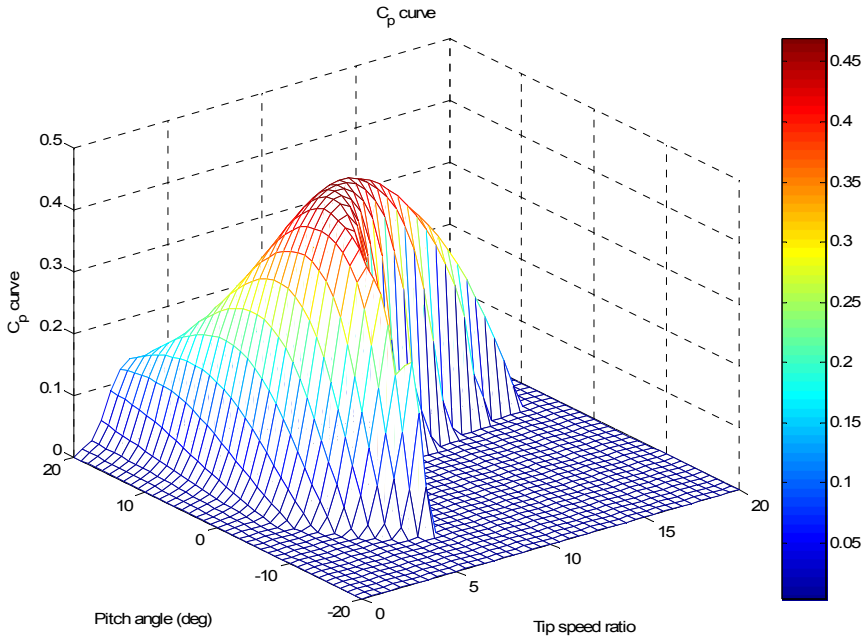

Figure 2.1 C_p curve

Figure 2.1 reveals that C_p^{max} = 0.4712 is achieved for λ^* = 7, θ_{Bi}^* = 2º. This result is pretty close to the expected one, except for the pitch angle, which should be around 0º or even negative.
The linearization tool of FAST can calculate the optimal generator torque and rotor speed given the wind speed, and the pitch angle, so that the C_p coefficient is maximized. The result is C_p^{max} = 0.4606 for λ^* = 6.75, θ_{Bi}^* = 0º.

	λ^*	θ_{Bi}^* (deg)	C_p^{max}	Error C_p^{max} (%)
BEM code	7.00	2.0	0.4712	2.25
FAST linearization tool	6.75	0.0	0.4606	0.00

Table 2.3 Validation of results of optimal C_p

In this project it has been made use of the results from FAST.

The boundaries of mode II regarding modes I and III are defined by the generated power P_L = 70 kW and P_H = 1392 kW, respectively.

Mode II	Operation range	Linearization point
Wind speed (m/s)	4 – 10.86	7
Rotor speed (rpm)	$\omega_{r,min}$ - $\omega_{r,rated}$	12.89
Generated power (kW)	P_L - P_H	372
Pitch angle (deg)	0	0

Table 2.4 Description of operation mode II

2.2.3 Mode III

The existence of the mode III is due to the fact that variable-speed wind turbines are not able to achieve the rated torque (and therefore rated power) at rated rotor speed. The generated power is P_H at this point.

As the wind speed increases, the rotor speed is kept constant at its rated value and the power efficiency at nearly its optimal value. The tip speed ratio decreases, whereas the generated power increases from P_H to the rated power. Moreover, a variation in the pitch angle occurs as well, but it has been neglected for simplicity.

Mode III	Operation range	Linearization point
Wind speed (m/s)	10.86 – 11.25	11
Rotor speed (rpm)	$\omega_{r,rated}$	$\omega_{r,rated}$
Generated power (kW)	P_H – $P_{el,rated}$	1445
Pitch angle (deg)	0	0

Table 2.5 Description of operation mode III

2.2.4 Mode IV

Mode IV is characterized by the rated performance of the wind turbine at high wind speeds. Generated power and rotor speed should be kept as constant as possible.

Mode IV	Operation range	Linearization point
Wind speed (m/s)	11.25 - 25	17
Rotor speed (rpm)	$\omega_{r,rated}$	$\omega_{r,rated}$
Generated power (kW)	$P_{el,rated}$	$P_{el,rated}$
Pitch angle (deg)	0 - 30	18.25

Table 2.6 Description of operation mode IV

2.2.5 Full-range operation

This section can be considered as a summary of the operation modes, and it also goes into the linearization tool of FAST to get the previous optimal equilibrium points.

The procedure for determining analytically the optimal equilibrium points is by maximizing the power produced by the wind turbine, given a steady wind speed:

$$\omega_r^*, \theta_{Bi}^* = \arg\max P_{el} = \frac{1}{2} \cdot \rho \cdot \pi \cdot R^2 \cdot v^3 \cdot C_p \left(\frac{\omega_r \cdot R}{v}, \theta_{Bi} \right) \tag{2.4}$$

Subjected to all constraints specified previously for each operational mode:

$$\begin{aligned} &\omega_{r,\min} \le \omega_r \le \omega_{r,rated} \\ &0 \le P_{el} \le P_{el,rated} \end{aligned} \tag{2.5}$$

First of all, this would require the computation of a mathematical model for the C_p curve.

However, it is extremely simple to carry out a similar calculation by means of the linearization tool of FAST, which is also a way of avoiding hypothetical disagreements between both methods.

Given a wind speed strategically chosen, the operational mode and an initial guess of the rotor speed (for modes III and IV it must be the rated one), it tries a number of either generator torques (modes I, II and III) or collective pitch angles (mode IV) until the solution converges within previously specified tolerances. This procedure is called trim analysis.

The objective in modes I, II and III is to maximize the C_p coefficient for a fixed collective pitch angle, which is done by computing the AeroDyn code, whereas the objective in mode IV is to keep rotor speed and power at its rated value (for a fixed generator torque).

It must be noticed that when trimming the generator torque, the collective pitch angle is fixed, and vice-versa.

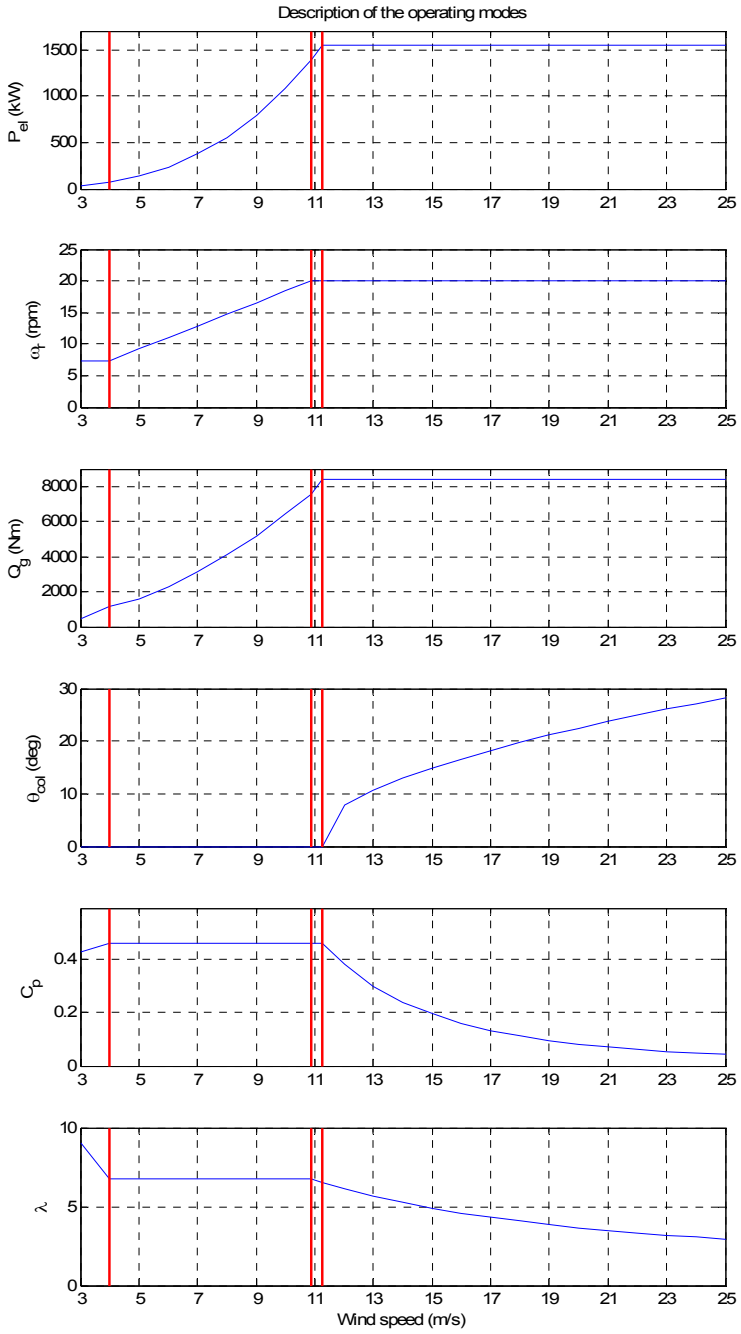

Figure 2.2 Description of the full-range operation modes

2.3 Mathematical model of the wind turbine

2.3.1 Linear model of the Wind turbine

2.3.1.1 Linear Model

The linear model has been obtained for each operation mode by means of the FAST linearization tool. The wind field must be steady, although it is possible to include wind shears and yaw/tilt errors.

The linearization process consists of 2 steps:

1. Search of a steady state (equilibrium) operating point
2. Linearization around this operating point

Since the wind field is steady, operating points are periodic, as they are driven just by aerodynamic and gravitational loads, which depend on the azimuth angle. An accurate linear model has been obtained for a revolution of the rotor with a precision of 1º of azimuth angle.

As the flexibility in the components of the wind turbine is not considered in the present work, the only state of this linear model is the rotor speed.

The variables which are manipulated for control are the generator torque and the pitch angle of the blades.

Throughout this work, the pitch angle of the i-th blade has been split into a collective, common to all blades, and individual components, as each one are governed by a different controller:

$$\theta_{Bi} = \theta_{collective} + \Delta\theta_{Bi} \tag{2.6}$$

Collective pitch angle is used for power regulation, whereas the individual component is ruled for load reduction, as described in later sections.

FAST can provide a list of over 250 measurements of the wind turbine; the number of them used in this project is 37, although only some of them have been used for the design of the controllers. The rest have been interesting at different stages of the project in order to check the correct behaviour of the model. The complete list of measurements is available at the end of the FAST primary input file, in the appendix A.

Out of these 37 measurements, only the generated power and the rotor speed are controlled by a linear-model-based controller, namely for power regulation.

The hub-height wind speed has been considered as a disturbance, so that it has been included for simulations with the linear model, but not for design of controllers or observers. A list of the possible wind disturbances is available in the linearization baseline, in the appendix A.

State (x)	ω_r	n = 1
Manipulated variables (u)	$Q_{g,ref}$, $\theta_{col,ref}$, $\Delta\theta_{B1,ref}$, $\Delta\theta_{B2,ref}$, $\Delta\theta_{B3,ref}$,	m = 5
Measured variables (y)	P_{el}, ω_r, loads, deflections, etc.	p = 37
Controlled variables (z)	P_{el}, ω_r	nc = 2
Disturbance	u_{wind}	

Table 2.7 Variables involved in the linear model

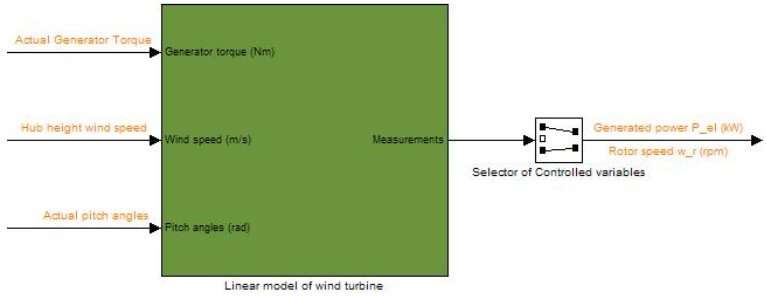

Figure 2.3 Linear model of the wind turbine

In state space (and continuous time) it has been implemented as:

$$\omega_r\big|_{k+1} = A\cdot\omega_r\big|_k + B\cdot\begin{bmatrix} Q_g \\ \theta_{col} \\ \Delta\theta_{B1} \\ \Delta\theta_{B2} \\ \Delta\theta_{B3} \end{bmatrix}_k + \left(B_{d,wind}\cdot u_{wind}\big|_k\right)^* + w_k$$

$$y_k = C\cdot\omega_r\big|_k + D\cdot\begin{bmatrix} Q_g \\ \theta_{col} \\ \Delta\theta_{B1} \\ \Delta\theta_{B2} \\ \Delta\theta_{B3} \end{bmatrix}_k + \left(D_{d,wind}\cdot u_{wind}\big|_k\right)^* + v_k \qquad (2.7)$$

$$\underbrace{\begin{bmatrix} P_{el} \\ \omega_r \end{bmatrix}_k}_{z_k} = C_z\cdot\omega_r\big|_k + D_z\cdot\begin{bmatrix} Q_g \\ \theta_{col} \\ \Delta\theta_{B1} \\ \Delta\theta_{B2} \\ \Delta\theta_{B3} \end{bmatrix}_k + \left(D_{zd,wind}\cdot u_{wind}\big|_k\right)^* + v_k = H_z\cdot y_k$$

Remark: C_z, D_z and $D_{zd,wind}$ are the corresponding rows to the generated power and rotor speed, out of C, D and $D_{d,wind}$, respectively. H_z is a matrix such that the desired measurements are selected, namely the generated power and the rotor speed. If necessary, it could be used for selecting a linear combination of measurements, but it is not the case.

Remark: w_k and v_k are the state and measurements noise, respectively, which have been modelled as white noise.

2.3.3.1 Analysis of the dynamics

At the time of writing the report, and as stated previously, only the rotor speed has been considered as a state. The eigenvalues calculated for each mode at its linearization point, and their time constants are shown in table 2.8. As all the eigenvalues are located in the negative semi-plane, the system is stable.

Mode I	Mode II	Mode III	Mode IV
λ_I = -0.0519	λ_{II} = -0.0740	λ_{III} = -0.1138	λ_{IV} = -0.2431
τ_I = 19.2678 s	τ_{II} = 13.5135 s	τ_{III} = 8.7873 s	τ_{IV} = 4.1135 s

Table 2.8 Eigenvalues and time constants

Figure 2.4 depicts the step response for a unitary increase of ω_r, where the difference in speed of response can be appreciated:

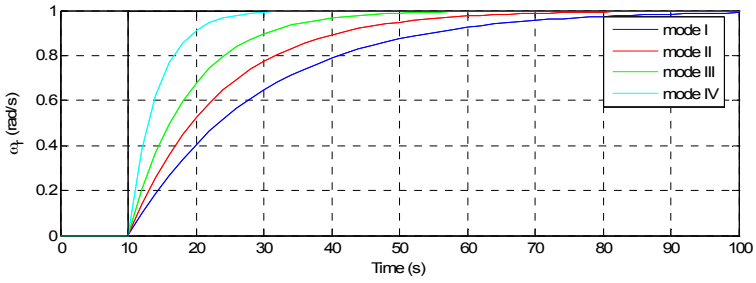

Figure 2.4 Step response of each mode

The controllers in this project have been designed in discrete with a sampling period T_s = 0.005 s, yielding a sampling frequency of F_s = 200Hz.

2.3.2 Generator model

The generator model, suggested by reference [9], is described by a first order transfer function:

$$\dot{Q}_g = \frac{1}{\tau_g} \cdot \left(Q_{g,ref} - Q_g \right) \tag{2.8}$$

Figure 2.5 Generator model

In state space (and continuous time) it has been implemented as:

$$\dot{Q}_g = \underbrace{-\frac{1}{\tau_g}}_{A_g} \cdot Q_g + \underbrace{\frac{1}{\tau_g}}_{B_g} \cdot Q_{g,ref} \tag{2.9}$$

A rather small time constant is desired so that the generator torque can achieve the demanded value quickly. A τ_g = 0.1s has been chosen.

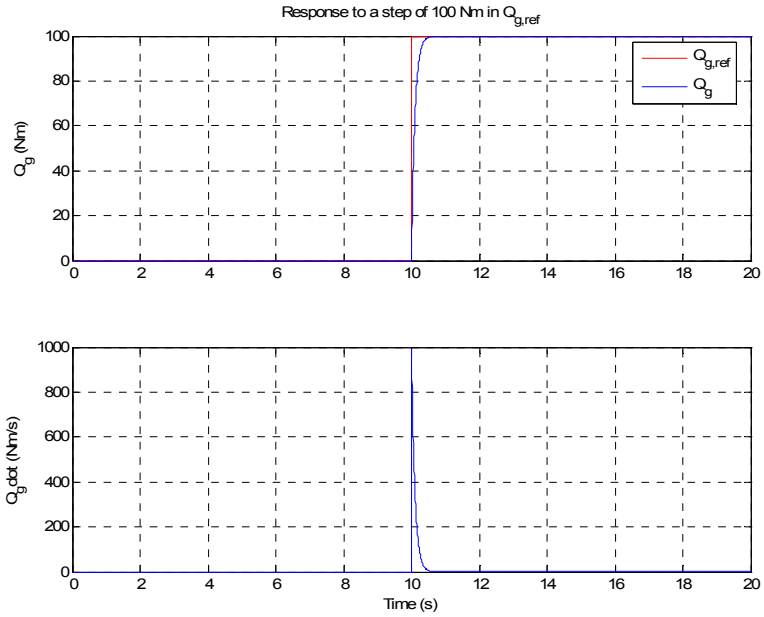

Figure 2.6 Response for a 100 Nm step in $Q_{g,ref}$

2.3.3 Model of the pitch actuator

The model of the pitch actuator, suggested by reference [9], is described by a second order transfer function:

$$\ddot{\theta}_{Bi} + \omega_n^2 \cdot \theta_{Bi} + 2\xi\omega_n \cdot \dot{\theta}_{Bi} = \omega_n^2 \cdot \theta_{Bi,ref} \tag{2.10}$$

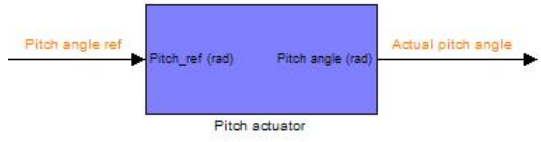

Figure 2.7 Pitch actuator

In state space (and continuous time) it has been implemented as:

$$\begin{bmatrix} \dot{\theta}_{col} \\ \Delta\dot{\theta}_{B1} \\ \Delta\dot{\theta}_{B2} \\ \Delta\dot{\theta}_{B3} \\ \ddot{\theta}_{col} \\ \Delta\ddot{\theta}_{B1} \\ \Delta\ddot{\theta}_{B2} \\ \Delta\ddot{\theta}_{B3} \end{bmatrix} = \underbrace{\begin{bmatrix} 0 & 0 & 0 & 0 & 1 & 0 & 0 & 0 \\ 0 & 0 & 0 & 0 & 0 & 1 & 0 & 0 \\ 0 & 0 & 0 & 0 & 0 & 0 & 1 & 0 \\ 0 & 0 & 0 & 0 & 0 & 0 & 0 & 1 \\ -\omega_n^2 & 0 & 0 & 0 & -2\xi\omega_n & 0 & 0 & 0 \\ 0 & -\omega_n^2 & 0 & 0 & 0 & -2\xi\omega_n & 0 & 0 \\ 0 & 0 & -\omega_n^2 & 0 & 0 & 0 & -2\xi\omega_n & 0 \\ 0 & 0 & 0 & -\omega_n^2 & 0 & 0 & 0 & -2\xi\omega_n \end{bmatrix}}_{A_p} \cdot \begin{bmatrix} \theta_{col} \\ \Delta\theta_{B1} \\ \Delta\theta_{B2} \\ \Delta\theta_{B3} \\ \dot{\theta}_{col} \\ \Delta\dot{\theta}_{B1} \\ \Delta\dot{\theta}_{B2} \\ \Delta\dot{\theta}_{B3} \end{bmatrix} + \underbrace{\begin{bmatrix} 0 & 0 & 0 & 0 \\ 0 & 0 & 0 & 0 \\ 0 & 0 & 0 & 0 \\ 0 & 0 & 0 & 0 \\ \omega_n^2 & 0 & 0 & 0 \\ 0 & \omega_n^2 & 0 & 0 \\ 0 & 0 & \omega_n^2 & 0 \\ 0 & 0 & 0 & \omega_n^2 \end{bmatrix}}_{B_p} \cdot \begin{bmatrix} \theta_{col,ref} \\ \Delta\theta_{B1,ref} \\ \Delta\theta_{B2,ref} \\ \Delta\theta_{B3,ref} \end{bmatrix} \tag{2.11}$$

Physical limitations of the pitch actuator have been taken into account for controllers design:

	Lower boundary	Upper boundary
θ_{Bi} (deg)	-5	85
$\dot{\theta}_{Bi}$ (deg/s)	-10	10
$\ddot{\theta}_{Bi}$ (deg/s^2)	-15	15

Table 2.9 Physical limitations of the pitch actuator

Remark: The width of the feasible range of pitch angles for the actuator is typically around 90º. However, when taking into account other aspects of the wind turbine, this range becomes much smaller. Values for this are discussed in Chapter 5.

Values for the natural frequency and damping ratio have been selected for providing a fast and bumpless response:

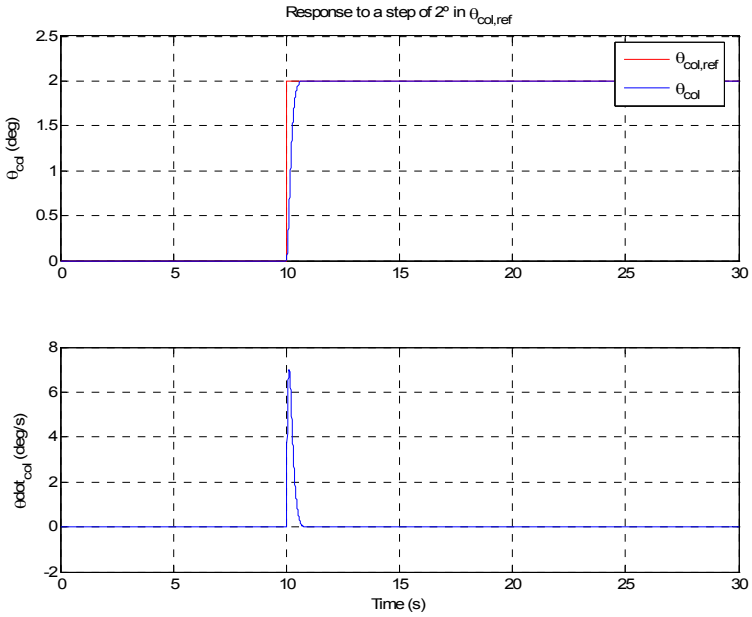

Figure 2.8 Response for a 2º step in $\theta_{col,ref}$ for $\omega_{n,p}$ = 8.88 rad/s and ξ_p = 0.9

2.3.4 Coupled model of the wind turbine

The overall response of the wind turbine to the signals from the controller can be obtained by including the model of the generator and the pitch actuator, resulting in what so called coupled or integrated model of the wind turbine.

This is of special interest when considering constraints with the power regulation controller, as the number of states is increased as follows:

State (x):	$\omega_r, Q_g, \theta_{col}, \Delta\theta_{B1}, \Delta\theta_{B2}, \Delta\theta_{B3}, \dot{\theta}_{col}, \Delta\dot{\theta}_{B1}, \Delta\dot{\theta}_{B2}, \Delta\dot{\theta}_{B3}$
Manipulated variables (u)	$Q_{g,ref}, \theta_{col,ref}, \Delta\theta_{B1,ref}, \Delta\theta_{B2,ref}, \Delta\theta_{B3,ref}$
Measured variables (y):	P_{el}, ω_r , loads, deflections, etc.
Controlled variables (z)	P_{el}, ω_r
Disturbance	u_{wind}

Table 2.10 Variables involved in the coupled model

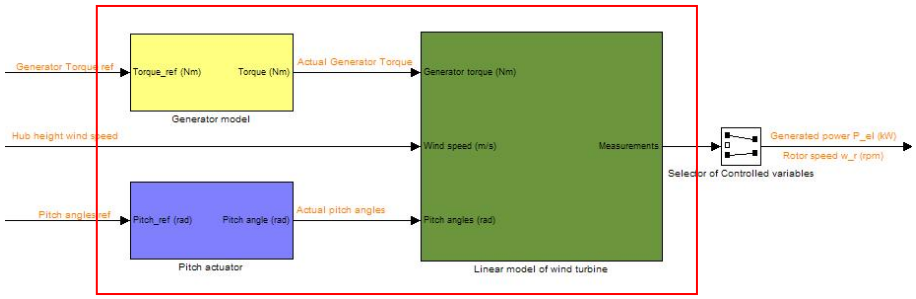

Figure 2.9 Coupled model of the wind turbine

In state space (and continuous time) it has been implemented as:

$$\begin{bmatrix} \dot{\omega}_r \\ \dot{Q}_g \\ \dot{\theta}_{col} \\ \Delta\dot{\theta}_{B1} \\ \Delta\dot{\theta}_{B2} \\ \Delta\dot{\theta}_{B3} \\ \ddot{\theta}_{col} \\ \Delta\ddot{\theta}_{B1} \\ \Delta\ddot{\theta}_{B2} \\ \Delta\ddot{\theta}_{B3} \end{bmatrix} = \underbrace{\begin{bmatrix} A_{wt} & B_{wt} & 0_{1x4} \\ 0 & A_g & 0_{1x8} \\ 0_{8x1} & 0_{8x1} & A_p \end{bmatrix}}_{A_{\text{int}}} \cdot \begin{bmatrix} \omega_r \\ Q_g \\ \theta_{col} \\ \Delta\theta_{B1} \\ \Delta\theta_{B2} \\ \Delta\theta_{B3} \\ \dot{\theta}_{col} \\ \Delta\dot{\theta}_{B1} \\ \Delta\dot{\theta}_{B2} \\ \Delta\dot{\theta}_{B3} \end{bmatrix} + \underbrace{\begin{bmatrix} 0_{1x5} \\ B_g & 0_{1x4} \\ 0_{8x1} & B_p \end{bmatrix}}_{B_{\text{int}}} \cdot \begin{bmatrix} Q_{g,ref} \\ \theta_{col,ref} \\ \Delta\theta_{B1,ref} \\ \Delta\theta_{B2,ref} \\ \Delta\theta_{B3,ref} \end{bmatrix} + \left(\begin{bmatrix} B_{d,wind} \\ 0_{9x1} \end{bmatrix} \cdot u_{wind}\big|_k \right)^* + w_k \tag{2.12}$$

The eigenvalues in continuous time of the integrated wind turbine model are:

	Mode I	Mode II	Mode III	Mode IV
Wind turbine	$\lambda_{WT,I}$ = -0.0519	$\lambda_{WT,II}$ = -0.0740	$\lambda_{WT,III}$ = -0.1138	$\lambda_{WT,IV}$ = -0.2431
Generator	λ_g = -10.0000			
Pitch actuator	λ_p = -7.9920 ± 3.8707j			

Table 2.11 Eigenvalues of the coupled wind turbine model

Remark: As it can be derived from table 2.11, the models for the generator and pitch actuator are stable as well.

CHAPTER 3

Aerodynamics modelling

In this chapter, it is presented the aerodynamic model used for calculating the C_p-curve described in used in Chapter 2, and the flow measurements necessary for the Individual pitch controller described in Chapter 7.

It is based on an unsteady Blade Element Momentum (BEM) formulation, which is widely used to calculate the induced velocities and the aerodynamic loads on each blade.

The implementation has been done in Simulink. For computational reasons, each variable such as angle of attack or loads is described as a vector of as many components as blade stations.

3.1 Theoretical basis

The BEM code is composed by two main theories, as its name depicts: Blade Element theory and Momentum theory.

Blade Element theory assumes that each blade can be discretized into a number of radial blade stations where local aerodynamic loads can be

calculated independently, reducing it into a 2D-problem. Then, these loads are integrated to determine the total aerodynamic load on each blade.

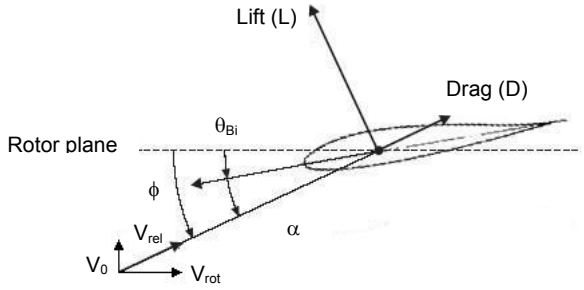

Figure 3.1 Distribution of velocities and aerodynamic loads for a certain blade station

On the other hand, the Momentum theory describes the rotor of the wind turbine as a homogeneous disc of radius R that causes a pressure drop Δp across it, reducing the speed of the wind as depicted in figure 3.2, and generating a thrust in the stream-wise direction, such that:

$$T = \pi \cdot R^2 \cdot \Delta p \tag{3.1}$$

The pressure drop in figure 3.2 is defined as the difference between p^+_d and p^-_d

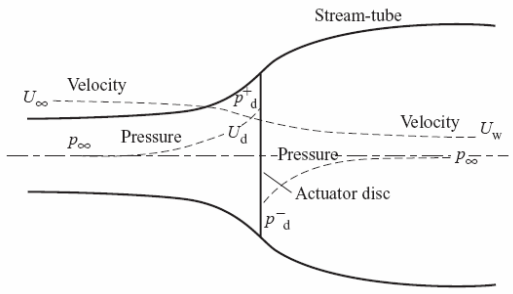

Figure 3.2 Evolution of wind speed and pressure from far upstream to far downstream, and across rotor

This thrust induces a velocity modifying the inflow in the rotor plane, and therefore also affecting the loads calculated by Blade Element theory. Here it is when Blade Element theory and Momentum theory result in the Blade Element Momentum theory, as depicted in figure 3.3:

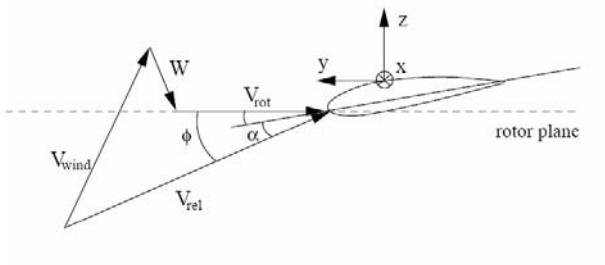

Figure 3.3 Distribution of velocities and aerodynamic loads in a certain blade station

Observation: It has been assumed that only the lift contributes to the induced velocity, in the opposite direction, according to reference [7].

The aerodynamic modelling by means of the BEM formulation involves the calculation of the induced velocity, relative velocity and aerodynamic loads at each time step, each blade station and for each blade.

The steady (classical) BEM formulation assumes steady distribution of the loads, independently from the azimuth position, as the wind speed is uniform and perpendicular to the rotor plane. On the other hand, the unsteady BEM formulation has been upgraded to include varying loads caused by yaw/tilt errors, wind shears and tower shadow.

The flow chart for the BEM code for the blade 1 is depicted in figure 3.4

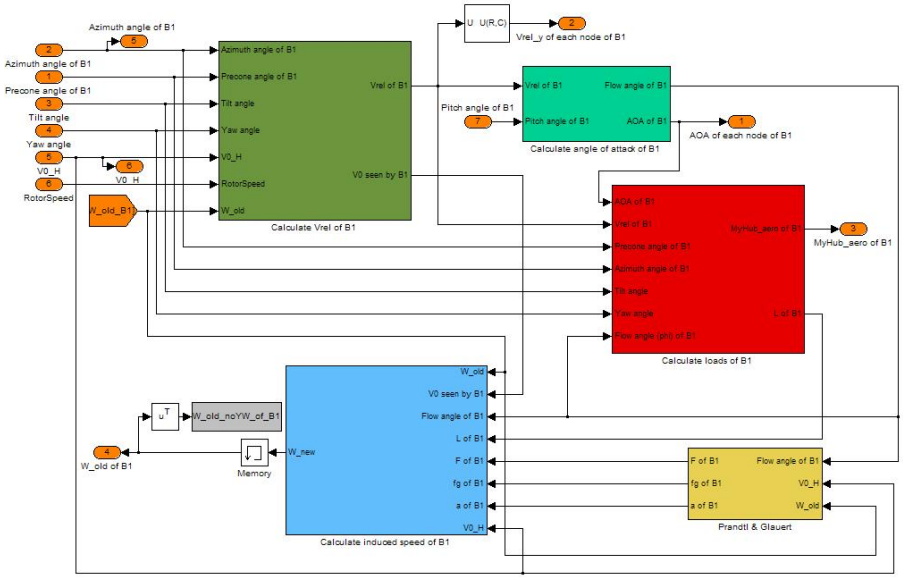

Figure 3.4 Flow chart of the unsteady BEM code for a blade

3.1.1 Calculation of the relative velocity

3.1.1.1 Specification of the coordinates systems

Correct implementation of an unsteady BEM requires coordinate transformations between various turbine components. Figure 3.5 depicts a simple 4 degree-of-freedom (DOF) system representing a wind turbine.

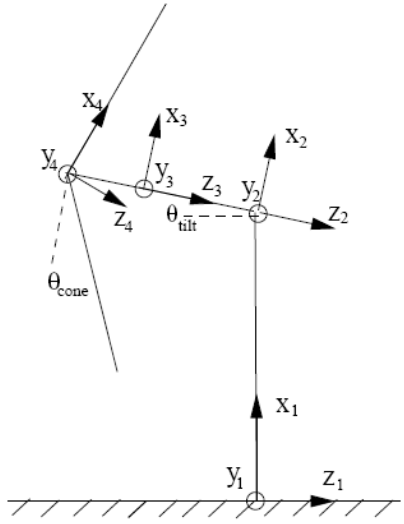

Figure 3.5 Coordinate Systems Representing 4 DOF Wind Turbine

Each coordinate system is described in the following way:

Coordinate System 1: Inertial reference frame where wind turbine tower is fixed to the ground.

Coordinate System 2: Reference frame located on the rotor shaft axis. Orientated relative to Coordinate System 1 through the tower vector and ψ and γ angles. It is described by the transformation matrix:

$$a_{12} = \begin{bmatrix} \cos\gamma & \sin\gamma \cdot \sin\psi & -\sin\gamma \cdot \cos\psi \\ 0 & \cos\psi & \sin\psi \\ -\sin\gamma & -\cos\gamma \cdot \sin\psi & \cos\gamma \cdot \cos\psi \end{bmatrix} \tag{3.2}$$

Coordinate System 3: Reference frame rotating on the rotor shaft axis. Orientated relative to Coordinate System 2 via the azimuth angle (φ_r). It is described by the transformation matrix:

$$a_{23} = \begin{bmatrix} \cos\varphi_r & \sin\varphi_r & 0 \\ -\sin\varphi_r & \cos\varphi_r & 0 \\ 0 & 0 & 1 \end{bmatrix} \tag{3.3}$$

Coordinate System 4: Reference frame located in the blade. Orientated relative to Coordinate System 3 via the cone angle (δ). It is described by the transformation matrix:

$$a_{34} = \begin{bmatrix} \cos\delta & 0 & -\sin\delta \\ 0 & 1 & 0 \\ \sin\delta & 0 & \cos\delta \end{bmatrix} \tag{3.4}$$

3.1.1.2 Calculation of the relative velocity

Figure 3.3 depicts the distribution of the velocities seen by a certain station of a blade (coordinate system 4). At the time of writing this report, both tower and blades have been considered stiff. Otherwise, their velocities should be included here.

$$\vec{V}_{rel} = \vec{V}_{wind} + \vec{V}_{rot} + \vec{W} + \left(\vec{V}_{blade} + \vec{V}_{tower}\right) \tag{3.5}$$

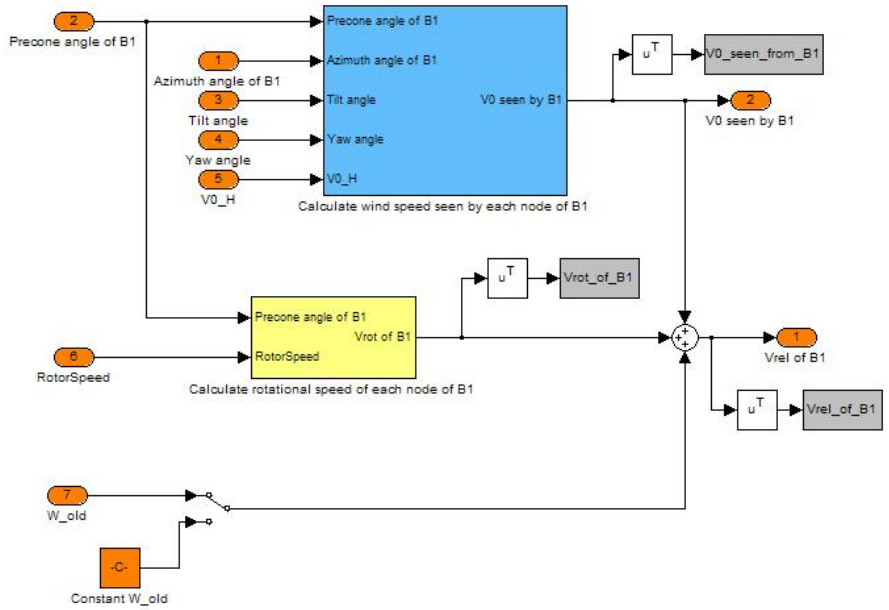

Figure 3.6 Calculation of V_{rel}

Observation: For the first iteration it is necessary to assume:

$$\vec{W} = 0 \tag{3.6}$$

3.1.2 Calculation of the loads

3.1.2.1 Calculation of the flow angle and AOA

The flow angle (ϕ), in the coordinate system of the blade described in previous sections is defined as:

$$\phi = \arctan\left(\frac{V_{rel,z}}{-V_{rel,y}}\right) \tag{3.7}$$

On the other hand, the angle of attack is defined as:

$$\alpha = \phi - \beta \tag{3.8}$$

Where the local pitch angle (β) is defined by means of the pitch angle of the blade and the twist angle at each station as:

$$\beta = \theta_{Bi} + twist \tag{3.9}$$

Remark: The twist angle is a structural characteristic of the blades, which is introduced in order to modify the angle of attack at each station.

3.1.2.2 Calculation of the aerodynamic loads

It is well known that the force resulting from the inflow in the blade is decomposed in Lift and Drag as depicted in figure 3.1, and defined for each station as follows:

$$\begin{aligned} L &= \frac{1}{2} \cdot \rho \cdot c \cdot \left| V_{rel} \right|^2 \cdot C_l \\ D &= \frac{1}{2} \cdot \rho \cdot c \cdot \left| V_{rel} \right|^2 \cdot C_d \end{aligned} \tag{3.10}$$

Where c is the length of the chord, and C_l and C_d are the lift and drag coefficients, respectively.

The C_l and C_d coefficients are obtained from a lookup table depending on the angle of attack, and used for static airfoil aerodynamics. However, variations in wind velocity over the rotor disk caused by wind shear, vertical wind, yaw misalignment and turbulences yield oscillatory angle of attack time histories, and therefore, unsteady C_l and C_d values, since it takes some time until they achieve steady values. This phenomenon called *dynamic stall* has been neglected in this section.

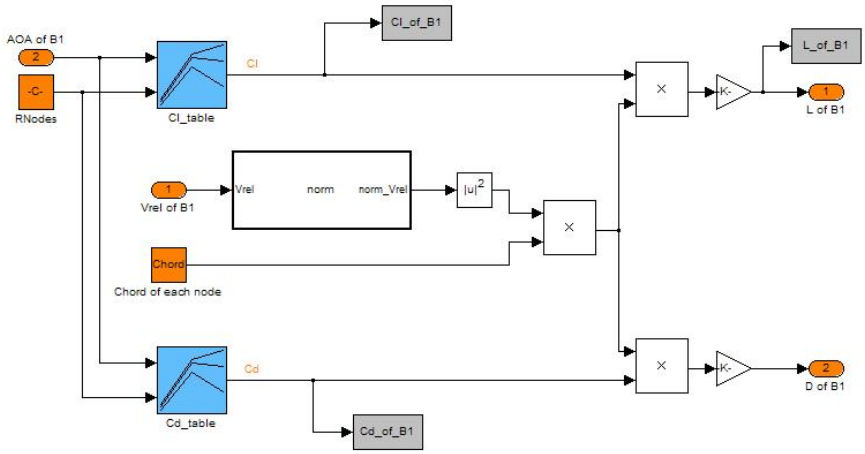

Figure 3.7 Calculation of Lift and Drag for static airfoil

Transforming them into the blade coordinate system:

$$P_y = L \cdot \sin\phi - D \cdot \cos\phi$$
$$P_z = L \cdot \cos\phi + D \cdot \sin\phi \qquad (3.11)$$

Finally, P_y and P_z calculated for every station must be integrated in order to obtain the total aerodynamic loads of the blade.

3.1.2.3 Structural and airfoil data of the blades

In order to calculate the loads, structural and airfoil data is necessary:

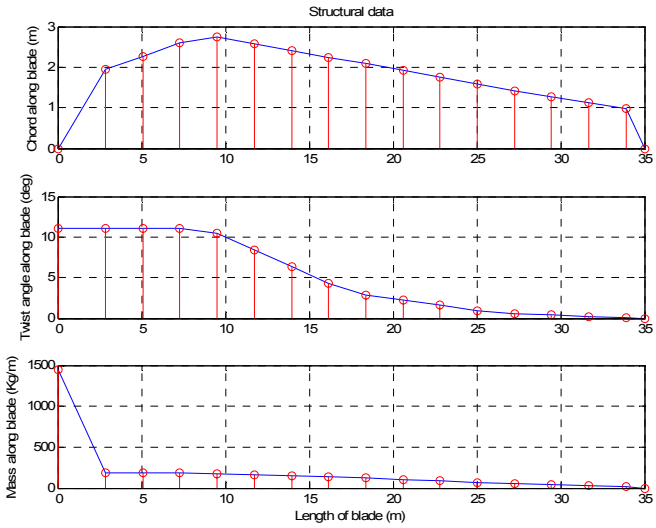

Figure 3.8 Structural data of the blades

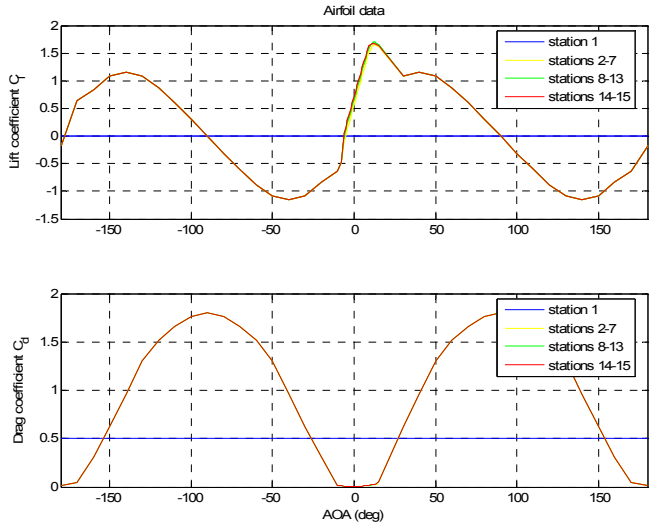

Figure 3.9 Airfoil data of the blades

Remark: Prevention of numerical errors when using FAST yields a ±180º scale for angles of attack, which is by far unrealistic from the point of view of

aerodynamics. Indeed, the airfoils are accurate only for small angles of attack, resulting in some difference among them.

The airfoils have been included in appendix A. Their distribution along the blade stations is as follows:

Station 1	*cylinder.dat*
Stations 2 – 7	*s818_2703.dat*
Stations 8 – 13	*s825_2103.dat*
Stations 13 – 15	*s826_1603.dat*

Table 3.1 Distribution of airfoils along blade

3.1.3 Calculation of the induced velocity

From the momentum theory assuming zero-yaw misalignment, equation (3.1) can be rewritten as:

$$T = 2 \cdot \rho \cdot A \cdot a \cdot V_0^2 \cdot (1 - a) \tag{3.12}$$

Where the axial (normal) induced velocity is:

$$W_n = a \cdot V_0 \tag{3.13}$$

However, when yaw misalignment is considered, V_0 is not perpendicular to the rotor plane. In this case, the axial (normal) induced velocity and the thrust are not in the opposite direction to the wind speed, yielding a deformation of the wake in the direction of V', namely the wind speed in the wake, as depicted in figure 3.10:

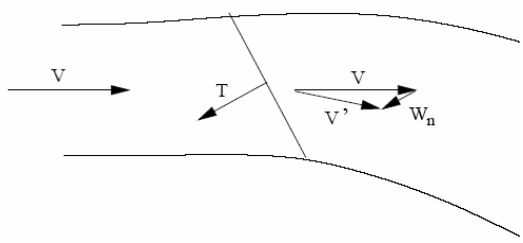

Figure 3.10 Deflected wake of a yawed wind turbine

Therefore, the thrust is now calculated as:

$$T = 2 \cdot \rho \cdot A \cdot W_n \cdot \left| \vec{V}' \right| \tag{3.14}$$

Where the wind speed in the wake can be calculated as:

$$\vec{V}' = \vec{V}_0 + \vec{n} \cdot \left(\vec{n} \cdot \vec{W} \right) \tag{3.15}$$

For a certain blade station at radius r, the thrust caused can be described as:

$$dT = T \cdot dA = -P_z \cdot dr \tag{3.16}$$

Where dA depicts the differential area of the annulus swept by one blade, described in figure 3.11:

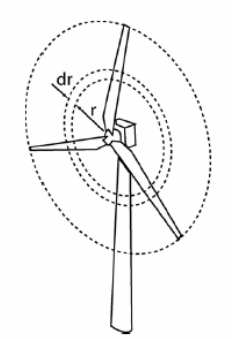

Figure 3.11 Annulus area swept by a blade station

$$dA = \frac{2 \cdot \pi \cdot r \cdot dr}{3} \tag{3.17}$$

It can be derived thus:

$$T = \frac{-3 \cdot P_z}{2 \cdot \pi \cdot r} \tag{3.18}$$

By combining equations (3.14) and (3.17), the normal induced velocity can be calculated as:

$$W_z = W_n = \frac{-3 \cdot P_z}{4 \cdot \rho \cdot \pi \cdot r \cdot F \cdot \left| V' \right|} \tag{3.19}$$

Finally, according to reference [7] it is assumed that only the lift contributes to the induced velocity, yielding:

$$W_z = W_n = \frac{-3 \cdot L \cdot \cos\phi}{4 \cdot \rho \cdot \pi \cdot r \cdot F \cdot \left| V' \right|} \tag{3.20}$$

Similarly, the tangential component of the induced velocity has been calculated as:

$$W_y = W_t = \frac{-3 \cdot L \cdot \sin\phi}{4 \cdot \rho \cdot \pi \cdot r \cdot F \cdot |V'|} \tag{3.21}$$

Remark 1: In equations from (3.19) to (3.21), a correction has been introduced by means of the Prandtl's tip loss factor (F), described in section 1.4 (Corrections applied for unsteady BEM).

Remark 2: The new induced velocity resulting from equations (3.20) and (3.21) has to be relaxed in usteady BEM formulation, as it has been calculated by means of past values of flow angle, wind speed and old induced velocity. This relaxation can be done in two different ways, described in section 3.1.4.

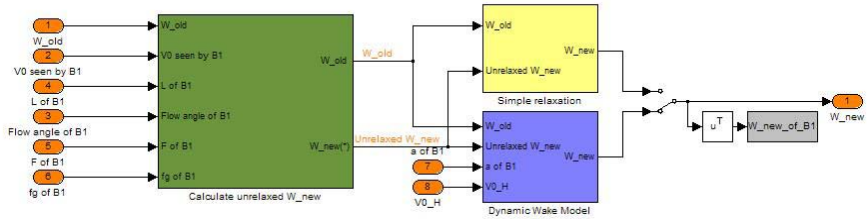

Figure 3.12 Calculation of induced velocity

3.1.4 Corrections applied throughout the unsteady BEM formulation

The following corrections have been implemented:

- Prandtl's tip loss model
- Glauert's correction for high values of the induction factor
- Relaxation of the induced velocity:
  - (a) Simple relaxation
  - (b) Dynamic wake model (DWM) of Snel and Schepers
- Vortex cylinder model for turbine operating in yaw

3.1.4.1 Prandtl's tip loss model

Prandtl's tip loss model is a correction to the assumption that the rotor disc can be considered homogeneous, equivalently to an infinite number of blades.

The factor F is calculated as follows:

$$F = \frac{2}{\pi} \cdot \arccos\left(e^{-f}\right) \tag{3.22a}$$

Where:

$$f = \frac{3}{2} \cdot \frac{R - r}{r \cdot \sin\phi} \tag{3.22b}$$

For very small flow angles, though, it has been assumed F = 1

3.1.4.2 Glauert's correction for high values of the induction factor

For values of the axial induction factor approximately higher than 0.3, the Momentum theory is not valid, according to empirical results.

In some literature though, and particularly in the AeroDyn model, the upper boundary of the axial induction factor is 0.4.

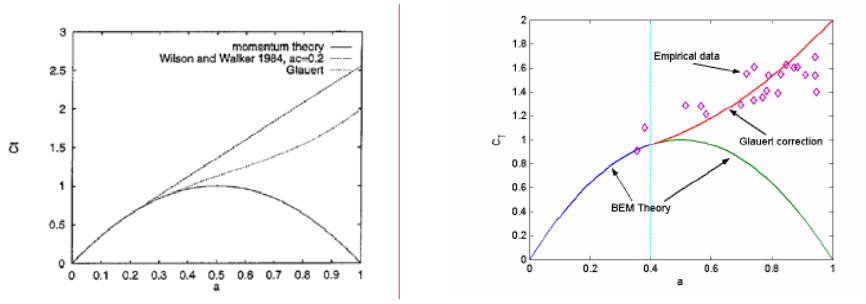

Figure 3.13 Glauert correction for a Prandtl's tip loss factor F = 1.0

Therefore, for high values of the axial (normal) induction factor, the calculation of its corresponding induced velocity must be modified, by correcting the wind speed in the wake as:

$$\vec{V}' = \vec{V}_0 + fg \cdot \vec{n} \cdot \left(\vec{n} \cdot \vec{W} \right) \tag{3.23}$$

Remark: This correction only affects W_n (3.20), not W_t (3.21).

The fg factor has been calculated as:

$$fg = \begin{cases} 1 & , \quad a \le a_c \\ \frac{a_c}{a} \cdot \left(2 - \frac{a_c}{a} \right) & , \quad a > a_c \end{cases} \tag{3.24}$$

3.1.4.3 Relaxation of the induced velocity

3.1.4.3.1 Simple relaxation

It is based on a weighted average such as:

$$W_{new} = aR \cdot W_{new} + \left(1 - aR\right) \cdot W_{old} \tag{3.25}$$

The value of the factor aR has been set to aR = 0.2

3.1.4.3.2 Dynamic wake model

The simplest way to calculate induced velocities is by assuming instantaneous equilibrium between load and induction. This is described by the equations (3.20) and (3.21), and the simple relaxation from previous section.

However, the former quasi-static approach is not suitable for load predictions in cases with load variations. It has been demonstrated that the introduction of a simple first order differential equation describing a time lag between the load and the induced velocity would improve the results. This is the basis of the DWM.

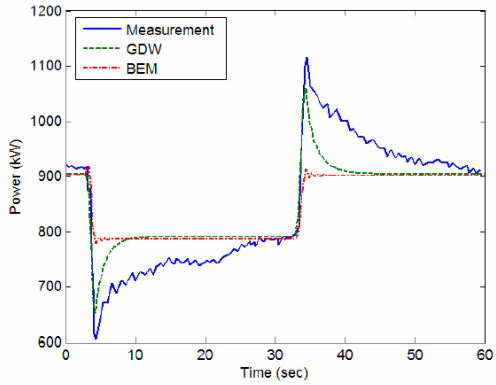

Figure 3.14 Comparison between measurements, DWM and quasi-static model. Generator power output during rapid pitch changes (from 0.2° to 3.9° and back) for the Tjæreborg turbine

Remark: The DWM model used in this work is the one suggested in reference [1]. However, the DWM model used for figure 3.14 is slightly different, called Generalized Dynamic Wake, developed by Suzuki (2000) and used in AeroDyn.

The DWM model consists of two first order lag filters with different time constants applied in series. It has been formulated as:

$$\begin{aligned} W_{\text{int}} + \tau_1 \cdot \frac{dW_{\text{int}}}{dt} &= W_{qs} + k_{DWM} \cdot \tau_1 \cdot \frac{dW_{qs}}{dt} \\ W_{DWM} + \tau_2 \cdot \frac{dW_{DWM}}{dt} &= W_{\text{int}} \end{aligned} \tag{3.26}$$

Where:

- W_{qs} is the quasi-static induced velocity calculated from equations (3.19) and (3.20)
- W_{int} is an intermediate value calculated from the first filter
- W_{DWM} is the resulting induced velocity from the Dynamic Wake Model

The time constants of the filters are calculated as follows:

$$\begin{aligned} \tau_1 &= \frac{1.1}{1 - 1.3 \cdot a} \cdot \frac{R}{V_0} \\ \tau_2 &= \tau_1 \cdot \left[0.39 - 0.26 \cdot \left(\frac{r}{R} \right)^2 \right] \end{aligned} \tag{3.27}$$

It has been implemented as suggested by reference [4].

3.1.4.4 Vortex cylinder model for turbine operating in yaw

The induced velocity is smaller when the blade is pointing upstream than when it is downstream (deep into the wake), yielding to an azimuth variation of the induced velocity.

Under these circumstances, when the blades point upstream they see a higher wind speed, and therefore higher loads, than at downstream. This difference of loads yields a restoring yaw moment that tries to balance the wind turbine.

In order to take into account this yaw moment, the induced velocity has to be modified according to:

$$W_{Bi} = W_{average} \cdot \left[1 + \frac{r}{R} \cdot \tan\left(\frac{\chi}{2}\right) \cdot \cos\left(\varphi_{Bi} - \varphi_0\right) \right] \tag{3.28}$$

Where:

- The wake skew angle (χ) is defined as the one between the wind speed in the wake (V') and the rotor axis, as depicted in figure 3.15
- $W_{average}$ is the mean value of the induced velocities of the blades
- φ_0 is the azimuth angle at which the blades are at their deepest position in the wake.

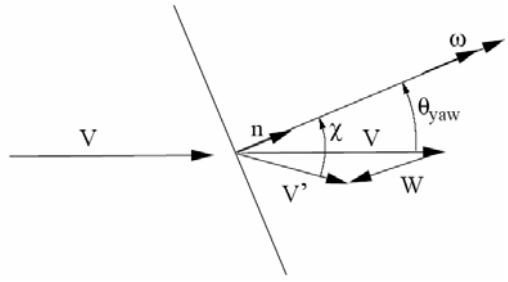

Figure 3.15 Zoom of the figure 3.10, depicting the yaw error (ψ) and skew angle (χ)

Remark: The wake skew angle is assumed to be constant along the blade, and it is calculated at r = 0.75·R

The yaw model has been implemented as follows:

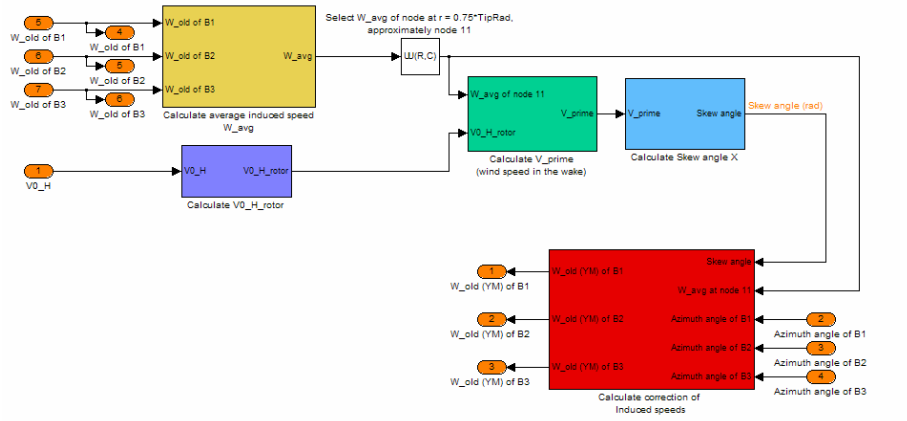

Figure 3.16 Implementation of the Yaw model

Remark: For simplicity, this correction is often referred as Yaw mode

3.2 Deterministic model of wind

3.2.1 Wind shear

The atmospheric boundary layer described can be modelled as:

$$V(x) = V_0(H) \cdot \left(\frac{x}{H} \right)^{\nu} \tag{3.29}$$

Throughout the project, the wind shear has been calculated for an exponent $\nu = 0.2$.

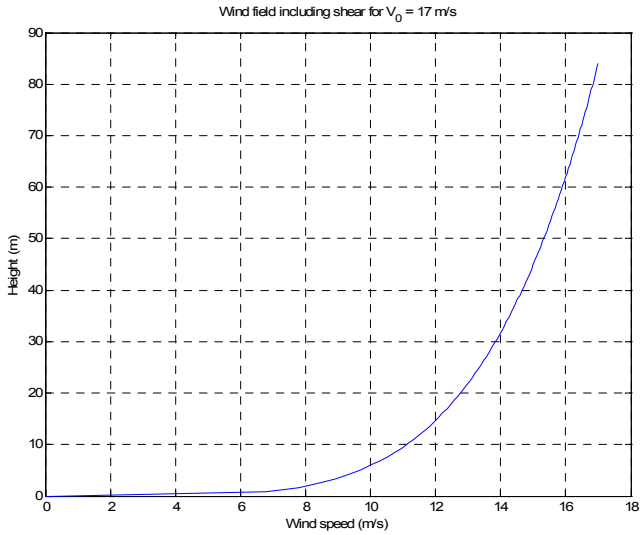

Figure 3.17 Wind field when introducing shear for V_0 = 17m/s

3.2.2 Tower shadow

The tower shadow model used in this project assumes potential flow as depicted in Figure 3.18:

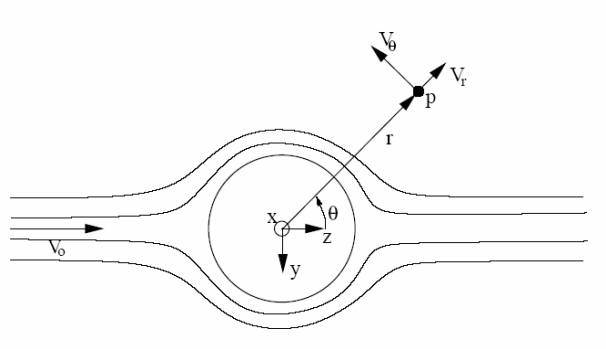

Figure 3.18 Potential flow model

The coordinate system is oriented so that the wind speed is aligned with the z-axis. The radial and tangential components around the tower are computed as follows:

$$V_r = V_0 \cdot \left(1 - \left(\frac{a}{r}\right)^2\right) \cdot \cos\theta \tag{3.30a}$$

and

$$V_t = V_\theta = -V_0 \cdot \left(1 + \left(\frac{a}{r}\right)^2\right) \cdot \sin\theta \tag{3.30b}$$

Remark: The angle θ does not have any relation with the pitch angle, since it just depicts the position of a particle p in polar coordinates

Transforming the speed into a Cartesian coordinate system, it yields:

$$V_y = -V_r \cdot \sin\theta - V_t \cdot \cos\theta \tag{3.31}$$

and

$$V_z = V_r \cdot \cos\theta - V_t \cdot \sin\theta \tag{3.32}$$

3.3 Results

Power, In-plane and Out-of-plane moments, Angle of attack and Induced velocity have been plotted in figures 3.19 – 3.22 for different yaw errors.

(a) For Yaw error = 0º

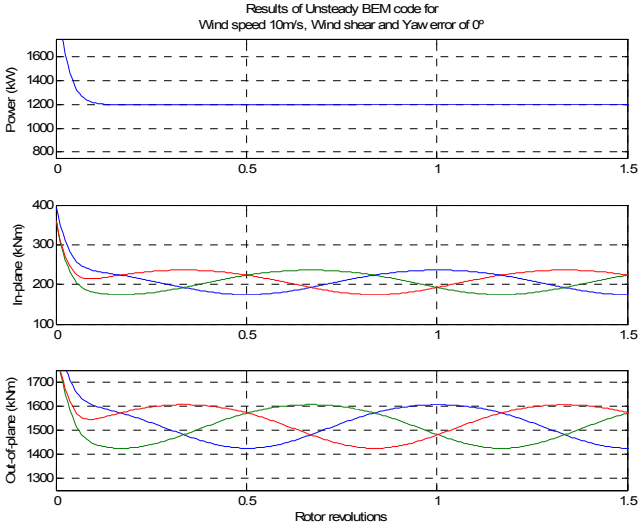

Figure 3.19 Power, In-plane moments and Out-of-plane moments, Wind speed 10m/s, Wind shear, Yaw error 0º

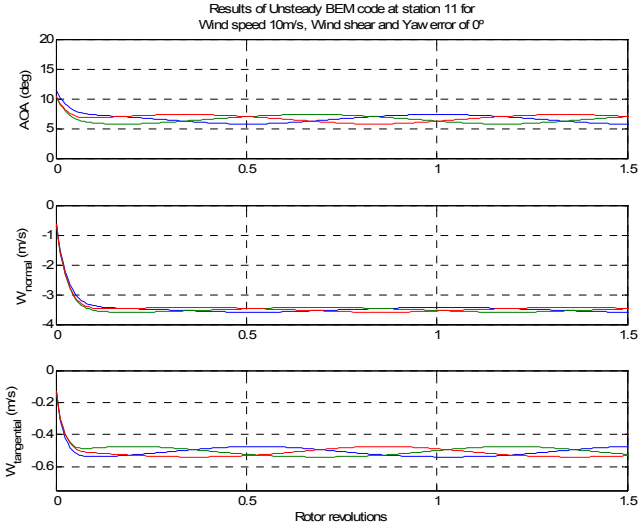

Figure 3.20 Angle of attack and Induced velocity Wind speed 10m/s, Wind shear, Yaw error 0º

(b) For Yaw error = 30º

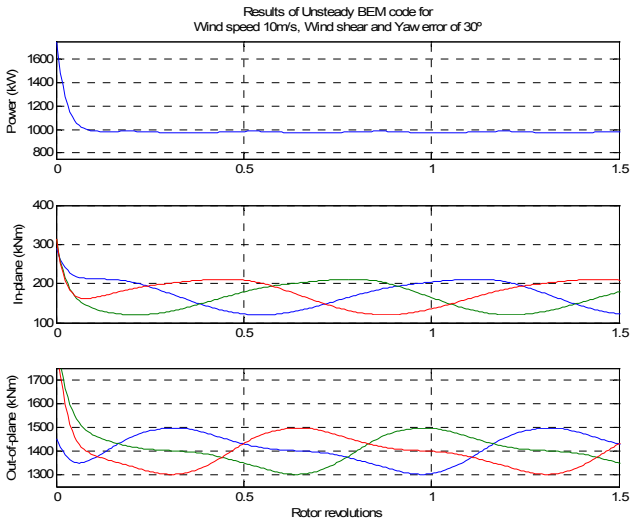

Figure 3.21 Power, In-plane moments and Out-of-plane moments Wind speed 10m/s, Wind shear, Yaw error 30º

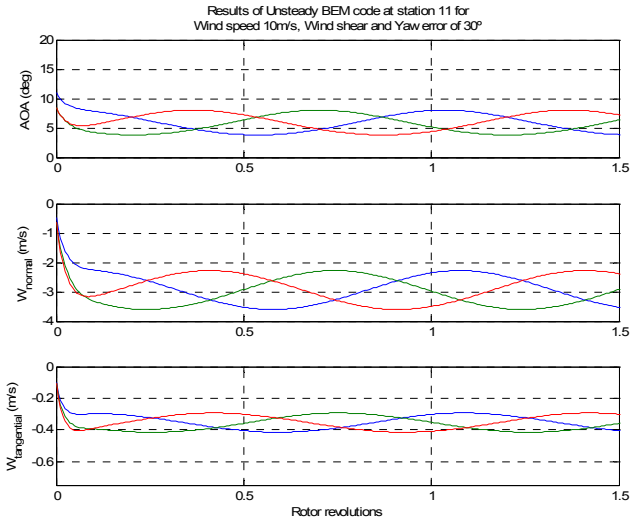

Figure 3.22 Angle of attack and Induced velocity Wind speed 10m/s, Wind shear, Yaw error 30º

3.4 Validation of the BEM code

The BEM code implemented in this section has been compared with the aerodynamic model of AeroDyn.

A good agreement between them is essential, as the Individual pitch controller (see Chapter 7) requires an online calculation of the angle of attack and the relative velocity. In the original format, it is not possible to obtain this from FAST-AeroDyn during the simulation, but only offline, so the unsteady BEM code has been used instead.

In the latter case, it is especially important the case for high wind speeds, where the load reduction becomes more relevant.

3.4.1 Conceptual differences

The aerodynamic model implemented in AeroDyn is based on the same steady BEM code as the one described in throughout this chapter. However, some corrections have been formulated in a different way:

1. Dynamic wake model
2. Yaw model
3. Tower shadow

For further information about the model used by AeroDyn, please refer to reference [5].

Last, the implementation of the unsteady BEM code has not been prepared for a turbulent wind field. By assuming a perfect knowledge about the wind field, namely deterministic wind field, the speed at any point of the rotor disc is derived from the hub height one. However AeroDyn is able to read a grid of wind speeds and interpolate for creating a 2D map.

3.4.2 Results

Angle of attack and coefficients C_l and C_d have been plotted in figures 3.23 and 3.24.

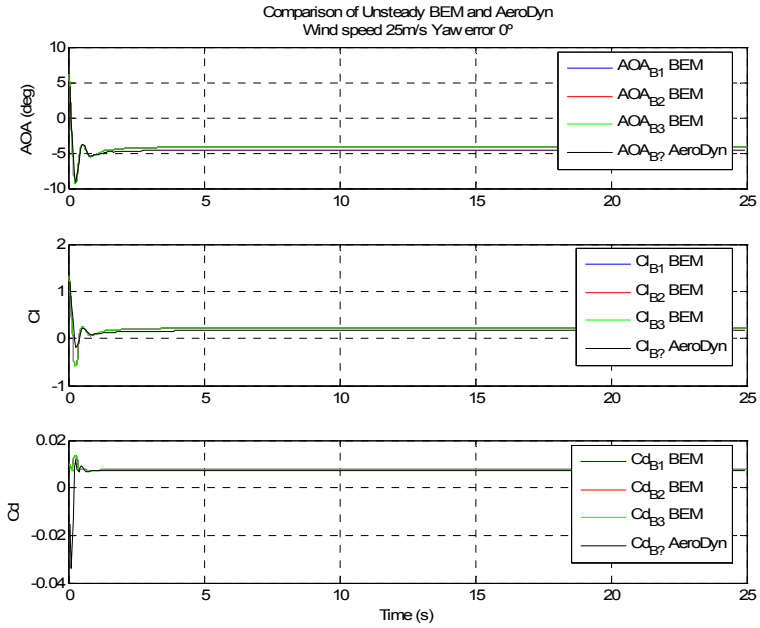

Figure 3.23 Angle of attack, Lift coefficient (C_l) and Drag coefficient (C_d) Wind speed 25m/s, Yaw error 0°

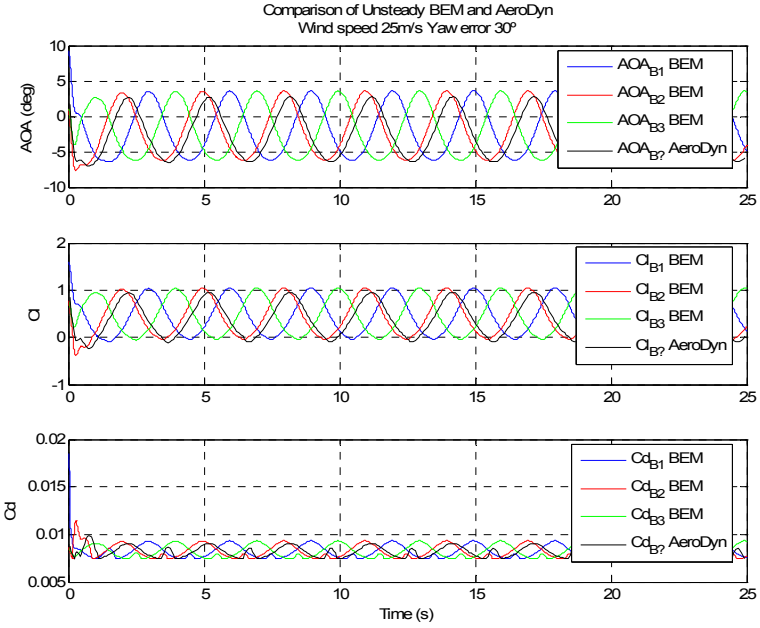

Figure 3.24 Angle of attack, Lift coefficient (C_l) and Drag coefficient (C_d) Wind speed 25m/s, Yaw error 30°

3.5 Nomenclature of Part I

Symbol	Units	Variable
H	[m]	Hub height of the wind turbine
R	[m]	Length of the blades
R	[m]	Distance between the blade root and a certain station
C	[m]	Chord of the airfoil
ρ	[kg/m^3]	Air density
ν	[-]	Wind shear exponent
P_{el}	[kW]	Generated power
C_p	[-]	Power coefficient or Power efficiency
T	[N]	Thrust force
C_T	[-]	Thrust coefficient
Q_g	[Nm]	Torque generator
λ	[-]	Tip speed ratio
	[-]	Eigenvalues of a model in state space formulation
V	[m/s]	Wind speed (for description of the operation modes)
ω_r	[rpm]	Rotor speed
φ_r	[deg]	Rotor azimuth angle
φ_{Bi}	[deg]	Azimuth angle of the i-th blade
ψ	[deg]	Yaw angle
γ	[deg]	Tilt angle
θ_{Bi}	[deg]	Pitch angle
$\Delta\theta_{Bi}$	[deg]	Cyclic or Individual (not specified) component of the pitch angle
θ_{col}	[deg]	Collective component of the pitch angle
β_{Bi}	[deg]	Local blade station pitch angle
δ_{Bi}	[deg]	Cone angle of the blade
ϕ_{Bi}	[deg]	Flow angle
α, AOA	[deg]	Angle of attack
χ	[deg]	Skew angle
L	[N]	Lift force
D	[N]	Drag force
C_l	[-]	Lift coefficient
C_d	[-]	Drag coefficient
V_{wind}, V_0, U_∞	[m/s]	Undisturbed wind speed
V'	[m/s]	Wind speed in the wake
V_{rel}	[m/s]	Relative velocity seen by blade
V_{rot}	[m/s]	Velocity component due to the azimuth rotation
W	[m/s]	Induced velocity
A	[-]	Axial (normal) induction factor
a'	[-]	Tangential induction factor
Fg	[-]	Glauert's correction factor
F	[-]	Prandtl's tip loss factor
τ_g	[s]	Time constant of the generator model
ξ	[-]	Damping ratio of the pitch actuator
ω_n	[rad/s]	Natural frequency of the pitch actuator
w_k	[-]	State noise
v_k	[-]	Measurement noise

3.6 Bibliography of Part I

[1] H. Snel, J. G. Schepers. *Joint Investigation of Dynamic Inflow Effects and Implementation of an Engineering Method*. ECN-C- 94-107, 1995

[2] M. O. L. Hansen. *Aerodynamics of Wind Turbines*. James & James 2000

[3] T. Burton, D. Sharpe, N. Jenkins, E. Bossanyi. *Wind Energy Handbook*. Ed. Wiley 2001

[4] M. O. L. Hansen. *A way of discretizing the dynamic wake model of Stig Øye*. 41325 Course notes 2005

[5] P. J. Moriarty, A. C. Hansen. *AeroDyn theory manual*. NREL 2005

[6] J. M. Jonkman, M. L. Buhl Jr. *FAST user's guide*. NREL 2005

[7] M. O. L. Hansen, J. N. Sørensen. *Unsteady BEM model of Aeroelasticity*. 41325 Course notes 2006

[8] K. Hammerum. *A fatigue approach to wind turbine control (master thesis)*. IMM 2006

[9] A. J. Larsen, T. S. Mogensen. *Individuel pitchregulering af vindmølle (master thesis)*. IMM 2006

[10] L. C. Henriksen. *Model predictive control of a wind turbine (master thesis)*. IMM 2007

Part II

Power Regulation

CHAPTER 4

Control Strategy

4.1 Introduction

The primary target of the design of a control system for a wind turbine is to optimize the production of power to be delivered to users.

Fixed-speed wind turbines require the control of the pitch angle of the blades in order to keep the generated power as close as possible to the rated one. However, below rated wind speeds, conventional fixed-speed wind turbines do not allow active control for optimizing the power, as the generator torque is directly determined by the slip speed of the induction generator.

Variable speed wind turbines include an additional control of the rotor speed below rated conditions, so that the tip speed ratio remains constant maximizing the power efficiency (defined in terms of the C_p coefficient).

The aim of this section is the design of a state-of-the-art controller for power and rotor speed of a variable-speed wind turbine. To do this, the generator torque and the collective pitch angle will be manipulated.

$$u = \begin{bmatrix} Q_{g,ref} \\ \theta_{col,ref} \end{bmatrix} \tag{4.1}$$

It is important to mention that in this section the pitch angle of all blades is assumed to be the same, namely $\theta_{Bi} = \theta_{col}$, as the concept of the load reduction is not introduced until Part III.

The power-regulation controller is composed by 4 subcontrollers, one for each operation mode described in Chapter 2, and therefore, with different set points. Moreover, according to their nature, they can be classified into two groups:

(a) The controller for operation modes I, III and IV is an MPC

(b) The controller for operation mode II is a gain scheduling based on the torque – rotor speed curve.

Part II is divided into 3 chapters:

1. First, the control strategies of each operation mode in order to either maximize the generated power or keep it constant is defined.

2. Next, a description of the methodology for designing the MPC controllers of operation modes I, III and IV is given.

3. In Chapter 6, some results comparing different modalities of MPC controllers and depicting the transitions among operation modes have been discussed.

Throughout the project, this controller will be alternatively referred as Torque and Collective pitch or Power-regulation controller, with no difference.

4.2 Control objectives

As a power generator object, the operation modes of a wind turbine define the control objectives at each one of them, in order to maximize the generated power or keep it as constant as possible, depending on the case.

As described in detailed in Chapter 2, below rated power and wind speed, namely modes I, II and III, the objective is to maximize the generated power, in other words, keep the operation point as close as possible to the top of the C_p curve. To do that, in agreement with reference [11], it has been set:

$$\theta_{col,ref} = \theta_{col}^{*} = 0^{o} \tag{4.2}$$

Otherwise, small variations in the collective pitch angle might yield stall, which at this range of wind speeds would be counterproductive.

Above rated values the control objective is orientated to keep the generated power as constant as possible in spite of the wind speed fluctuations.

4.2.1 Control objective of mode I

The objective is to keep the rotor speed constant at its minimum value, namely $\omega_r = \omega_{r,min}$, for maximizing the generated power. The wind turbine is only controlled by the generator torque at this mode, as stated in equation (4.2).

$$\begin{aligned} \overline{z}_I &= \omega_{r,\min} \\ u_I &= \begin{bmatrix} Q_{g,ref} \\ \theta_{col}^{*} = 0 \end{bmatrix} \end{aligned} \tag{4.3}$$

4.2.2 Control objective of mode II

The objective is to keep the operation at the top of the C_p-curve, by keeping constant the tip speed ratio and the pitch angle of the blades at their optimal values.

The control method in mode II is the so called *Pω control*, widely used to track the optimal generated power at this range of wind speeds, which makes use of the generator torque for achieving the set point.

Essentially it consists of a gain scheduling whose parameters are derived from:

$$P_{el} = \frac{1}{2} \cdot \rho \cdot \pi \cdot R^2 \cdot v^3 \cdot C_p \tag{4.4}$$

By expressing the wind speed as a function of the tip speed ratio, it is obtained:

$$P_{el} = \frac{1}{2} \cdot \rho \cdot \pi \cdot \frac{{\omega_r}^3 \cdot R^5}{\lambda^3} \cdot C_p \tag{4.5}$$

Therefore, it is possible to derive a relation between the rotor speed and the generator torque for control:

$$Q_{g,ref} = \frac{1}{2} \cdot \rho \cdot \pi \cdot \frac{{\omega_r}^2 \cdot R^5}{\lambda^3 \cdot N_g} \cdot C_p \tag{4.6}$$

Remark: N_g is the gearbox ratio

A look-up table has created based on this equation for every wind speed within this range, so for intermediate wind speeds a linear interpolation is carried out.

When the rotor speed decreases due to a drop in wind speed, then the demanded generator torque decreases as well, and vice-versa. Therefore, there is not a fixed set point for power and rotor speed, which is the reason why the theory of MPC controllers has not been applied for mode II.

4.2.3 Control objective of mode III

The objective is to keep the rotor speed constant at its rated value, namely $\omega_r = \omega_{r,rated}$, for maximizing the generated power. The wind turbine is only controlled by the generator torque:

$$\begin{aligned} \overline{z}_{III} &= \omega_{r,rated} \\ u_{III} &= \begin{bmatrix} Q_{g,ref} \\ \theta^*_{col} = 0 \end{bmatrix} \end{aligned} \tag{4.7}$$

4.2.4 Control objective of mode IV

The objective is to keep the generated power and rotor speed at their rated values, which is accomplished by means of the generator torque and the pitch angle of the blades simultaneously:

$$\overline{z}_{IV} = \begin{bmatrix} P_{el,rated} \\ \omega_{r,rated} \end{bmatrix}$$
$$u_{IV} = \begin{bmatrix} Q_{g,ref} \\ \theta_{col,ref} \end{bmatrix} \quad (4.8)$$

4.3 Transition between modes

The transition between 2 modes is done according to the measured power and rotor speed, and the previous mode. In principle it could also be implemented according to the wind speed, but that would require extremely fast response of the wind turbine, which is not possible due to its inertia. Therefore, the former solution is more robust. For simulations, only the initialization of the operation mode is based on the wind speed.

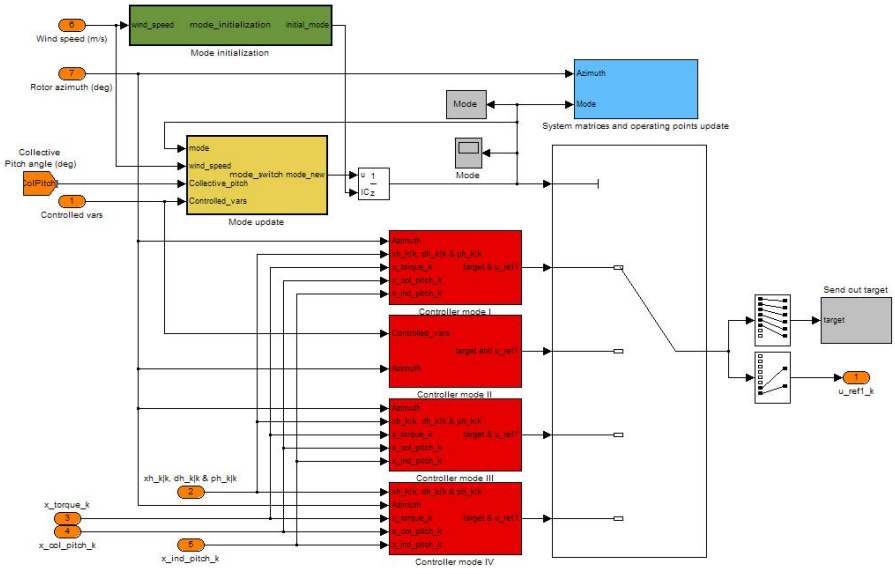

Figure 4.1 Power regulation controller

The criteria for switching modes have been inspired from both references [8] and [11], as follows:

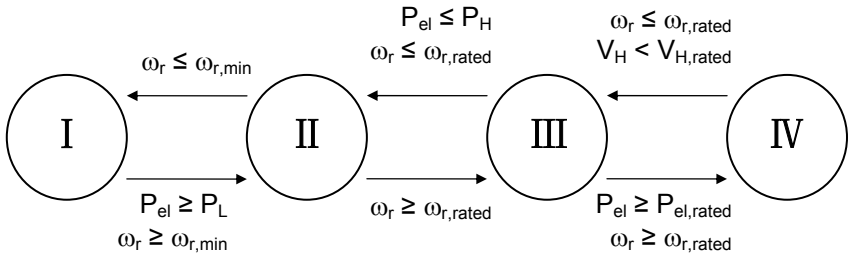

Figure 4.2 Diagram of transition among modes

The transition from mode IV to mode III is often done by assuming a negative pitch angle, as it can perform as a good estimator of the wind speed at this range. However, in this work the hub height wind speed measurement has been considered instead.

Once the mode has been updated, it is necessary to switch to the right linearized model and its corresponding operating points.

A very important issue when switching the mode is to carry it out smoothly, in other words, bumpless. However, as stated in reference [11], this is not possible since each subcontroller has a different control objective.

CHAPTER 5

Theoretical basis of MPC controllers

The MPC (Model Predictive Control) is an advanced control theory whose goal is to obtain offset-free control in presence of unmeasured/unmodelled disturbances, and constraints of linear combinations of states in a systematically way.

Remark: To obtain offset-free control means to achieve the states such that the controlled variables satisfies the reference set point.

A state space formulation of MPC in discrete time has been used in this work.

The MPC controllers are divided into three modules based on a state space model of the system:

- Disturbance model and estimator
- Target calculation
- Dynamic optimization problem

In this work, it is referred as CLQ (Constrained Linear Quadratic) or ULQ (Unconstrained Linear Quadratic) to those MPC controllers whose target calculation is constrained or not. In general, MPC controllers also include this distinction regarding the Dynamic optimization problem, but in this case this module has been substituted by a classical LQR. This involves that the horizon is infinite, whereas the general description of the MPC controllers often considers a receding one.

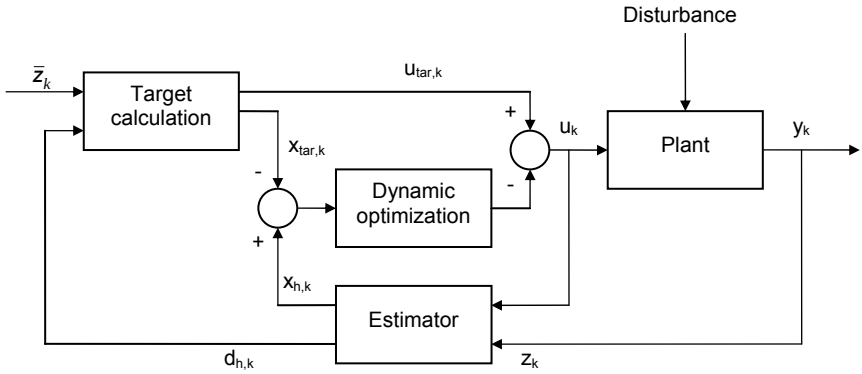

Figure 5.1 Modules of the MPC controller

5.1 Disturbance model and estimator

The linear system of the wind turbine described in Chapter 2 must be augmented with a number of integrating disturbance variables in order to counteract an incidental model-plant mismatch or some unmeasured event. In this case, it is possible to obtain offset-free control.

Remark: The model-plant mismatch refers to the discrepancy between the linear model used for designing the controller and the non-linear plant. In earlier stages of design, it can also be appreciated when the linear model of the plant is used away from the linearization points.

With no loss of generality, the models of the generator and the pitch actuator have not been included, as hypothetical unmeasured disturbances in these systems are out of interest in this project.

Before getting deeper into the description of the disturbance model, it has been considered interesting to redefine the list of variables introduced for first time in Chapter 2, in order to describe the disturbance model:

State (x):	ω_r	n = 1
Manipulated variables (u)	$Q_{g,ref}$, $\theta_{col,ref}$	m = 2
Measured variables (y):	P_{el}, ω_r, loads, deflections, etc.	p = 37
Controlled variables (z)	P_{el}, ω_r	nc = 2
State disturbance (d)		nd = 1
Output disturbance (p)		np = 1

Table 5.1 *Redefinition of variables involved in the linear model*

5.1.1 Augmented system

In this section, first the structure of the augmented system has been discussed. Next, a number of requirements that the augmented system must fulfil in order to get offset-free control have been introduced and proved.

5.1.1.1 Structure of the augmented model

The structure of the augmented system including is a matter of discussion in reference [3], where three disturbance models are presented:

a) State disturbance model

$$\begin{aligned} x_{k+1} &= A \cdot x_k + B \cdot u_k + B_d \cdot d_k + w_{x,k} \\ d_{k+1} &= d_k + w_{d,k} \\ y_k &= C \cdot x_k + D \cdot u_k + v_k \end{aligned} \tag{5.1a}$$

b) Output disturbance model

$$\begin{aligned} x_{k+1} &= A \cdot x_k + B \cdot u_k + w_{x,k} \\ p_{k+1} &= p_k + w_{p,k} \\ y_k &= C \cdot x_k + D \cdot u_k + C_d \cdot p_k + v_k \end{aligned} \tag{5.1b}$$

c) State and output disturbance model

$$\begin{aligned} x_{k+1} &= A\cdot x_k + B\cdot u_k + B_d\cdot\left[\begin{matrix} d \\ p \end{matrix}\right]_k + w_{x,k} \\ d_{k+1} &= d_k + w_{d,k} \\ p_{k+1} &= p_k + w_{p,k} \\ y_k &= C\cdot x_k + D\cdot u_k + C_d\cdot\left[\begin{matrix} d \\ p \end{matrix}\right]_k + v_k \end{aligned} \tag{5.1c}$$

The number of state disturbances (nd) is equal to the number of states among the controlled variables. Similarly, each output disturbance (np) has associated a measurement among the controlled variables, excluding states.

The structure in (5.1c), which separates state and output disturbances, seems to be the most intuitive, so this is the one selected for this project. Reference [11] confirms this idea.

Therefore, the augmented linear system of the wind turbine is:

$$\begin{aligned} \omega_r\big|_{k+1} &= A\cdot\omega_r\big|_k + B\cdot\left[\begin{matrix} Q_g \\ \theta_{col} \\ \Delta\theta_{B1} \\ \Delta\theta_{B2} \\ \Delta\theta_{B3} \end{matrix}\right]_k + B_d\cdot\left[\begin{matrix} d \\ p \end{matrix}\right]_k + \left(B_d\cdot u_{wind}\big|_k\right)^* + w_{x,k} \\ d\big|_{k+1} &= d\big|_k + w_{d,k} \\ p\big|_{k+1} &= p\big|_k + w_{p,k} \\ y_k &= C\cdot\omega_r\big|_k + D\cdot\left[\begin{matrix} Q_g \\ \theta_{col} \\ \Delta\theta_{B1} \\ \Delta\theta_{B2} \\ \Delta\theta_{B3} \end{matrix}\right]_k + C_d\cdot\left[\begin{matrix} d \\ p \end{matrix}\right]_k + \left(D_{d,wind}\cdot u_{wind}\big|_k\right)^* + v_k \\ \underbrace{\left[\begin{matrix} P_{el} \\ \omega_r \end{matrix}\right]_k}_{z_k} &= H_z\cdot y_k \end{aligned} \tag{5.2}$$

Each controlled variable has associated one integrating disturbance, so that the integrating disturbance d_1 of a controlled variable z_1 does not have any relation with other controlled variables z_2, z_3...

Therefore, the state disturbance d is directly related to ω_r, whereas the output disturbance p is related to P_{el}. This yields the equation (5.2) can be expressed as:

$$
\begin{aligned}
&\left[\begin{matrix}\omega_r\\ d\\ p\end{matrix}\right]\Big|_{k+1} = \underbrace{\left[\begin{matrix}A & I_{n,nd} & 0_{n,np}\\ 0_{nd,n} & I_{nd,nd} & 0_{nd,np}\\ 0_{np,n} & 0_{np,nd} & I_{np,np}\end{matrix}\right]}_{A^{aug}} \cdot \left[\begin{matrix}\omega_r\\ d\\ p\end{matrix}\right]\Big|_k + \\
&+ \underbrace{\left[\begin{matrix}B\\ 0_{nd,5}\\ 0_{np,5}\end{matrix}\right]}_{B^{aug}} \cdot \left[\begin{matrix}Q_g\\ \theta_{col}\\ \Delta\theta_{B1}\\ \Delta\theta_{B2}\\ \Delta\theta_{B3}\end{matrix}\right]\Big|_k + \left(\underbrace{\left[\begin{matrix}B_{d,wind}\\ 0_{nd,1}\\ 0_{np,1}\end{matrix}\right]}_{B^{aug}_{d,wind}} \cdot u_{wind}\big|_k \right)^* + w_k \\
&y_k = \underbrace{\left[\begin{matrix}C & 0_{p,nd} & I_{p,np}\end{matrix}\right]}_{C^{aug}} \cdot \left[\begin{matrix}\omega_r\\ d\\ p\end{matrix}\right]\Big|_k + \\
&+ \underbrace{D}_{D^{aug}} \cdot \left[\begin{matrix}Q_g\\ \theta_{col}\\ \Delta\theta_{B1}\\ \Delta\theta_{B2}\\ \Delta\theta_{B3}\end{matrix}\right]\Big|_k + \left(\underbrace{D_{d,wind}}_{D^{aug}_{d,wind}} \cdot u_{wind}\big|_k \right)^* + v_k \\
&\underbrace{\left[\begin{matrix}P_{el}\\ \omega_r\end{matrix}\right]\Big|_k}_{z_k} = H_z \cdot y_k
\end{aligned}
\tag{5.3}
$$

Remark: w_k depicts the state and disturbance noises, respectively, which are discussed in section 5.1.2.1.

Rearranging from equations (5.2) and (5.3):

$$
\begin{aligned}
B_d &= \left[\begin{matrix}I_{n,nd} & 0_{n,np}\end{matrix}\right] \\
C_d &= \left[\begin{matrix}0_{p,nd} & I_{p,np}\end{matrix}\right]
\end{aligned}
\tag{5.4}
$$

5.1.1.2 Requirements for offset-free control

1. **The pair (A,B) is stabilizable**

   The stability of the non-augmented system had been proved in Chapter 2 by means of the eigenvalues (in continuous time):

Mode I	Mode III	Mode IV
λ_I = -0.0519	λ_{III} = -0.1138	λ_{IV} = -0.2431

2. **The pair (C,A) is detectable**

   The non-augmented system is observable

3. **The augmented system must be detectable**

   This requirement is fulfil as long as the pair (C,A) is detectable and:

$$rank\begin{bmatrix} I-A & -B_d \\ C_z & C_d \end{bmatrix} = n + nd + np \tag{5.5a}$$

   The detectability of the augmented system is not a trivial issue, as the disturbances introduced are not stable. Note that when augmenting the system as described previously, there is a number of nd+np eigenvalues $\lambda = 1$ (discrete time)

4. **The unconstrained target calculation must have a feasible solution**

$$rank\begin{bmatrix} I-A & -B \\ C_z & D_z \end{bmatrix} = n + nc \tag{5.5b}$$

   This can only be satisfied if $nc \leq m$

5. **Finally, the main result:**

$$rank\begin{bmatrix} I-A & -B_d \\ C_z & C_d \end{bmatrix} = n + nc \tag{5.5c}$$

   Remark: According to reference [3], the number of integrating disturbances should be the same as the number of measurements (nd + np = p). In that paper, it is assumed that all

the measurements need to be controlled, and only in case p > m, a linear combination of measurements (named controlled variables) has to be created, so that nc = m.

In this work, though, it has been assumed that not all the measurements need to be controlled, so that this lemma has been adapted. Instead, the number of disturbances should be the same as the controlled variables (nd + np = nc).

5.1.2 State and disturbances estimator

The integrating disturbances included in the augmented model are unmeasured, but must be estimated together with the states by means of a Kalman filter.

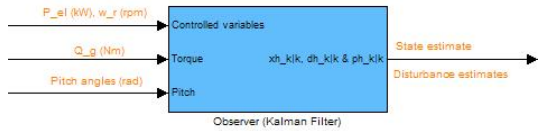

Figure 5.2 Estimator module

$$\begin{bmatrix}\hat{x}\\ \hat{d}\\ \hat{p}\end{bmatrix}_{k+1|k} = A^{aug}\cdot\begin{bmatrix}\hat{x}\\ \hat{d}\\ \hat{p}\end{bmatrix}_{k|k-1} + B^{aug}\cdot\begin{bmatrix}Q_g\\ \theta_{col}\\ \Delta\theta_{B1}\\ \Delta\theta_{B2}\\ \Delta\theta_{B3}\end{bmatrix}_k + L\cdot\left(z_k - C_z^{aug}\cdot\begin{bmatrix}\hat{x}\\ \hat{d}\\ \hat{p}\end{bmatrix}_{k|k-1} - D^{aug}\cdot\begin{bmatrix}Q_g\\ \theta_{col}\\ \Delta\theta_{B1}\\ \Delta\theta_{B2}\\ \Delta\theta_{B3}\end{bmatrix}_k\right) \quad (5.6)$$

Observation: The wind model has not been included in the Kalman filter, since it will be estimated by means of the state disturbance d.

The Kalman filter gain, L, is obtained by solving the ARE (in discrete time):

$$\Pi = A^{aug} \cdot \Pi \cdot \left[A^{aug} \right]^T + Q_w + \\ -A^{aug} \cdot \Pi \cdot \left[C^{aug} \right]^T \cdot \left(C^{aug} \cdot \Pi \cdot \left[C^{aug} \right]^T + R_v \right)^{-1} \cdot C^{aug} \cdot \Pi \cdot \left[A^{aug} \right]^T \quad (5.7)$$

And, then:

$$L = A^{aug} \cdot \Pi \cdot \left[C^{aug} \right]^T \cdot \left(C^{aug} \cdot \Pi \cdot \left[C^{aug} \right]^T + R_v \right)^{-1} \quad (5.8)$$

In this work, as the wind speed has been excluded from the model, it is considered as a disturbance. Thus, the state disturbance estimate will be strongly correlated with the wind speed. To highlight this fact, a simple test of the disturbance estimator is depicted in figure 5.3, where the linear model is subjected to a wind speed of 25m/s, yielding a model-plant mismatch as the linearization point of mode IV is at 17m/s, as stated in Chapter 2. Wind speed is thus the only disturbing element.

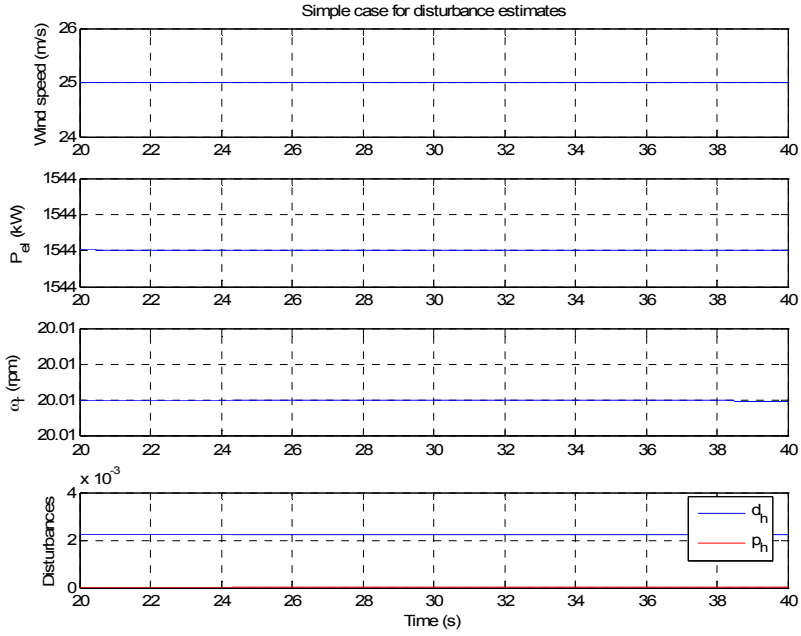

Figure 5.3 *Simple test of the disturbance estimator for a model-plant mismatch*

It can be observed that d_h = 0.0022. If this is divided by the matrix for mode IV, $B_{d,wind}$ = $2.7878 \cdot 10^{-4}$, then the result is 8m/s, which is exactly the difference between the actual wind speed (25m/s) and the wind speed at the linearization point (17m/s)

On the other hand, it can be observed that the output disturbance estimator is zero, as expected.

5.1.2.1 Discussion of the variances

Matrices Q_w and R_v are the variance matrices of the states and disturbances, and the controlled variables, respectively. In other words:

$$Q_w = \begin{bmatrix} R_x & 0 & 0 \\ 0 & R_d & 0 \\ 0 & 0 & R_p \end{bmatrix}$$
$$R_v = \begin{bmatrix} R_{v,z_1} & 0 \\ 0 & R_{v,z_2} \end{bmatrix} \quad (5.9)$$

The criterion for tuning state and output disturbance variances has been obtained from reference [11], where it is suggested that:

- R_d is small in order to get a disturbance compensation without noise
- R_p is larger than the state variance since the state measurements are more reliable than other controlled variables

On the other hand, state and measurement noises are given in real life, and they are hopefully small.

Values corresponding to the set 4 (s4) in reference [11] have been selected for this project as well. A more exhaustive analysis should have been carried out, but these values have worked out fine.

5.2 Target calculation

The target values are those states and manipulated variables which keep the controlled variables as close as possible to the reference set point, after having estimated the disturbances by means of the Kalman filter.
In section 5.1, only the wind turbine model was taken into account, excluding the generator and pitch actuator models. However, when calculating the target calculation, it is necessary to consider the coupled model of the wind

turbine, as they include a number of physical limitations, such as the feasible torque and pitch rates, accelerations, ranges…

For the case of unconstrained target calculation, these limitations are neglected, so it is possible to work only with the augmented wind turbine model. However, in order to set the same framework regardless the constrained or unconstrained target calculation, the coupled model has been used.

Another important issue is that the cyclic/individual contribution to the pitch angle of each blade from the load-reduction controllers must be taken into account, so that the collective pitch angle will counteract their action in order to guarantee offset-free power regulation.

5.2.1 Unconstrained target calculation

The state and manipulated variables targets are calculated as follows:

$$\underbrace{\begin{bmatrix} \omega_r^{tar} \\ Q_g^{tar} \\ \theta_{col}^{tar} \\ \theta_{col}^{'tar} \end{bmatrix}}_{x_{tar}^{\text{int},MPC}} = \underbrace{\begin{bmatrix} A & B_{Q_g} & B_{\theta_{col}} & 0 \\ 0 & A_g & 0 & 0 \\ 0 & 0 & A_p^{(1,1)} & A_p^{(1,5)} \\ 0 & 0 & A_p^{(5,1)} & A_p^{(5,5)} \end{bmatrix}}_{A_1^{\text{int},MPC}} \cdot \underbrace{\begin{bmatrix} \omega_r^{tar} \\ Q_g^{tar} \\ \theta_{col}^{tar} \\ \theta_{col}^{'tar} \end{bmatrix}}_{x_{tar}^{\text{int},MPC}} + \underbrace{\begin{bmatrix} 0 & 0 \\ B_g & 0 \\ 0 & B_p^{(1,1)} \\ 0 & B_p^{(5,1)} \end{bmatrix}}_{B_1^{\text{int},MPC}} \cdot \underbrace{\begin{bmatrix} Q_{g,ref}^{tar} \\ \theta_{col,ref}^{tar} \end{bmatrix}}_{u_{tar}^{\text{int},MPC}} +$$

$$+ \underbrace{\begin{bmatrix} B_{\Delta\theta_{B1}} & B_{\Delta\theta_{B2}} & B_{\Delta\theta_{B3}} & 0 & 0 & 0 \\ 0 & 0 & 0 & 0 & 0 & 0 \\ A_p^{(1,2)} & A_p^{(1,3)} & A_p^{(1,4)} & A_p^{(1,6)} & A_p^{(1,7)} & A_p^{(1,8)} \\ A_p^{(5,2)} & A_p^{(5,3)} & A_p^{(5,4)} & A_p^{(5,6)} & A_p^{(5,7)} & A_p^{(5,8)} \end{bmatrix}}_{A_2^{\text{int},MPC}} \cdot \left. \begin{bmatrix} \Delta\theta_{B1} \\ \Delta\theta_{B2} \\ \Delta\theta_{B3} \\ \Delta\theta_{B1}^{'} \\ \Delta\theta_{B2}^{'} \\ \Delta\theta_{B3}^{'} \end{bmatrix} \right|_k + \tag{5.10}$$

$$+ \underbrace{\begin{bmatrix} 0 & 0 & 0 \\ 0 & 0 & 0 \\ B_p^{(1,2)} & B_p^{(1,3)} & B_p^{(1,4)} \\ B_p^{(5,2)} & B_p^{(5,3)} & B_p^{(5,4)} \end{bmatrix}}_{B_2^{\text{int},MPC}} \cdot \left. \begin{bmatrix} \Delta\theta_{B1,ref} \\ \Delta\theta_{B2,ref} \\ \Delta\theta_{B3,ref} \end{bmatrix} \right|_k + \underbrace{\begin{bmatrix} B_d \\ 0_{3x2} \end{bmatrix}}_{B_d^{\text{int},MPC}} \cdot \left. \begin{bmatrix} \hat{d} \\ \hat{p} \end{bmatrix} \right|_{k|k}$$

Whereas, the feasible generated power and rotor speed are expressed by means of equation (5.11):

$$\underbrace{\begin{bmatrix} P_{el} \\ \omega_r \end{bmatrix}}_{z} = \underbrace{\begin{bmatrix} C_z & D_{z,Q_g} & D_{z,\theta_{col}} & 0_{px1} \end{bmatrix}}_{C_{z1}^{\text{int,MPC}}} \cdot \underbrace{\begin{bmatrix} \omega_r^{tar} \\ Q_g^{tar} \\ \theta_{col}^{tar} \\ \theta_{col}^{'tar} \end{bmatrix}}_{x_{tar}^{\text{int,MPC}}} + \underbrace{\begin{bmatrix} 0 & 0 \\ 0 & 0 \end{bmatrix}}_{D_{z1}^{\text{int,MPC}}} \cdot \underbrace{\begin{bmatrix} Q_{g,ref}^{tar} \\ \theta_{col,ref}^{tar} \end{bmatrix}}_{u_{tar}^{\text{int,MPC}}} +$$

$$+ \underbrace{\begin{bmatrix} D_{z,\Delta\theta_{B1}} & D_{z,\Delta\theta_{B2}} & D_{z,\Delta\theta_{B3}} & 0_{2x3} \end{bmatrix}}_{C_{z2}^{\text{int,MPC}}} \cdot \begin{bmatrix} \Delta\theta_{B1} \\ \Delta\theta_{B2} \\ \Delta\theta_{B3} \\ \Delta\theta_{B1}^{'} \\ \Delta\theta_{B2}^{'} \\ \Delta\theta_{B3}^{'} \end{bmatrix}_k + \underbrace{C_{zd}}_{C_{zd}^{\text{int,MPC}}} \cdot \begin{bmatrix} \hat{d} \\ \hat{p} \end{bmatrix}_{k|k} + \tag{5.11}$$

$$\underbrace{\begin{bmatrix} 0 & 0 & 0 \\ 0 & 0 & 0 \end{bmatrix}}_{D_{z2}^{\text{int,MPC}}} \cdot \begin{bmatrix} \Delta\theta_{B1,ref} \\ \Delta\theta_{B2,ref} \\ \Delta\theta_{B3,ref} \end{bmatrix}_k$$

Observations:

$$\omega_r, Q_g, \theta_{col}, \dot{\theta}_{col} \neq f(\Delta\dot{\theta}_{Bi}, \Delta\theta_{Bi,ref}) \forall i = 1,2,3 \tag{5.12a}$$

$$P_{el}, \omega_r \neq f(Q_{g,ref}, \theta_{col,ref}, \Delta\theta_{Bi,ref}) \forall i = 1,2,3 \tag{5.12b}$$

Therefore, equations (5.10) and (5.11) can be reformulated as equations (5.13) and (5.14):

$$\underbrace{\begin{bmatrix}\omega_r^{tar}\\ Q_g^{tar}\\ \theta_{col}^{tar}\\ \theta_{col}^{'tar}\end{bmatrix}}_{x_{tar}^{int,MPC}}=\underbrace{\begin{bmatrix}A & B_{Q_g} & B_{\theta_{col}} & 0\\ 0 & A_g & 0 & 0\\ 0 & 0 & A_p^{(1,1)} & A_p^{(1,5)}\\ 0 & 0 & A_p^{(5,1)} & A_p^{(5,5)}\end{bmatrix}}_{A_1^{int,MPC}}\cdot\underbrace{\begin{bmatrix}\omega_r^{tar}\\ Q_g^{tar}\\ \theta_{col}^{tar}\\ \theta_{col}^{'tar}\end{bmatrix}}_{x_{tar}^{int,MPC}}+\underbrace{\begin{bmatrix}0 & 0\\ B_g & 0\\ 0 & B_p^{(1,1)}\\ 0 & B_p^{(5,1)}\end{bmatrix}}_{B_1^{int,MPC}}\cdot\underbrace{\begin{bmatrix}Q_{g,ref}^{tar}\\ \theta_{col,ref}^{tar}\end{bmatrix}}_{u_{tar}^{int,MPC}}+$$
$$+\underbrace{\begin{bmatrix}B_{\Delta\theta_{B1}} & B_{\Delta\theta_{B2}} & B_{\Delta\theta_{B3}}\\ 0 & 0 & 0\\ A_p^{(1,2)} & A_p^{(1,3)} & A_p^{(1,4)}\\ A_p^{(5,2)} & A_p^{(5,3)} & A_p^{(5,4)}\end{bmatrix}}_{A_2^{int,MPC}}\cdot\begin{bmatrix}\Delta\theta_{B1}\\ \Delta\theta_{B2}\\ \Delta\theta_{B3}\end{bmatrix}\Bigg|_k+\underbrace{\begin{bmatrix}B_d\\ 0_{3x2}\end{bmatrix}}_{B_d^{int,MPC}}\cdot\begin{bmatrix}\hat{d}\\ \hat{p}\end{bmatrix}\Bigg|_{k|k} \tag{5.13}$$

$$\underbrace{\begin{bmatrix}P_{el}\\ \omega_r\end{bmatrix}}_{z}=\underbrace{\begin{bmatrix}C_z & D_{z,Q_g} & D_{z,\theta_{col}} & 0_{px1}\end{bmatrix}}_{C_{z1}^{int,MPC}}\cdot\underbrace{\begin{bmatrix}\omega_r^{tar}\\ Q_g^{tar}\\ \theta_{col}^{tar}\\ \theta_{col}^{'tar}\end{bmatrix}}_{x_{tar}^{int,MPC}}+\underbrace{C_{zd}}_{C_{zd}^{int,MPC}}\cdot\begin{bmatrix}\hat{d}\\ \hat{p}\end{bmatrix}\Bigg|_{k|k}$$
$$+\underbrace{\begin{bmatrix}D_{z,\Delta\theta_{B1}} & D_{z,\Delta\theta_{B2}} & D_{z,\Delta\theta_{B3}}\end{bmatrix}}_{C_{z2}^{int,MPC}}\cdot\begin{bmatrix}\Delta\theta_{B1}\\ \Delta\theta_{B2}\\ \Delta\theta_{B3}\end{bmatrix}\Bigg|_k \tag{5.14}$$

In an unconstrained target calculation, it is assumed that the reference set point of generated power and rotor speed is feasible, in other words:

$$z=\overline{z} \tag{5.15}$$

Combining equations (5.13), (5.14) and (5.15), the states and manipulated variables targets can be calculated as follows:

$$\begin{bmatrix} I - A_1^{\text{int},MPC} & -B_1^{\text{int},MPC} \\ C_{z1}^{\text{int},MPC} & D_{z1}^{\text{int},MPC} \end{bmatrix} \cdot \begin{bmatrix} x_{tar}^{\text{int},MPC} \\ u_{tar}^{\text{int},MPC} \end{bmatrix} =$$

$$= \begin{bmatrix} B_d^{\text{int},MPC} & 0_{4x2} & A_2^{\text{int},MPC} \\ -C_{zd}^{\text{int},MPC} & I_{2x2} & -C_{z2}^{\text{int},MPC} \end{bmatrix} \cdot \begin{bmatrix} \begin{bmatrix} \hat{d} \\ \hat{p} \end{bmatrix}_{k|k} \\ \overline{z} \\ \begin{bmatrix} \Delta\theta_{B1} \\ \Delta\theta_{B2} \\ \Delta\theta_{B3} \end{bmatrix}_k \end{bmatrix} \tag{5.16}$$

The solution of this equation can be computed offline, as the matrices involved are deterministic, depending only on:

a) Rotor azimuth

b) Operation mode

This has a particular importance when implementing in the Simulink model, in order to reduce the computational cost. Therefore:

$$\begin{bmatrix} x_{tar}^{\text{int},MPC} \\ u_{tar}^{\text{int},MPC} \end{bmatrix} = M \cdot \begin{bmatrix} \begin{bmatrix} \hat{d} \\ \hat{p} \end{bmatrix}_{k|k} \\ \overline{z} \\ \begin{bmatrix} \Delta\theta_{B1} \\ \Delta\theta_{B2} \\ \Delta\theta_{B3} \end{bmatrix}_k \end{bmatrix} \tag{5.17a}$$

Where:

$$M = \begin{bmatrix} I - A_1^{\text{int},MPC} & -B_1^{\text{int},MPC} \\ C_{z1}^{\text{int},MPC} & D_{z1}^{\text{int},MPC} \end{bmatrix}^{-1} \cdot \begin{bmatrix} B_d^{\text{int},MPC} & 0_{4x2} & A_2^{\text{int},MPC} \\ -C_{zd}^{\text{int},MPC} & I_{2x2} & -C_{z2}^{\text{int},MPC} \end{bmatrix} \tag{5.17b}$$

Finally, by decomposing the matrix M according to (5.18):

$$M = \begin{bmatrix} M_{11}^{[4x2]} & M_{12}^{[4x2]} & M_{13}^{[4x3]} \\ M_{21}^{[2x2]} & M_{22}^{[2x2]} & M_{23}^{[2x3]} \end{bmatrix} \tag{5.18}$$

The target values for states and manipulated variables have been calculated as:

$$\begin{aligned} x_{tar}^{\text{int},MPC} &= M_{11} \cdot \left[\begin{matrix} \hat{d} \\ \hat{p} \end{matrix} \right]_{k|k} + M_{12} \cdot \overline{z} + M_{13} \cdot \left[\begin{matrix} \Delta\theta_{B1} \\ \Delta\theta_{B2} \\ \Delta\theta_{B3} \end{matrix} \right]_k \\ u_{tar}^{\text{int},MPC} &= M_{21} \cdot \left[\begin{matrix} \hat{d} \\ \hat{p} \end{matrix} \right]_{k|k} + M_{22} \cdot \overline{z} + M_{23} \cdot \left[\begin{matrix} \Delta\theta_{B1} \\ \Delta\theta_{B2} \\ \Delta\theta_{B3} \end{matrix} \right]_k \end{aligned} \tag{5.19}$$

5.2.2 Constrained target calculation

The performance of the wind turbine is correct only if certain variables achieve values within the physical limitations of the wind turbine components.

In some cases, though, the unconstrained targets calculated according to the procedure described in section 5.2.1 violate those limitations, yielding a situation in which the wind turbine does not achieve the demands from the controller. Then, the wind turbine performance is unpredictable.

In this case, one or more constraints are active, and thus it is impossible to get offset-free control, in other words:

$$z \neq \overline{z} \tag{5.20}$$

However, this offset can be minimized subjected to certain constraints.

(1) Objective function to be minimized:

$$J = \left\| \overline{z} - z \right\|^2 \tag{5.21a}$$

(2) Constraints:

a. Constraints regarding the steady-state targets:

b. Constraints regarding the boundaries

This problem has been formulated as a quadratic program (QP), whose objective function has been rewritten as:

$$J = \frac{1}{2} \cdot \begin{bmatrix} \begin{bmatrix} x_{tar}^{\text{int},MPC} \end{bmatrix}^T & \begin{bmatrix} u_{tar}^{\text{int},MPC} \end{bmatrix}^T \end{bmatrix} \cdot H \cdot \begin{bmatrix} x_{tar}^{\text{int},MPC} \\ u_{tar}^{\text{int},MPC} \end{bmatrix} + q \cdot \begin{bmatrix} x_{tar}^{\text{int},MPC} \\ u_{tar}^{\text{int},MPC} \end{bmatrix} \tag{5.21b}$$

5.2.2.1 Objective function

$$\begin{aligned} &\min_{x_{tar}^{\text{int},MPC}, u_{tar}^{\text{int},MPC}} J = \min_{x_{tar}^{\text{int},MPC}, u_{tar}^{\text{int},MPC}} \left\| \bar{z} - z \right\|^2 = \bar{z}^T \cdot \bar{z} + z^T \cdot z - 2 \cdot \bar{z}^T \cdot z = \\ &= \begin{bmatrix} \begin{bmatrix} x_{tar}^{\text{int},MPC} \end{bmatrix}^T & \begin{bmatrix} u_{tar}^{\text{int},MPC} \end{bmatrix}^T \end{bmatrix} \cdot Q \cdot \begin{bmatrix} x_{tar}^{\text{int},MPC} \\ u_{tar}^{\text{int},MPC} \end{bmatrix} + 2 \cdot q \cdot \begin{bmatrix} x_{tar}^{\text{int},MPC} \\ u_{tar}^{\text{int},MPC} \end{bmatrix} + \\ &+ \begin{bmatrix} \begin{bmatrix} \begin{bmatrix} \hat{d} \\ \hat{p} \end{bmatrix}_{k|k} \end{bmatrix}^T & \begin{bmatrix} \begin{bmatrix} \Delta\theta_{B1} \\ \Delta\theta_{B2} \\ \Delta\theta_{B3} \end{bmatrix}_k \end{bmatrix}^T \end{bmatrix} \cdot f \cdot \begin{bmatrix} \begin{bmatrix} \hat{d} \\ \hat{p} \end{bmatrix}_{k|k} \\ \begin{bmatrix} \Delta\theta_{B1} \\ \Delta\theta_{B2} \\ \Delta\theta_{B3} \end{bmatrix}_k \end{bmatrix} \end{aligned} \tag{5.22a}$$

Where:

$$Q = \begin{bmatrix} \begin{bmatrix} C_{z1}^{\text{int},MPC} \end{bmatrix}^T \cdot \begin{bmatrix} C_{z1}^{\text{int},MPC} \end{bmatrix} & \begin{bmatrix} C_{z1}^{\text{int},MPC} \end{bmatrix}^T \cdot \begin{bmatrix} D_{z1}^{\text{int},MPC} \end{bmatrix} \\ \begin{bmatrix} D_{z1}^{\text{int},MPC} \end{bmatrix}^T \cdot \begin{bmatrix} C_{z1}^{\text{int},MPC} \end{bmatrix} & \begin{bmatrix} D_{z1}^{\text{int},MPC} \end{bmatrix}^T \cdot \begin{bmatrix} D_{z1}^{\text{int},MPC} \end{bmatrix} \end{bmatrix}$$

$$q = \begin{bmatrix} \left\{ \begin{bmatrix} \begin{bmatrix} \hat{d} \\ \hat{p} \end{bmatrix}_{k|k} \end{bmatrix}^T \cdot \begin{bmatrix} C_{zd}^{\text{int},MPC} \end{bmatrix}^T + \begin{bmatrix} \begin{bmatrix} \Delta\theta_{B1} \\ \Delta\theta_{B2} \\ \Delta\theta_{B3} \end{bmatrix}_k \end{bmatrix}^T \cdot \begin{bmatrix} C_{z2}^{\text{int},MPC} \end{bmatrix}^T - \bar{z} \right\} \cdot C_{z1}^{\text{int},MPC} \\ \left\{ \begin{bmatrix} \begin{bmatrix} \hat{d} \\ \hat{p} \end{bmatrix}_{k|k} \end{bmatrix}^T \cdot \begin{bmatrix} C_{zd}^{\text{int},MPC} \end{bmatrix}^T + \begin{bmatrix} \begin{bmatrix} \Delta\theta_{B1} \\ \Delta\theta_{B2} \\ \Delta\theta_{B3} \end{bmatrix}_k \end{bmatrix}^T \cdot \begin{bmatrix} C_{z2}^{\text{int},MPC} \end{bmatrix}^T - \bar{z} \right\} \cdot D_{z1}^{\text{int},MPC} \end{bmatrix}^T \tag{5.22b}$$

$$f = \begin{bmatrix} \begin{bmatrix} C_{zd}^{\text{int},MPC} \end{bmatrix}^T \cdot \begin{bmatrix} C_{zd}^{\text{int},MPC} \end{bmatrix} & \begin{bmatrix} C_{zd}^{\text{int},MPC} \end{bmatrix}^T \cdot \begin{bmatrix} C_{z2}^{\text{int},MPC} \end{bmatrix} \\ \begin{bmatrix} C_{z2}^{\text{int},MPC} \end{bmatrix}^T \cdot \begin{bmatrix} C_{zd}^{\text{int},MPC} \end{bmatrix} & \begin{bmatrix} C_{z2}^{\text{int},MPC} \end{bmatrix}^T \cdot \begin{bmatrix} C_{z2}^{\text{int},MPC} \end{bmatrix} \end{bmatrix}$$

The Q matrix should be symmetric in order avoid numerical errors. This can be done by defining a new matrix, H, as:

$$H = \frac{1}{2}(Q + Q^T) \tag{5.22c}$$

On the other hand, the last term can be ignored as long as it does not contain any target variable. The QP program can thus be formulated as:

$$\min \frac{1}{2} \cdot \begin{bmatrix} \begin{bmatrix} x_{tar}^{\text{int},MPC} \end{bmatrix}^T & \begin{bmatrix} u_{tar}^{\text{int},MPC} \end{bmatrix}^T \end{bmatrix} \cdot H \cdot \begin{bmatrix} x_{tar}^{\text{int},MPC} \\ u_{tar}^{\text{int},MPC} \end{bmatrix} + q \cdot \begin{bmatrix} x_{tar}^{\text{int},MPC} \\ u_{tar}^{\text{int},MPC} \end{bmatrix} \tag{5.23}$$

5.2.2.2 Constraints

5.2.2.2.1 Constraints regarding the steady-state targets

This constraint is actually the unconstrained target calculation, except for an unfeasible reference set point.

$$\begin{bmatrix} I - A_1^{\text{int},MPC} & -B_1^{\text{int},MPC} \end{bmatrix} \cdot \begin{bmatrix} x_{tar}^{\text{int},MPC} \\ u_{tar}^{\text{int},MPC} \end{bmatrix} = \begin{bmatrix} B_d^{\text{int},MPC} & A_2^{\text{int},MPC} \end{bmatrix} \cdot \begin{bmatrix} \begin{bmatrix} \hat{d} \\ \hat{p} \end{bmatrix}_{k|k} \\ \begin{bmatrix} \Delta\theta_{B1} \\ \Delta\theta_{B2} \\ \Delta\theta_{B3} \end{bmatrix}_k \end{bmatrix} \tag{5.24}$$

5.2.2.2.2 Constraints regarding the boundaries

The variables to be constrained in this project are:

- Rotor speed
- Rotor acceleration*
- Generator torque
- Generator torque rate*
- Pitch angle of all blades
- Collective pitch rate
- Collective pitch acceleration

The constraints regarding the boundaries have been formulated as:

$$\underbrace{M^{ctc,MPC}\cdot\left[E_1^{ctc,MPC} \quad F^{ctc,MPC}\right]}_{Variables\_to\_be\_constrained(cv)}\cdot\begin{bmatrix} x_{tar}^{int,MPC} \\ u_{tar}^{int,MPC}\end{bmatrix} \le \underline{c} - M^{ctc,MPC}\cdot\left[E_d^{ctc,MPC} \quad E_2^{ctc,MPC}\right]\cdot\begin{bmatrix}\begin{bmatrix}\hat{d}\\ \hat{p}\end{bmatrix}_{k|k} \\ \begin{bmatrix}\Delta\theta_{B1}\\ \Delta\theta_{B2}\\ \Delta\theta_{B3}\end{bmatrix}_k\end{bmatrix} \quad (5.25)$$

Where matrix $M^{ctc,MPC}$ is used for defining the sign of the inequality, such that:

$$M^{ctc,MPC} = \begin{bmatrix} I_{9x9} \\ -I_{9x9}\end{bmatrix} \quad (5.26)$$

And c is the vector of boundaries such as:

$$\underline{c} = \begin{bmatrix} ub \\ -lb\end{bmatrix} \quad (5.27)$$

The boundaries specified in this project are:

(a) For wind turbine

	Lower boundary	Upper boundary
ω_r (rpm)	0	$\omega_r^{rated}\cdot(1+tol_{\omega_r})$
$\dot{\omega}_r$ (rad/s^2)	-4	4

Table 5.2 Boundaries for the wind turbine

Comments:

1. The tolerance for the maximum rotor speed allowed has been set to 5%, yielding to: ω_r^{max} = 21 rpm.

2. The rotor acceleration constraint has been chosen rather loose so that it is not active in this work. It has left out of scope to analyze the importance of constraining this variable. However, it might be useful for future implementations

(b) For generator model

	Lower boundary	Upper boundary
Q_g (Nm)	0	$Q_g^{rated} \cdot (1 + tol_{Q_g})$
$\dot{Q}_g$ (N·m/s)	$-1.5 \cdot 10^4$	$1.5 \cdot 10^4$

Table 5.3 Boundaries for the generator model

Comments:

3. The tolerance for the maximum generator torque allowed has been set to 1%, yielding to: Q_g^{max} = 8.4604 kN·m.

4. As the rotor acceleration, the generator torque rate constraint has been chosen rather loose, like for rotor acceleration. It has left out of scope to analyze the importance of constraining this variable. However, it might be useful for future implementations

(c) For pitch actuator

	Lower boundary	Upper boundary
θ_{Bi} (deg)	-5	30
$\dot{\theta}_{collective}$ (deg/s)	-10	10
$\ddot{\theta}_{collective}$ (deg/s^2)	-15	15

Table 5.4 Boundaries for the pitch actuator

Remark: The pitch angle in the table includes the cyclic or individual component from the Cyclic or Individual pitch controller, respectively:

Cyclic pitch controller: $\theta_{Bi} = \theta_{collective} + \Delta\theta_{cyclic,Bi}$ (5.28a)

Individual pitch controller: $\theta_{Bi} = \theta_{collective} + \Delta\theta_{individual,Bi}$ (5.28b)

Remark: The ideal situation would be to constrain the pitch rate and acceleration of the blade, not only the collective component. This has been done like this due to the current formulation of the load-reduction controller, as the power-regulation controller is not able to control those states.

Observation: Some of the constraints, such as the rotor acceleration or the generator torque rate, might be modified in a real implementation; the aim of this section is to analyze the performance of the wind turbine under certain constraints, not their accuracy.

Back to equation (5.25), matrices $E_1^{ctc,MPC}$, $E_2^{ctc,MPC}$, $F^{ctc,MPC}$ and $E_d^{ctc,MPC}$ are used in order to constrain variables which are linear combination of states and manipulated variables, such as the generator torque rate and the collective pitch acceleration. In this case:

$$\underbrace{\begin{bmatrix} \omega_r \\ Q_g \\ \theta_{B1} \\ \theta_{B2} \\ \theta_{B3} \\ \omega_r^{'} \\ Q_g^{'} \\ \theta_{col}^{'} \\ \theta_{col}^{''} \end{bmatrix}}_{cv} = \underbrace{\begin{bmatrix} 1 & 0 & 0 & 0 \\ 0 & 1 & 0 & 0 \\ 0 & 0 & 1 & 0 \\ 0 & 0 & 1 & 0 \\ 0 & 0 & 1 & 0 \\ A_1^{\text{int},MPC} \end{bmatrix}}_{E_1^{ctc,MPC}} \cdot \underbrace{\begin{bmatrix} \omega_r^{tar} \\ Q_g^{tar} \\ \theta_{col}^{tar} \\ \theta_{col}^{'tar} \end{bmatrix}}_{x_{tar}^{\text{int},MPC}} + \underbrace{\begin{bmatrix} 0 & 0 \\ 0 & 0 \\ 0 & 0 \\ 0 & 0 \\ 0 & 0 \\ B_1^{\text{int},MPC} \end{bmatrix}}_{F^{ctc,MPC}} \cdot \underbrace{\begin{bmatrix} Q_{g,ref}^{tar} \\ \theta_{col,ref}^{tar} \end{bmatrix}}_{u_{tar}^{\text{int},MPC}} +$$

$$+ \underbrace{\begin{bmatrix} 0 & 0 & 0 \\ 0 & 0 & 0 \\ 1 & 0 & 0 \\ 0 & 1 & 0 \\ 0 & 0 & 1 \\ A_2^{\text{int},MPC} \end{bmatrix}}_{E_2^{ctc,MPC}} \cdot \begin{bmatrix} \Delta\theta_{B1} \\ \Delta\theta_{B2} \\ \Delta\theta_{B3} \end{bmatrix}_k + \underbrace{\begin{bmatrix} 0_{5x2} \\ B_d^{\text{int},MPC} \end{bmatrix}}_{E_d^{ctc,MPC}} \cdot \begin{bmatrix} \hat{d} \\ \hat{p} \end{bmatrix}_{k|k} \tag{5.29}$$

5.3 Dynamic optimization problem

The dynamic optimization problem deals with the calculation of the torque and collective pitch references in order to achieve the steady-state targets calculated in the previous module.

For simplicity a conventional LQR has been used for calculating the torque and collective pitch references.

Cost function:

$$J=\sum_{k=0}^{\infty}\left[x_k^{\text{int},MPC}\right]^T\cdot Q_x\cdot x_k^{\text{int},MPC}+\left[u_k^{\text{int},MPC}\right]^T\cdot R_u\cdot u_k^{\text{int},MPC} \tag{5.30}$$

Weight matrices Q_x and R_u have been tuned according to the rule of thumb:

$$Q_x=\begin{bmatrix}\frac{1}{\left(\max\left(\omega_r\right)\right)^2} & 0 & 0 & 0\\ 0 & \frac{1}{\left(\max\left(Q_g\right)\right)^2} & 0 & 0\\ 0 & 0 & \frac{1}{\left(\max\left(\theta_{col}\right)\right)^2} & 0\\ 0 & 0 & 0 & \frac{1}{\left(\max\left(\dot{\theta}_{col}\right)\right)^2}\end{bmatrix} \tag{5.31}$$

$$R_u=\begin{bmatrix}\frac{1}{\left(\max\left(Q_g\right)\right)^2} & 0\\ 0 & \frac{1}{\left(\max\left(\theta_{col}\right)\right)^2}\end{bmatrix}$$

The LQR gain has been calculated as the solution to the ARE:

$$\begin{aligned}&S=A_1^{\text{int},MPC}\cdot S\cdot\left[A_1^{\text{int},MPC}\right]^T+Q_k+\\&-A_1^{\text{int},MPC}\cdot S\cdot\left[B_1^{\text{int},MPC}\right]^T\cdot\left(B_1^{\text{int},MPC}\cdot S\cdot\left[B_1^{\text{int},MPC}\right]^T+R_k\right)^{-1}\cdot\\&\cdot B_1^{\text{int},MPC}\cdot S\cdot\left[A_1^{\text{int},MPC}\right]^T\end{aligned} \tag{5.32}$$

And, then:

$$K=A_1^{\text{int},MPC}\cdot S\cdot\left[B_1^{\text{int},MPC}\right]^T\cdot\left(B_1^{\text{int},MPC}\cdot S\cdot\left[B_1^{\text{int},MPC}\right]^T+R_k\right)^{-1} \tag{5.33}$$

Finally, the torque and collective pitch angle references are computed as:

$$\left[\begin{array}{c} Q_{g,ref} \\ \theta_{col,ref} \end{array}\right]_k = u_{tar}^{\text{int},MPC} - K \cdot \left(\left[\begin{array}{c} \hat{x}_{k|k-1} \\ Q_g \\ \theta_{col} \\ \theta_{col}^{'} \end{array}\right] - x_{tar}^{\text{int},MPC} \right) \tag{5.34}$$

CHAPTER 6

Results

6.1 Results

Several tests have been carried out orientated to evaluate the performance of the Power-regulation controller in both versions ULQ and CLQ, in terms of:

1. Keeping the power and rotor speed constant at rated values for high wind speeds
2. Performance of the switch among operation modes

Different scenarios have been considered. The TurbSim code has been used for creating realistic wind data files:

Wind field #1 is a turbulent wind field with a mean hub-height wind speed of 18.2 m/s, and a spectral model Risø smooth terrain.

Wind field #2 is a deterministic and uniform wind field, whose hub-height wind speed is 12.8 m/s with a large wind gust for about 10s, achieving a maximum value of 17.5 m/s.

Wind field #3 is a turbulent wind field with a mean hub-height wind speed of 10.0 m/s, an IEC 61400-1 Ed. 2: 1999 class 1A, and an IEC Kaimal spectral model.

Wind field #4 has the same characteristics of the wind field #2, but for a hub-height wind speed of 9 m/s and a peak at 13.7 m/s.

Further details of each wind field is available in Appendix B

Wind fields #1 and #2 have been used for testing the performance of the power regulation controller at high wind speeds, whereas wind fields #3 and #4 are considered for analysing the transition among modes.

6.1.1 Analysis of the controller for power regulation at high wind speeds

Figures 6.1 and 6.2 depict the performance of the wind turbine with the controller for power regulation described in previous chapters in the wind field #1. The controller works very well, as the generated power remains within an interval of 1% of the rated value.

The disturbance from the wind speed has been estimated and rejected correctly, as a strong correlation between wind speed and the state disturbance d_h can be observed in the last subplot of figure 6.2.

On the other hand, it can be observed that the constraints are all inactive, which means that the ULQ performs the same as CLQ. In other words, it was possible to obtain offset-free control.

For a large and fast disturbance like the wind gust from in wind field #2, the controller is not able to reject it immediately, and as a consequence, the generated power increases. However, it barely overcomes 1% of the rated power, which is still an excellent result.

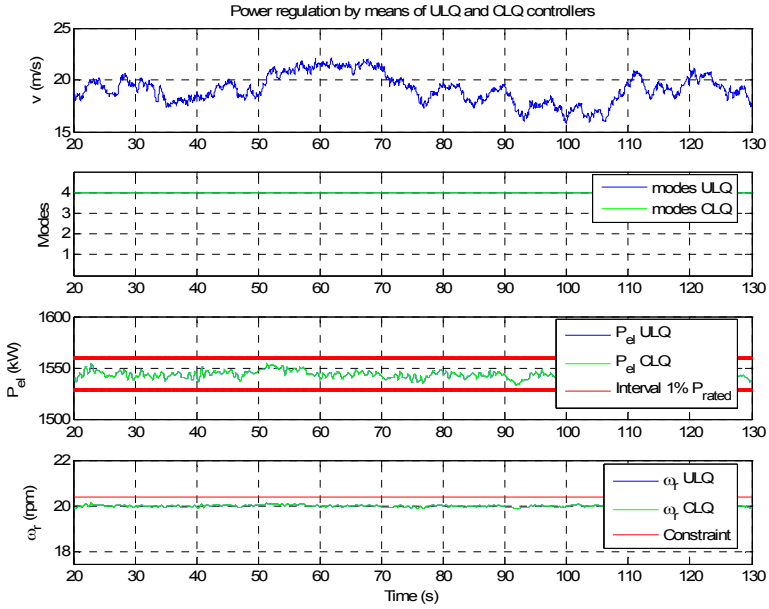

Figure 6.1 Response of the controller for power regulation at wind field #1

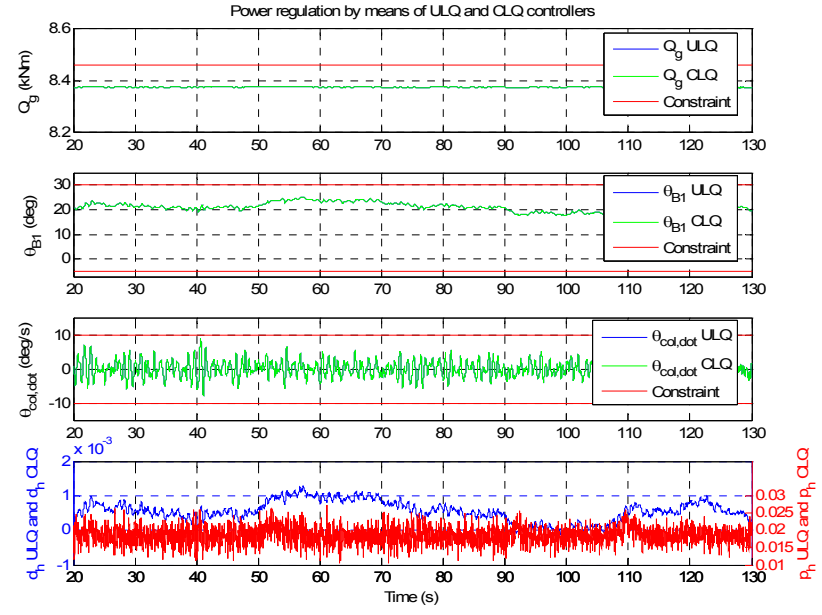

Figure 6.2 Response of the controller for power regulation at wind field #1

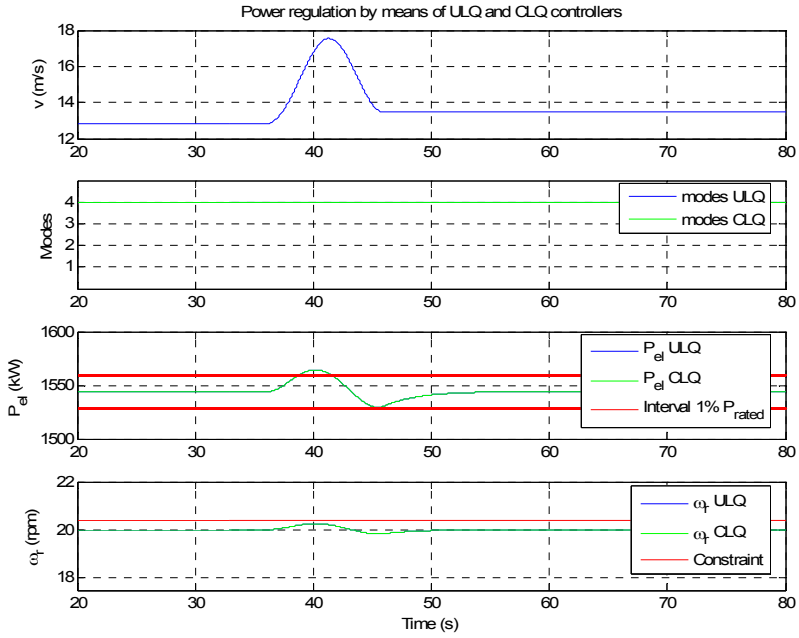

Figure 6.3 Response of the controller for power regulation at wind field #2

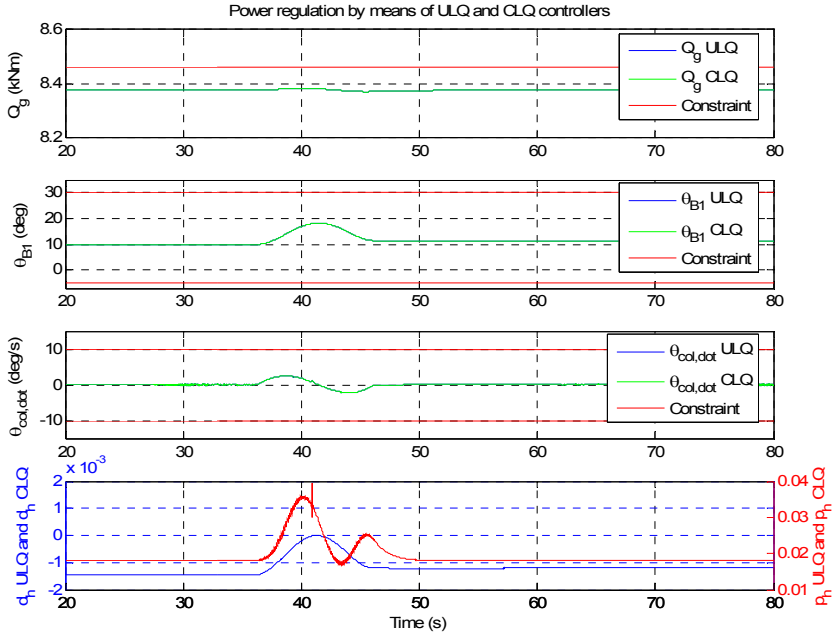

Figure 6.4 Response of the controller for power regulation at wind field #2

6.1.2 Analysis of the controller for power regulation with transition of modes

Unfortunately, some bug has been recently found in the controller for power regulation below rated wind speed. It has been observed that in mode III, torque and collective pitch act simultaneously (only torque should do). In the case of CLQ, due to the constraints in torque and collective pitch, it can still work acceptably well; however, in the case of ULQ, the transients are very severe, yielding extremely large dips in power and rotor speed.

Comparison between CLQ and ULQ should be appreciated when switching operation modes and their controllers. For large fluctuations of wind speed in the same mode, it has been observed that the constraints are always inactive, yielding to the same performance. Another way that has not been explored could be by defining very tight constraints.

6.2 Nomenclature of Part II

Symbol	Units	Variable
R	[m]	Length of the blades
r	[m]	Distance between the blade root and a certain station
ρ	[kg/m^3]	Air density
P_{el}	[kW]	Generated power
C_p	[-]	Power coefficient or Power efficiency
Q_g	[Nm]	Torque generator
λ	[-]	Tip speed ratio
	[-]	Eigenvalues of a model in state space formulation
v	[m/s]	Wind speed (for description of the operation modes)
ω_g	[rpm]	Generator speed
N_g	[-]	Gearbox ratio
ω_r	[rpm]	Rotor speed
θ_{Bi}	[deg]	Pitch angle
$\Delta\theta_{Bi}$	[deg]	Cyclic or Individual (not specified) component of the pitch angle
θ_{col}	[deg]	Collective component of the pitch angle
w_k	[-]	Augmented state noise
$w_{x,k}$	[-]	State noise
$w_{d,k}$	[-]	State disturbance noise
$w_{p,k}$	[-]	Output disturbance noise
v_k	[-]	Measurement noise
R_x	[-]	Variance of state noise
R_d	[-]	Variance of state disturbance noise
R_p	[-]	Variance of output disturbance noise
R_v	[-]	Variance of the controlled variables noise
$\bar{z}$	[kW,rpm]	Reference set point
K	[-]	LQR gain
L	[-]	Kalman filter gain

6.3 Bibliography of Part II

[1] T. Burton, D. Sharpe, N. Jenkins, E. Bossanyi. *Wind Energy Handbook*. Ed. Wiley 2001

[2] K. R. Muske, T. A. Badgwell. *Disturbance modeling for offset-free linear model predictive control*. Ed. Elsevier 2002

[3] G. Pannocchia, J. B. Rawlings. *Disturbance Models for Offset-Free Model-Predictive Control*. AIChE Journal 2003

[4] G. Pannocchia, N. Laachi, J. B. Rawlings. *A Candidate to Replace PID Control: SISO-Constrained LQ Control*. Ed. Wiley InterScience 2005

[5] E. Hendricks, O. Jannerup, P. H. Sørensen. *Linear systems control*. Ørsted·DTU 2005

[6] J. M. Jonkman, M. L. Buhl Jr. *FAST user's guide*. NREL 2005

[7] N. K. Poulsen. *Stochastic adaptive control*. 02421 Course notes 2006

[8] K. Hammerum. *A fatigue approach to wind turbine control (master thesis)*. IMM 2006

[9] A. J. Larsen, T. S. Mogensen. *Individuel pitchregulering af vindmølle (master thesis)*. IMM 2006

[10] J. M. Jonkman, M. L. Buhl Jr. *TurbSim user's guide*. NREL 2007

[11] L. C. Henriksen. *Model predictive control of a wind turbine (master thesis)*. IMM 2007

[12] N. K. Poulsen. *State space based MPC*. IMM 2007

Part III

Load Reduction

CHAPTER 7

Control for Load Reduction

The reduction of the loads has recently become an essential goal for the design of controllers, as the lifespan of the wind turbines can be extended.

In this chapter, two different controllers presented in reference [2] have been applied to the model in order to reduce the loads:

1. Cyclic pitch controller

2. Individual pitch controller

In order to do this, the manipulated variables are the individual components of the pitch angle:

$$u = \begin{bmatrix} \Delta\theta_{B1} \\ \Delta\theta_{B2} \\ \Delta\theta_{B3} \end{bmatrix} \tag{7.1}$$

On the other hand, only the reduction of the loads for wind speeds above rated has been considered. This is due to the fact that the current version of the power regulation controller for mode II described Chapter 4 does not take into account the cyclic/individual component of the pitch angle. Therefore,

different pitch angles from the collective component yield an inefficient power regulation.

Moreover, the loads at wind speeds below rated are less relevant, and in some cases, as it occurs in reference [2], it may become counterproductive, as loads get increased.

Chapter 7 has been structured as follows:

1. First, the cyclic pitch controller is presented

2. Next, the individual pitch controller has been described

3. Last, results regarding loads obtained by using both controllers with and without the power-regulation controller have been compared.

Remark: Throughout part III load reduction, the controller power regulation has been referred as just collective pitch controller for simplicity, with no loss of meaning.

7.1 Cyclic pitch controller

Cyclic pitch control is a modern method for reducing the loads in a wind turbine, originally developed for helicopters and recently adapted to wind turbines.

The cyclic pitch control is based on the measurement of the Yaw and Tilt moments in the rotor, which must be counteracted by means of a variation in the pitch angle of each blade.

As the term *cyclic* depicts, this contribution to the pitch angle varies sinusoidally, achieving the same values after 120º of rotor rotation.

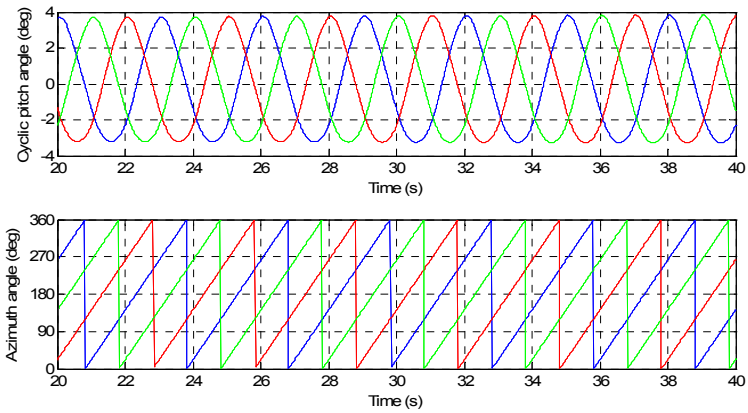

Figure 7.1 Example of Cyclic pitch angle Vs Azimuth angle

The cyclic pitch control is useful in skew inflow and/or large wind shears, yielding slow variations in yaw and tilt moments. In general, fast-varying loads cannot be reduced with this method because the response to a certain load in blades, tower or nacelle is not instantaneously measured.

7.1.1 Theoretical basis

The concept of cyclic pitch control yields the calculation of the necessary variation in the pitch angle to reduce the loads to some extent. The pitch angle of the i-th blade when using a cyclic pitch controller can be expressed as:

$$\theta_{Bi} = \theta_{collective} + \Delta\theta_{cyclic,Bi} \tag{7.2}$$

The term $\Delta\theta_{cyclic,Bi}$ is calculated as a composition of the amplitudes $\Delta\theta_y$ and $\Delta\theta_z$ in top and side rotor position, in other words, 90º and 0º, and therefore associated directly to the Yaw and Tilt moments, respectively:

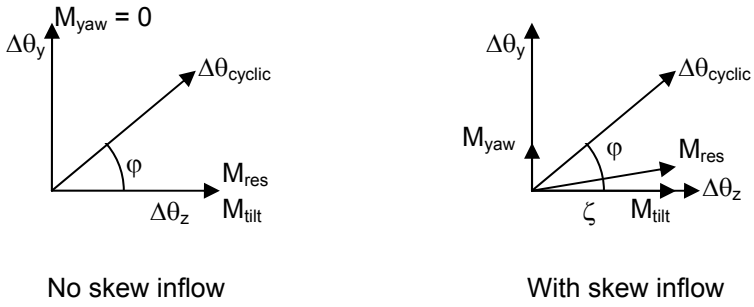

Figure 7.2 Diagram of the relationship between cyclic amplitudes $\Delta\theta_y$ and $\Delta\theta_z$, and Yaw and Tilt moments

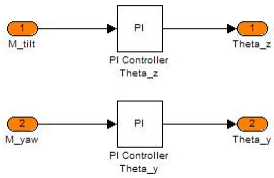

Figure 7.3 Diagram of the PI actions of the cyclic pitch controller

7.1.2 Discussion of the Phase shift angle

When no skew inflow or wind shear is considered, these amplitudes are expressed as follows:

$$\Delta\theta_{cyclic,Bi} = \Delta\theta_y \cdot \sin(\varphi_{Bi}) + \Delta\theta_z \cdot \cos(\varphi_{Bi}) \tag{7.3}$$

However, when skew inflow or wind shear is introduced, it is well known that the distribution of the loads varies, so that the Yaw moment has a mean value away from 0. In this case thus, the resulting moment in the rotor is not equal to the Tilt moment.

This can barely be appreciated due to the fact that the Yaw moment is still small compared to the Tilt moment, and thus the variation in the resulting moment is not large, so it has been carried out a zoom in.

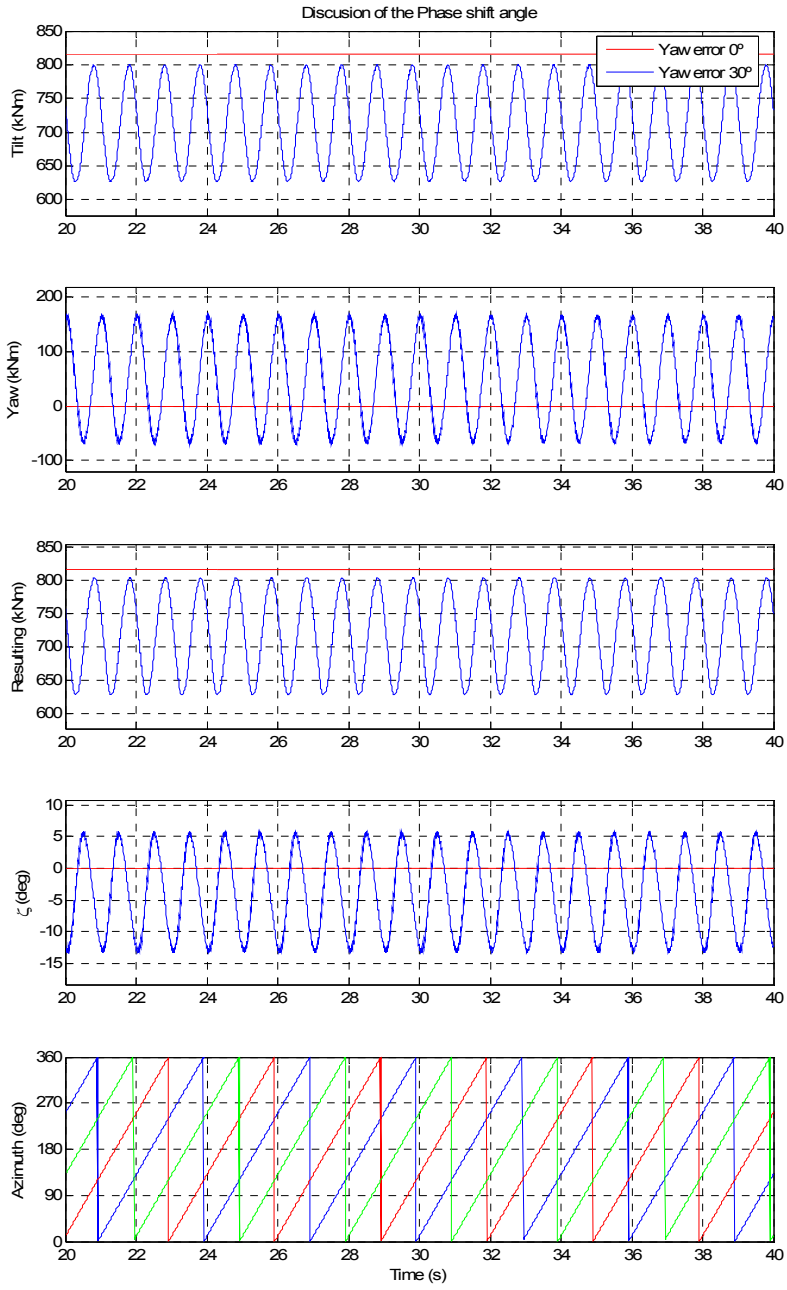

Figure 7.4 Discussion of the Phase shift angle in the case of a WTG with just a controller for power regulation, subjected to a Wind speed of 25m/s and different Yaw angles

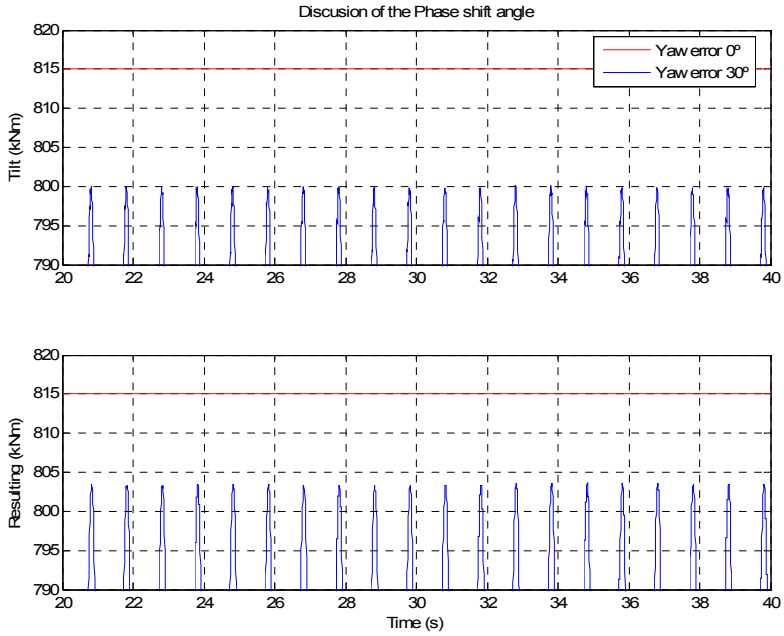

Figure 7.5 Zoom in Tilt and Resulting moment for discussion of the Phase shift angle

Therefore, the phase angle of the resulting moment (ζ) has to be taken into account in order to make sure the PI action on Yaw and Tilt moments yield independently $\Delta\theta_y$ and $\Delta\theta_z$, respectively.

$$\Delta\theta_{cyclic,Bi} = \Delta\theta_y \cdot \sin(\varphi_{Bi} + \zeta) + \Delta\theta_z \cdot \cos(\varphi_{Bi} + \zeta) \tag{7.4}$$

7.1.3 Implementation

Figure 7.6 depicts how the cyclic pitch controller has been implemented in Simulink.

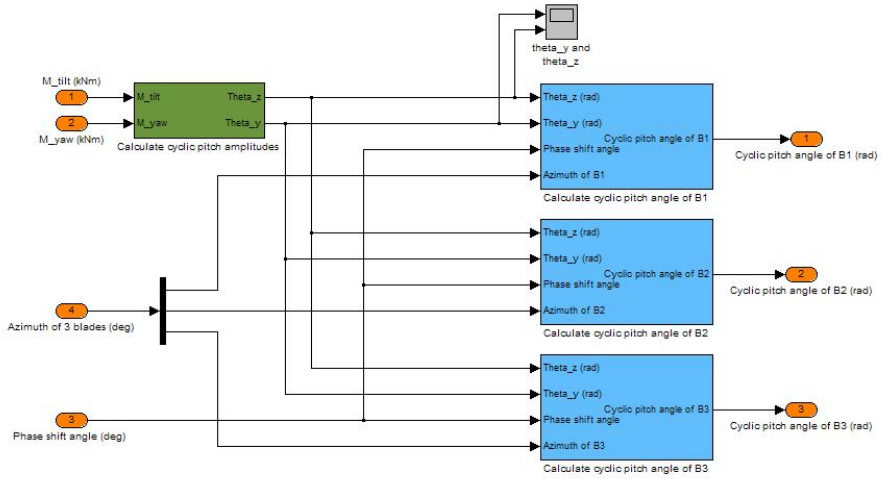

Figure 7.6 Implementation of the cyclic pitch controller

Yaw and Tilt moments have been obtained directly from FAST for convenience. However, it can also be derived either from the Flapwise and Edgewise moments (pitching frame) or the Out-of-plane moments (non-pitching frame) at the root of the 3 blades.

In this case, Hub Yaw and Tilt moments have been used, but it could have been done with the Tower top ones with no loss of meaning. It is important to remark that the coordinate system must not rotate with azimuth.

Another important point to remark is that the resulting moment from Yaw and Tilt moments must be located within the 1st and 4th quadrants, in other words:

$$\zeta \in \left[-\frac{\pi}{2}, \frac{\pi}{2} \right] \tag{7.5}$$

Therefore, depending on the sign criterion of the coordinate system, it may be necessary to change the sign of a certain moment.

7.1.3.1 Tuning the PI controllers of the cyclic pitch controller

The K_p parameters have been tuned based on a estimation of the pitch amplitude at top and side azimuth position, and the moments obtained from simulations using only the power-regulation controller.

Regarding the tuning of the K_i parameters, the system has experienced a high sensitivity. Therefore, the procedure to find the optimal K_i has been based on trial and error. The maximum value of K_i that keeps the system stable has been selected.

K_p will adjust the amplitude of the pitch angle in top and side positions, whereas K_i will approach the mean values of the Yaw and Tilt moments to zero.

7.2 Individual pitch controller

The individual pitch controller is based on the rotor flow measurements by means of a pitot tube located at a distance around 0.75 of the blade length, measured from the root.

Unfortunately, the computation of the angle of attack and the relative velocity is not available on-line while FAST is running, but *a posteriori*. Instead, the unsteady BEM code developed in Chapter 3. This fact involves a number of drawbacks:

1. Although the agreement observed is reasonably good, a small delay between them seems to exist, yielding pitch actions deviated from the right time.

2. Turbulent wind fields are not suitable, as the current version of the unsteady BEM code is prepared only for deterministic models, where the wind speed at every pitot tube is calculated by means of the hub-height wind speed, and its position.

A possible solution that has not been explored is to modify the source code of FAST in order to obtain flow measurements during the simulation.

Unlike the cyclic pitch controller, individual pitch controller is suitable for reducing the loads in fast-varying wind conditions, as they are not measured directly (with its corresponding delay), but estimated by the AOA and relative velocity. This yields a very promising load reduction.

On the other hand, the individual pitch controller implies some drawbacks compared to the cyclic one:

1. Extremely fast response of the actuator so that the pitch angle can be varied with as little delay as possible to the variation in flow measurements.

2. The pitot tube for measuring the angle of attack and relative velocity is located at a certain point of the blade, but it is not necessarily representative of the rest of the blade.

At the time of writing this report, this controller does not work out properly; compared to the cyclic pitch controller, individual pitch action is not carried out at the right time.

7.2.1 Theoretical basis

As stated previously, the individual pitch controller is based on the correlation between loads and flow measurements. Figure 7.7 depicts the reliability of this assumption.

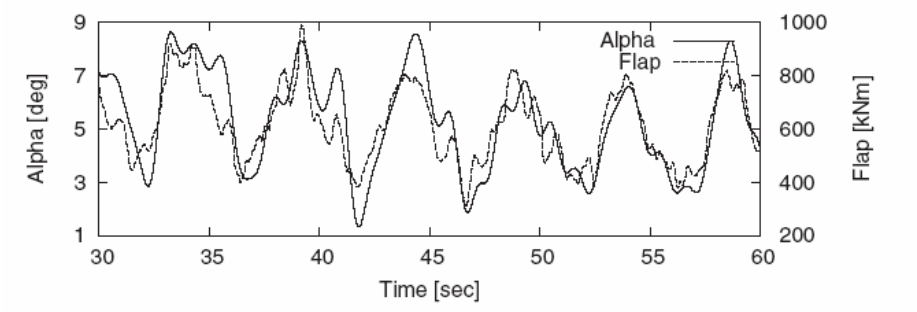

Figure 7.7 High correlation observed between AOA and the Flapwise moment Plot obtained from reference [2]

The pitch angle of the i-th blade when using an individual pitch controller can be expressed as:

$$\theta_{Bi} = \theta_{collective} + \Delta\theta_{individual,Bi} \tag{7.6}$$

The principle of the individual pitch controller is to carry out independent actions based on the angle of attack and the relative velocity, so that the term $\Delta\theta_{individual,Bi}$ is calculated as:

$$\Delta\theta_{individual,Bi} = \Delta\theta^{a}_{individual,Bi}(AOA) + \Delta\theta^{b}_{individual,Bi}(V_{rel}) \tag{7.7}$$

These two complementary actions deal with different source of varying loads:

1. Action based on angle of attack deals with any source of varying loads except the ones derived from skew inflow, such as wind shears or turbulences in wind field

2. Action based on the relative velocity counteracts the skew inflow (slow-varying loads), yielding relatively similar results as for the cyclic pitch controller

7.2.1.1 Action based on measurements of the angle of attack

The action based on angles of attack intends to minimize the difference between the AOA at each blade regarding the average one. Under these circumstances, the loads on the rotor are auto-balanced.

In this work, this controller has been implemented as a PI-controller that derives the individual component from the error between the angle of attack at each blade and the average one.

$$\Delta\theta^{a}_{individual,Bi}(AOA) = PI\left(AOA_{Bi} - AOA_{average}\right) \tag{7.8}$$

It is strongly recommended, though, to achieve a state space formulation of this problem, so that the minimization of the error between the angle of attack of each blade and the average one can be formulated as a cost function.

7.2.1.2 Action based on measurements of the relative velocity

In this case, a model-based feedforward control loop has been used:

$$\Delta\theta^{b}_{individual,Bi}(V_{rel}) = \left(V_{rel,Bi} - V_{rel,average}\right)\cdot K\left(\omega_r, \theta_{col}\right) \tag{7.9}$$

The gain function K is formulated in a different way depending essentially whether the wind speed is below (*low wind speed*) or above rated (*high wind speed*). However due to robustness issues, the rotor speed has been used as an estimator of the wind speed below rated, and the collective pitch angle above rated.

Moreover, during the transition between low wind speed and high wind speed, exactly when $\omega_r > 0.95 \cdot \omega_{r,rated}$, the gain function has been set to 0.

$$K\left(\omega_r, \theta_{col}\right) = \begin{cases} K_0 & , \ \omega_r \le \omega_{r,rated} \quad and \quad \theta_{col} \le \theta_0 \\ 0 & , \ \omega_r > \omega_{r,rated} \quad and \quad \theta_{col} \le \theta_0 \\ \beta \cdot \left(\theta_{col} - \theta_0\right), & \theta_{col} > \theta_0 \end{cases} \tag{7.10}$$

Where:

- K_0 is the gain at $\omega_r = \omega_{r,rated}$
- θ_0 is the collective pitch angle at which the gain function K = 0
- β is the slope of the linear regression in figure 7.12

In order to tune the gain function K, the cyclic pitch controller described in section 7.1 has been used, due to their good agreement.

7.2.2 Implementation

The implementation of the individual pitch controller has been depicted in figure 7.8:

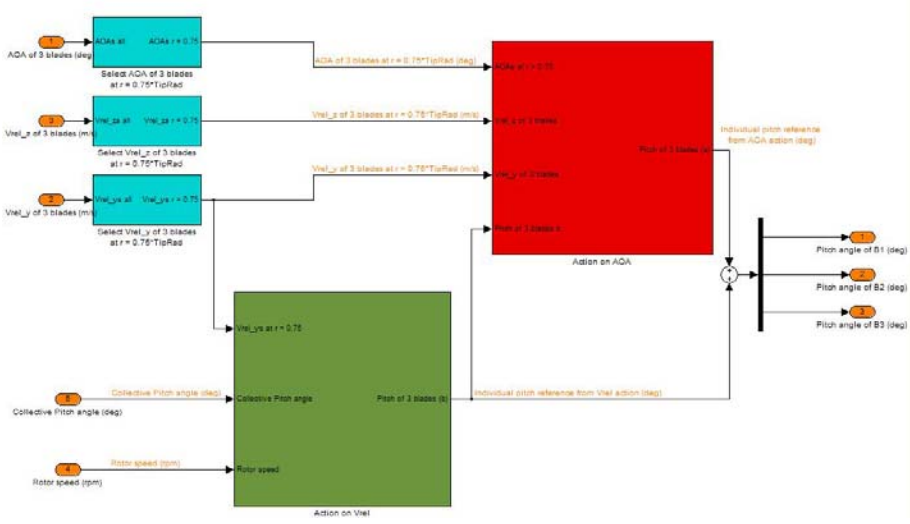

Figure 7.8 Implementation of the individual pitch controller

7.2.2.1 Implementation of the action based on the angle of attack

The implementation of the action based on AOA of the individual pitch controller has been depicted in figure 7.9:

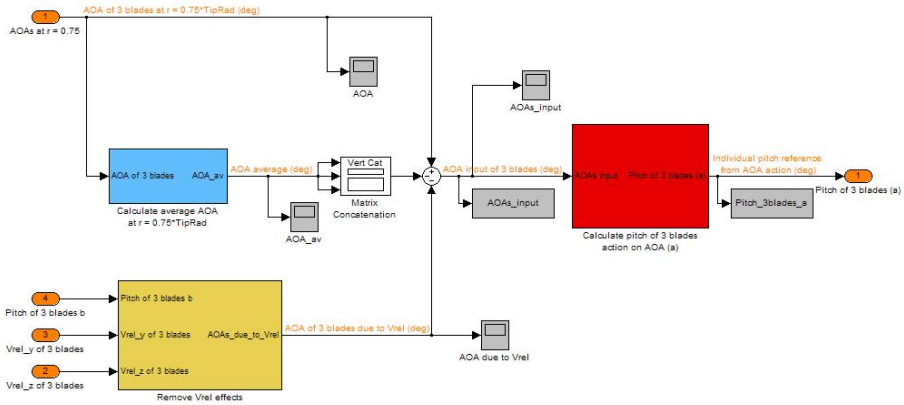

Figure 7.9 Implementation of the action based on AOA

In practice, the action on the relative velocity would have a certain influence on the action on the angle of attack if no corrections are carried out. The nature of this influence is:

1. Variations in the in-plane relative velocity ($V_{rel,y}$)
2. The component itself from the relative velocity, $\Delta\theta^{b}_{individual,Bi}(V_{rel})$

The variation in AOA due to changes in the in-plane relative velocity is quantified by means of:

$$AOA\left(V_{rel,y}\right) = \arctan\left(\frac{V_{rel,z,average}}{V_{rel,y}}\right) - \phi_{average} \tag{7.11}$$

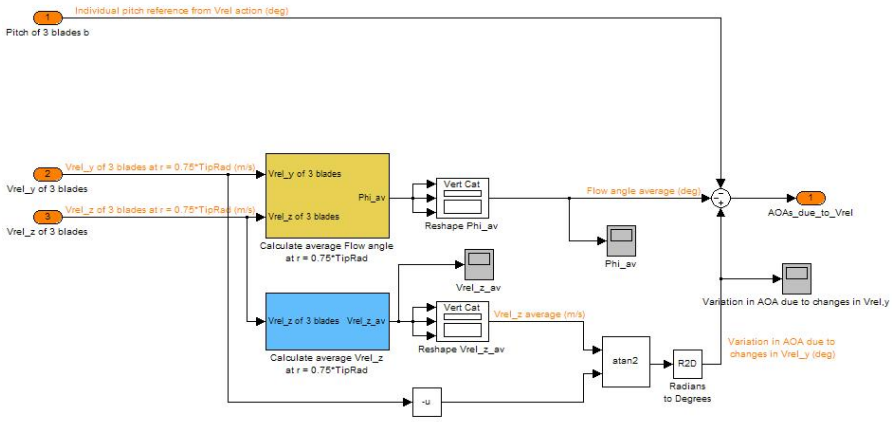

Figure 7.10 Rejection of the influence from the relative velocity

The corrected AOA_{input} is therefore calculated as:

$$AOA_{input} = AOA_{Bi} - AOA_{average} - \left[AOA\left(V_{rel,y}\right) - \Delta\theta^{b}_{individual,Bi}\left(V_{rel}\right) \right] \qquad (7.12)$$

7.2.2.2 Implementation of the action based on the relative velocity

The implementation of the action based on V_{rel} of the individual pitch controller has been depicted in figure 7.11:

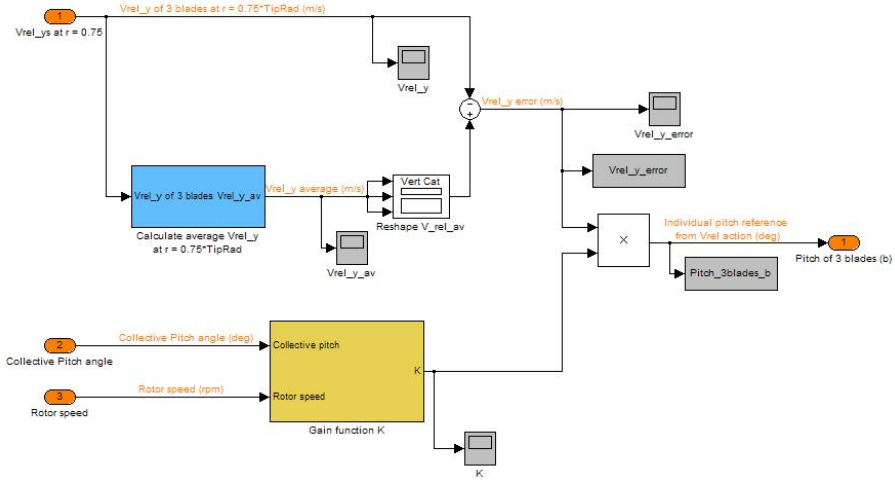

Figure 7.11 Implementation of the action based on V_{rel}

As the individual pitch controller has only been used for high wind speeds:

$$K\left(\omega_r, \theta_{col}\right) = \beta \cdot \left(\theta_{col} - \theta_0\right) \tag{7.13}$$

The parameters and have been calculated based on the curve depicted in figure 7.12, yielding:

θ_0	β
18.125°	0.01875 $(m/s)^{-1}$

Table 7.1 Parameters of the gain function K

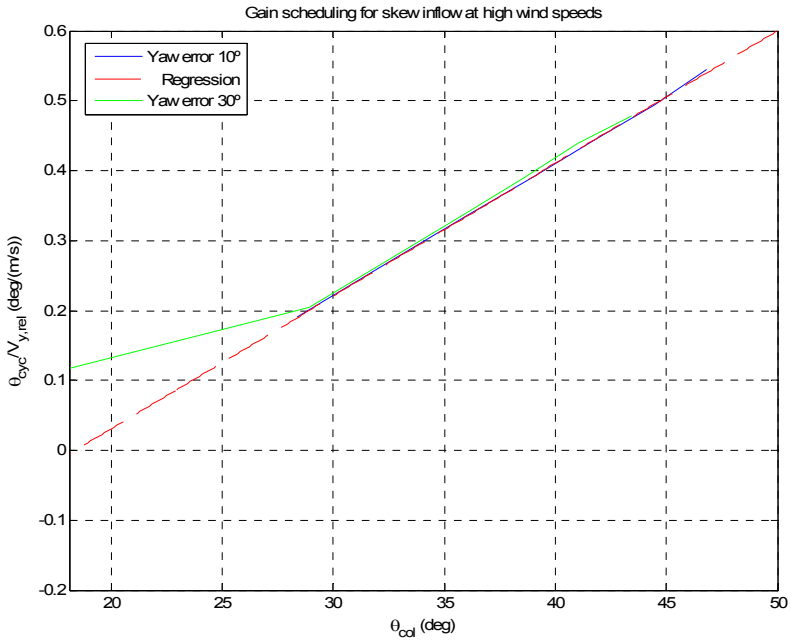

Figure 7.12 Gain scheduling for the gain function K at wind speed over rated

When using the power-regulation controller in combination with the either cyclic or individual pitch controller, the collective pitch angle needs to be varied to take into account the latter components. Therefore, in general it achieves larger values than when using just the power-regulation controller. That is the reason why figure 7.12 is defined for high values of the collective pitch angle. Note also that this is not the overall pitch angle, but just the collective component; otherwise, it would not make sense from the point of view of aerodynamics.

7.3 Comparison of controllers

Last, a comparison between the collective and the cyclic pitch controllers have been carried out. The individual pitch controller should be included here, but at the time of writing the report it does not work out well.

Different scenarios have been designed for carrying out this comparison:

1. Constant wind speed = 25m/s, Yaw error = 30º
2. Constant wind speed = 25m/s, Yaw error = 30º and Wind shear
3. Wind field #5

Wind field #5 is turbulent with a mean hub-height wind speed of 18.2 m/s, an IEC 61400-1 Ed. 3: 2005 class 1B, and an IEC Kaimal spectral model.

7.3.1 Plots of some results

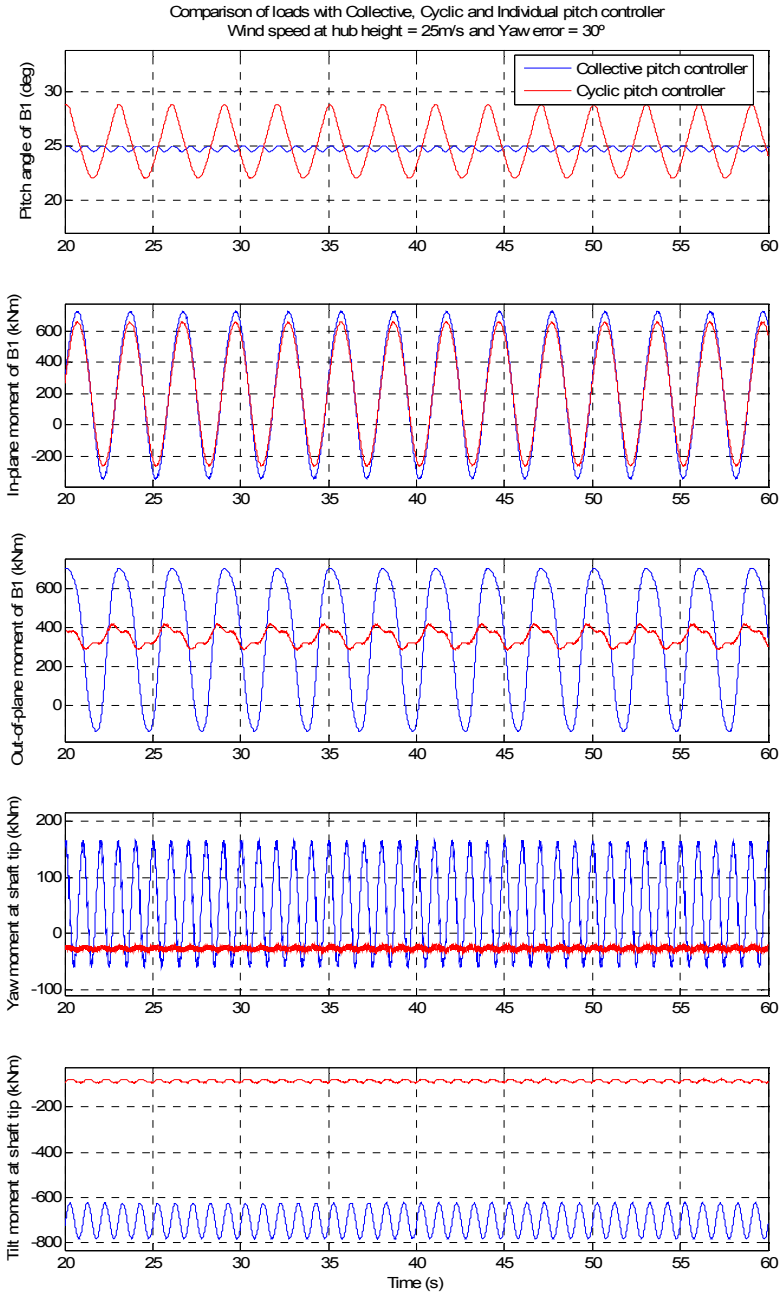

Figure 7.13 Constant wind speed 25m/s, Yaw error 30°

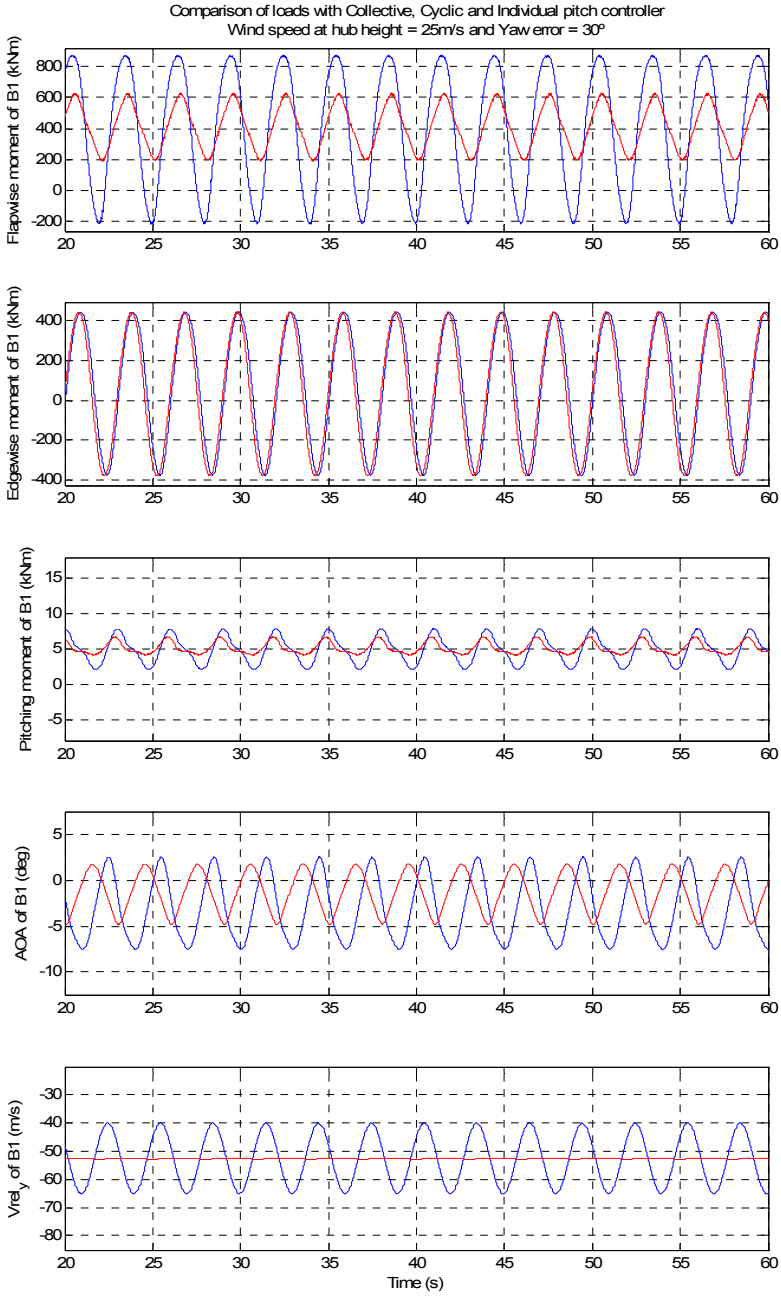

Figure 7.14 Constant wind speed 25m/s, Yaw error 30°

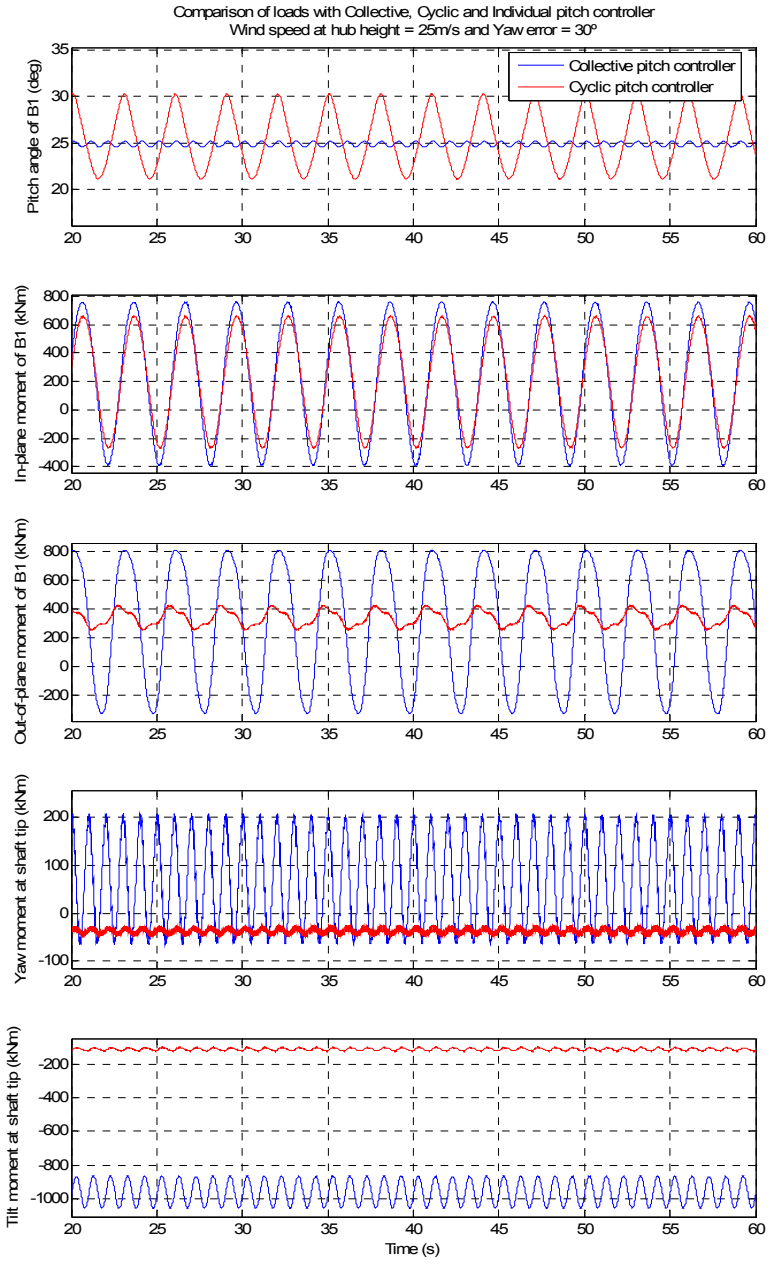

Figure 7.15 Constant wind speed 25m/s, Yaw error 30°, Wind shear with $\nu = 0.2$

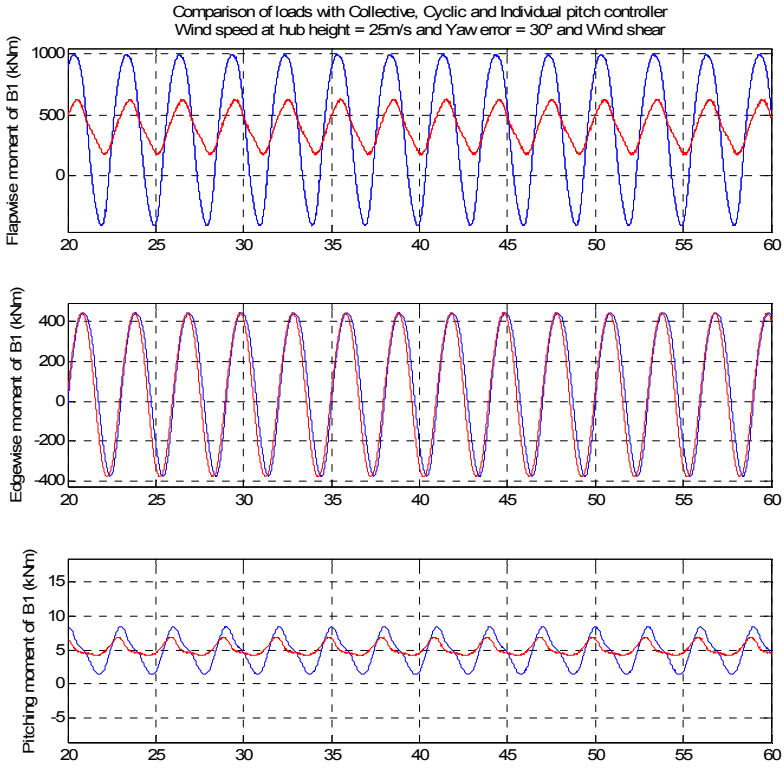

Figure 7.16 Constant wind speed 25m/s, Yaw error 30º, Wind shear with $\nu = 0.2$

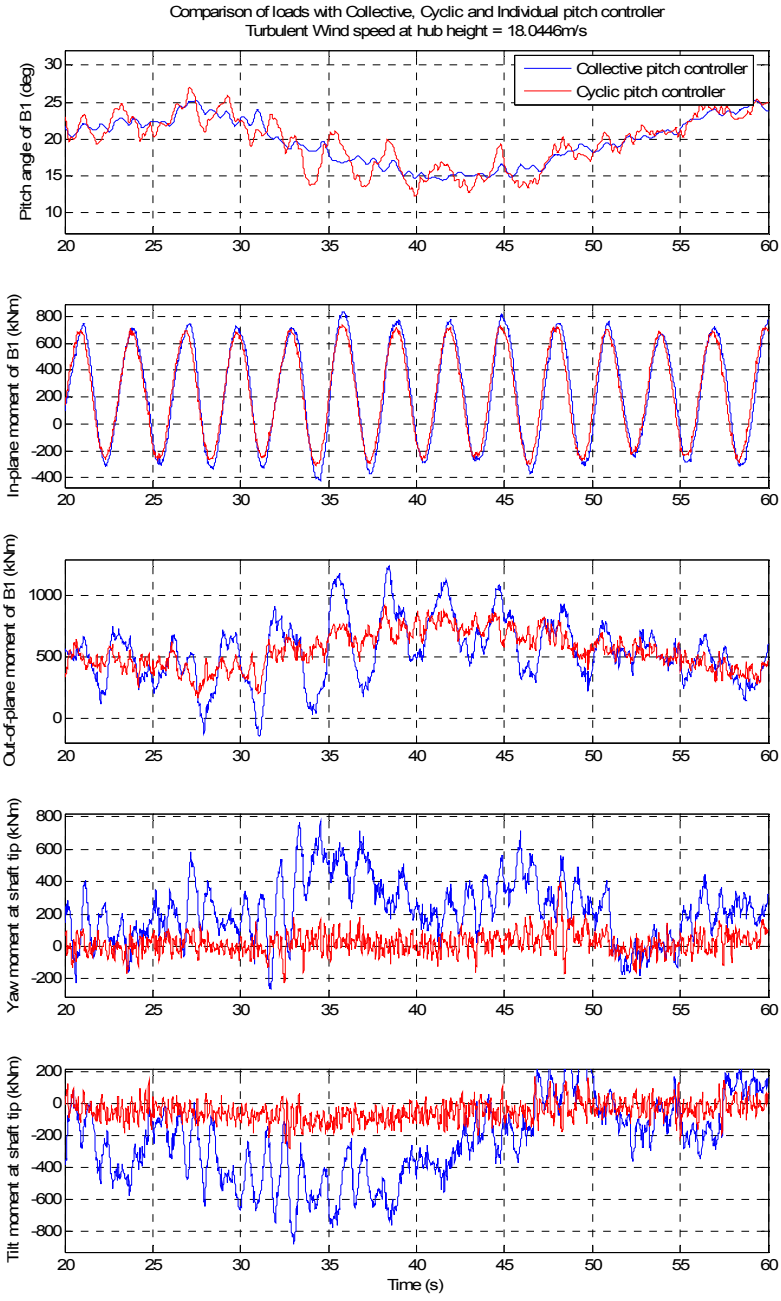

Figure 7.17 Wind field #5

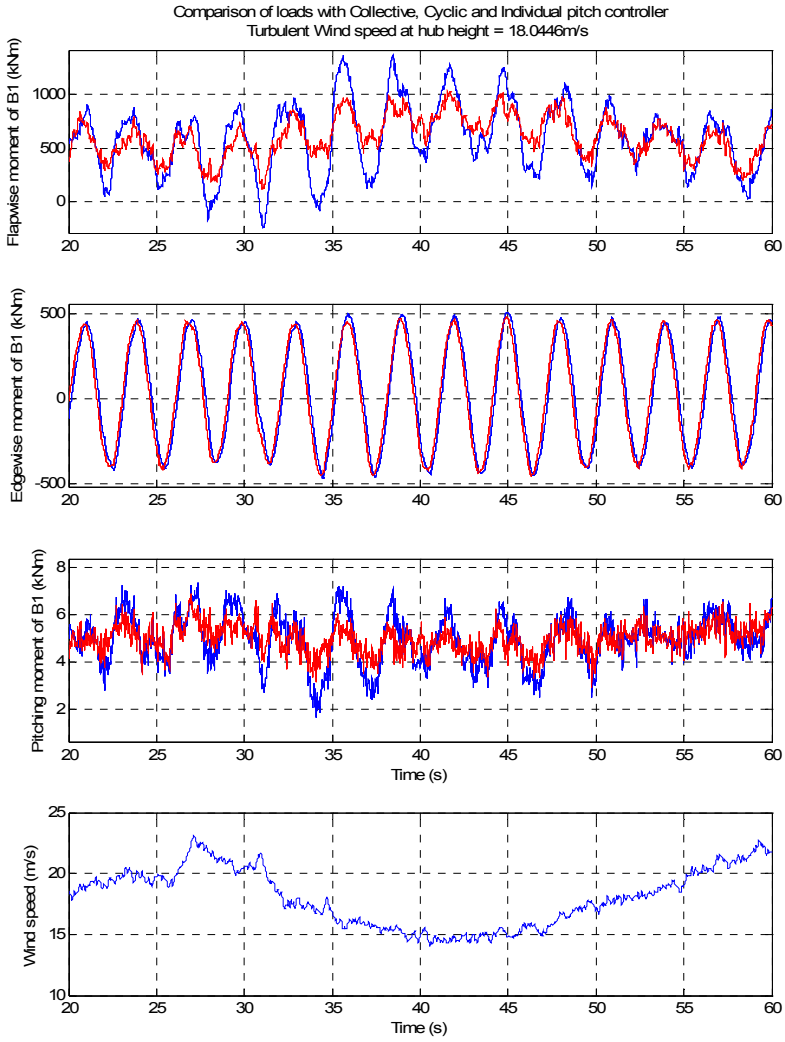

Figure 7.18 Wind field #5

7.3.2 Analysis of variance

Previous plots depict a great benefit when using the cyclic pitch controller in all three scenarios. For quantifying this advantage in terms of the amplitude of the loads, an analysis of variance has been carried out.

A fatigue analysis would be desirable for a sense of completion, but it has been discarded due to the constraining time.

Different loads have been selected from the measurements available from the FAST model.

Scenario 1

Moments (kNm)	Variances	
	Collective pitch controller	Cyclic pitch controller
Tower top Yaw moment	7721.1	87.193
Tower top Tilt moment	3802	148.79
Hub Yaw moment	5861.2	14.946
Hub Tilt moment	3246.4	24.905
Out-of-plane moment	96411	1544
In-plane moment	1.423e+5	1.0637e+5
Pitching moment	3.4643	0.64703
Flapwise moment	1.5286e+5	20042
Edgewise moment	85835	86168

Table 7.2 Analysis of variance for scenario 1

Scenario 2

Moments	Variances	
	Collective pitch controller	Cyclic pitch controller
Tower top Yaw moment	10906	110.36
Tower top Tilt moment	5356.9	212.44
Hub Yaw moment	8298.1	34.892
Hub Tilt moment	4585.2	50.862
Out-of-plane moment	1.7786e+5	2796.5
In-plane moment	1.648e+5	1.0706e+5
Pitching moment	5.26	0.74572
Flapwise moment	2.5738e+5	21863
Edgewise moment	85256	85798

Table 7.3 Analysis of variance for scenario 2

Scenario 3

Moments (kNm)	Variances	
	Collective pitch controller	Cyclic pitch controller
Tower top Yaw moment	35676	3973.1
Tower top Tilt moment	61868	4291.8
Hub Yaw moment	34542	4084
Hub Tilt moment	61630	3591.9
Out-of-plane moment	62492	22723
In-plane moment	1.3922e+5	1.1519e+5
Pitching moment	1.0412	0.31142
Flapwise moment	1.0283e+5	36191
Edgewise moment	96502	94156

Table 7.4 Analysis of variance for scenario 3

The reduction of the amplitude of the loads expressed in terms of the variance is depicted in table 7.5. The results must not be understood as a reduction of the load itself, as it would be necessary to carry out an analysis of fatigue and calculate the 1Hz equivalent loads.

Moments (kNm)	Reduction of variance (%)		
	Scenario 1	Scenario 2	Scenario 3
Tower top Yaw moment	98.871	98.988	88.863
Tower top Tilt moment	96.087	96.034	93.063
Hub Yaw moment	99.745	99.580	88.177
Hub Tilt moment	99.233	98.891	94.172
Out-of-plane moment	98.399	98.428	63.639
In-plane moment	25.249	35.036	17.260
Pitching moment	81.323	85.823	70.090
Flapwise moment	86.889	91.506	64.805
Edgewise moment	-0.388	-0.636	2.431

Table 7.5 Summary of the analysis of variance for all the scenarios

Remark: Both the plots and the analysis of variance show a relevant reduction of the loads except for the In-plane and Edgewise moments. The reason is that the load reduction is focused on the Out-of-plane moments, which are the ones which originate the Yaw and Tilt moments. In-plane moments are just out of the scope.

7.4 Nomenclature of Part III

Symbol	Units	Variable
H	[m]	Hub height of the wind turbine
R	[m]	Length of the blades
r	[m]	Distance between the blade root and a certain station
c	[m]	Chord of the airfoil
ρ	[kg/m^3]	Air density
ν	[-]	Wind shear exponent
ω_r	[rpm]	Rotor speed
φ_r	[deg]	Rotor azimuth angle
φ_{Bi}	[deg]	Azimuth angle of the i-th blade
ψ	[deg]	Yaw angle
γ	[deg]	Tilt angle
ζ	[deg]	Phase shift angle
θ_{Bi}	[deg]	Pitch angle
$\Delta\theta_{Bi}$	[deg]	Cyclic or Individual (not specified) component of the pitch angle
$\Delta\theta_{cyclic,Bi}$	[deg]	Cyclic component of the pitch angle
$\Delta\theta_y$	[deg]	Cyclic component of the pitch angle in top position
$\Delta\theta_z$	[deg]	Cyclic component of the pitch angle in side position
$\Delta\theta_{individual,Bi}$	[deg]	Individual component of the pitch angle
θ_{col}	[deg]	Collective component of the pitch angle
K	[deg/(m/s)]	Gain function of action based on V_{rel}
β_{Bi}	[deg]	Local blade station pitch angle
		Slope of linear regression in figure 7.12
θ_0		Collective pitch angle at which K = 0
δ_{Bi}	[deg]	Cone angle of the blade
ϕ_{Bi}	[deg]	Flow angle
$\phi_{average}$	[deg]	Average flow angle of 3 blades
α, AOA	[deg]	Angle of attack
$AOA_{average}$	[deg]	Average angle of attack of 3 blades
χ	[deg]	Skew angle
L	[N]	Lift force
D	[N]	Drag force
C_l	[-]	Lift coefficient
C_d	[-]	Drag coefficient
V_{wind}, V_0, U_∞	[m/s]	Undisturbed wind speed
V'	[m/s]	Wind speed in the wake
V_{rel}	[m/s]	Relative velocity seen by blade
$V_{rel,y}$	[m/s]	In-plane component of the relative velocity
$V_{rel,z}$	[m/s]	Out-of-plane component of the relative velocity
V_{rot}	[m/s]	Velocity component due to the azimuth rotation
W	[m/s]	Induced velocity
a	[-]	Axial (normal) induction factor
a'	[-]	Tangential induction factor
fg	[-]	Glauert's correction factor
F	[-]	Prandtl's tip loss factor
τ_g	[s]	Time constant of the generator model
ξ	[-]	Damping ratio of the pitch actuator
ω_n	[rad/s]	Natural frequency of the pitch actuator

7.5 Bibliography of Part III

[1] T. Burton, D. Sharpe, N. Jenkins, E. Bossanyi. *Wind Energy Handbook*. Ed. Wiley 2001

[2] T. J. Larsen, H. A. Madsen, K. Thomsen. *Active Load Reduction Using Individual Pitch, Based on Local Blade Flow Measurements*. Wind Energy 2005; 8: 67 – 80

Part IV

Conclusions and Perspectives

CHAPTER 8

Conclusions

8.1 Modelling

In Chapter 2, the FAST model of the variable-speed wind turbine has been presented, describing its behaviour for a given wind speed, by introducing the concepts of operation modes and power efficiency (C_p).

Next, a linear model for the wind turbine has been derived by means of the linearization FAST tool, and expressed as a state space. Moreover, a model for the generator and pitch actuator has been included for more accuracy.

In Chapter 3, an unsteady BEM code has been developed in order to determine the C_p-curve which defines the parameters for maximizing the generated power below rated wind speed in Chapter 2. Moreover, this BEM code is also used for generating the flow measurements necessary for the Individual pitch controller in Chapter 7.

It has been compared to the aerodynamic model used by FAST-AeroDyn, which is based on the classical (steady) BEM code as well. A good agreement between both formulations has been achieved, which is essential regarding the Individual pitch controller, as the aerodynamic model used by FAST-AeroDyn cannot be computed online.

However, the codes include different corrections for the steady BEM code, so it has been recommended to evaluate their influence in order to remove the small existing discrepancy.

8.2 Power regulation

In Chapter 4, the control objectives for power regulation have been defined based on the specification of the operation modes described in Chapter 2.

Moreover it has been designed the strategy for switching among them according to the wind speed, and therefore, the available power. At this point, it has been argued the switching criteria must be based on the measurements of the rotor speed and generated power rather than the wind speed itself, as the inertia of the wind turbine involve a certain time response. Unfortunately some error has been found in the implementation of the control objectives for operation modes I and III, so the performance of the mode switch has not been evaluated, although it seemed to work out fine in previous thesis.

In Chapter 5, the theory of the MPC control has been introduced, which is used for the controllers of modes I, III and IV. It has been proved MPC controllers are an excellent method for rejecting unmeasured disturbances in order to keep the states of the wind turbine at the set point. For high wind speeds in a turbulent wind field the controller is able to keep the power at its rated value.

MPC controllers are composed of 3 modules: state and disturbance estimator, target calculation and dynamic optimization. Two different implementations have been considered: unconstrained and constrained target calculations, so that the physical limitations of the wind turbine components are taken into account in the latter case. Good performance has been observed in both cases. Moreover, the setup is ready for including further constraints.

8.3 Load reduction

Chapter 7 deals with the design of a controller for reducing the loads. Two methods are proposed by varying individually the pitch angle of the blades: Cyclic and Individual pitch control.

The cyclic pitch control is based on the measurement of the Yaw and Tilt moments in the rotor, which must be counteracted by means of a variation in

the pitch angle of each blade. It is designed for alleviating slow-varying loads, as their measurement involves some delay until the effective action is carried out. However, it provided a significant reduction in the amplitude of the loads even for a turbulent wind field.

The Individual pitch control seems to be a very promising method, as it measures the inflow for estimation of the loads, so that they can be alleviated before they actually occur. Therefore, it is suitable for fast-varying loads. Unfortunately, at the time of writing this report it has not been able to be evaluated due to some bug.

CHAPTER 9

Perspectives

The interest of this project is not only the results obtained until the time of writing the report, but perhaps even more the wide range of possibilities that can derived from this setup.

In this chapter several issues which could be implemented in short term have been described.

9.1 Modelling

Regarding the modelling improvements, first step should be orientated to consider the elasticity of the components of the wind turbine, currently stiff, especially the blades in flap and edgewise, and tower in both fore-aft and side-to-side directions. Moreover, the torsion of the drivetrain is recommended as well.

Next, the unsteady BEM code described in Chapter 3 should be modified in order to deal with a turbulent wind field, rather than deterministic. In this case, it will be profitable for realistic simulations with the Individual pitch controller for load reduction. Last, after an analysis of the effect derived from having different implementations of the unsteady BEM code and the aerodynamic model used by FAST-AeroDyn, it might be necessary to change some correction.

9.2 Power regulation

First, the dynamic optimization problem may be updated in terms of considering constraints and a receding horizon.

On the other hand, more complex implementations of the MPC controller might also be investigated, such a robust MPC, and possibly a non-linear one.

9.3 Load reduction

A new implementation of the load reduction problem is the most promising part of the future work. By obtaining a state space description of it, the power regulation and the load reduction problems would be integrated as a single MPC controller, yielding a common target calculation and an optimization problem. Then, constraints for both problems would be considered simultaneously. On the other hand, a common cost function would make possible to tune the priority of each problem, and what is more important, to minimize analytically the loads.

Finally, if offset-free control is not possible in case some constraints cannot be satisfied, at least with this method the offset would be minimized. In terms of load reductions, this means the minimal loads possible for a given wind turbine and wind field.

Moreover, different studies, that have not been possible for this work due to the lack of time, should be carried out.

First, 20-year fatigue loads should be calculated in order to analyze the benefit of implementing the current or future versions of the Cyclic and Individual pitch controllers, as the analysis of variance is too simple. Once the damage in different components of the wind turbine after 20 years has been estimated, it is possible to calculate the comparative extension of its lifespan. For a given power demand to be covered by wind energy, if old wind turbines can work for longer time, less new ones are necessary, yielding a significant reduction of costs.

Last, it would be interesting a feasibility study taking into account on the one hand the cost of setting the pitot tube and upgrading the measurement setup, and on the other hand the benefits derived from the increase of produced power as a result of a longer-lasting wind turbine.

APPENDIX A

FAST INPUT FILES

A.1 Airfoils

cylinder.dat

```
   Round Root Section
   1      Number of airfoil tables in this file
   0.0    Table ID parameter
  14.0    Stall angle (deg)
   0.0    No longer used, enter zero
   0.0    No longer used, enter zero
   0.0    No longer used, enter zero
   0.0    Zero lift angle of attack (deg)
   0.0    Cn slope for zero lift (dimensionless)
   0.0    Cn at stall value for positive angle of attack
   0.0    Cn at stall value for negative angle of attack
   0.0    Angle of attack for minimum CD (deg)
   1.0    Minimum CD value

      AOA        Cl        Cd        Cm
   -180.0       0.0       0.5       0.0
      0.0       0.0       0.5       0.0
    180.0       0.0       0.5       0.0
```

s818_2703.dat

```
Re=4,000,000 (windward modified the flat Cl section near stall)
FROM Dayton Griffin, sept28 '00, post stall blended with flat plate.
Foilchcked by Windward on 10-Oct-2000 at 10:23.

     1          Number of airfoil tables in this file
     0.00       Table ID parameter
    12.50       Stall angle (deg)
     0.00       No longer used, enter zero
     0.00       No longer used, enter zero
     0.00       No longer used, enter zero
    -5.31       Zero lift angle of attack (deg)
     6.10840    Cn slope for zero lift (dimensionless)
     1.9560     Cn at stall value for positive angle of attack
    -0.8000     Cn at stall value for negative angle of attack
    -4.5000     Angle of attack for minimum CD (deg)
     0.0082     Minimum CD value
```

AOA	Cl	Cd	AOA	Cl	Cd
-180.00	-0.170	0.0200	4.00	0.990	0.0096
-170.00	0.640	0.0500	5.00	1.100	0.0099
-160.00	0.840	0.3100	6.00	1.200	0.0103
-150.00	1.080	0.6200	7.00	1.310	0.0108
-140.00	1.150	0.9600	8.00	1.410	0.0113
-130.00	1.090	13.000	9.00	1.510	0.0118
-120.00	0.880	15.200	10.00	1.560	0.0194
-110.00	0.600	16.600	11.00	1.610	0.0221
-100.00	0.310	17.600	12.00	1.650	0.0245
-90.00	0.000	18.000	13.00	1.650	0.0269
-80.00	-0.310	17.600	14.00	1.630	0.0296
-70.00	-0.600	16.600	15.00	1.620	0.0520
-60.00	-0.880	15.200	30.00	1.080	0.6200
-50.00	-1.090	13.000	40.00	1.150	0.9600
-40.00	-1.150	0.9600	50.00	1.090	13.000
-30.00	-1.080	0.6200	60.00	0.880	15.200
-20.00	-0.840	0.3100	70.00	0.600	16.600
-10.00	-0.640	0.0144	80.00	0.310	17.600
-8.00	-0.480	0.0124	90.00	0.000	18.000
-6.00	-0.090	0.0082	100.00	-0.310	17.600
-5.00	0.020	0.0082	110.00	-0.600	16.600
-4.00	0.130	0.0082	120.00	-0.880	15.200
-3.00	0.240	0.0082	130.00	-1.090	13.000
-2.00	0.350	0.0086	140.00	-1.150	0.9600
-1.00	0.460	0.0086	150.00	-1.080	0.6200
0.00	0.570	0.0087	160.00	-0.840	0.3100
1.00	0.670	0.0088	170.00	-0.640	0.0500
2.00	0.780	0.0090	180.00	-0.170	0.0200
3.00	0.890	0.0093			

s825_2103.dat

```
Re=3,000,000 (windward modified the flat Cl section near stall)
FROM Dayton Griffin, sept 28'00, post stall combined with flat plate.
Foilchcked by Windward on 10-Oct-2000 at 10:23.

     1          Number of airfoil tables in this file
     0.00       Table ID parameter
    12.50       Stall angle (deg)
     0.00       No longer used, enter zero
     0.00       No longer used, enter zero
     0.00       No longer used, enter zero
    -6.10       Zero lift angle of attack (deg)
     6.18827    Cn slope for zero lift (dimensionless)
     2.0641     Cn at stall value for positive angle of attack
    -0.8000     Cn at stall value for negative angle of attack
    -6.0000     Angle of attack for minimum CD (deg)
     0.0074     Minimum CD value
```

AOA	Cl	Cd
-180.00	-0.170	0.0200
-170.00	0.640	0.0500
-160.00	0.840	0.3100
-150.00	1.080	0.6200
-140.00	1.150	0.9600
-130.00	1.090	13.000
-120.00	0.880	15.200
-110.00	0.600	16.600
-100.00	0.310	17.600
-90.00	0.000	18.000
-80.00	-0.310	17.600
-70.00	-0.600	16.600
-60.00	-0.880	15.200
-50.00	-1.090	13.000
-40.00	-1.150	0.9600
-30.00	-1.080	0.6200
-20.00	-0.840	0.3100
-10.00	-0.640	0.0144
-8.00	-0.480	0.0124
-6.00	0.010	0.0074
-5.00	0.120	0.0075
-4.00	0.230	0.0077
-3.00	0.340	0.0078
-2.00	0.440	0.0080
-1.00	0.550	0.0082
0.00	0.660	0.0084
1.00	0.770	0.0086
2.00	0.880	0.0089
3.00	0.980	0.0091
4.00	1.090	0.0095
5.00	1.200	0.0098
6.00	1.300	0.0102
7.00	1.410	0.0107
8.00	1.490	0.0155
9.00	1.580	0.0179
10.00	1.660	0.0203
11.00	1.680	0.0250
12.00	1.700	0.0273
13.00	1.700	0.0297
14.00	1.680	0.0324
15.00	1.660	0.0520
30.00	1.080	0.6200
40.00	1.150	0.9600
50.00	1.090	13.000
60.00	0.880	15.200
70.00	0.600	16.600
80.00	0.310	17.600
90.00	0.000	18.000
100.00	-0.310	17.600
110.00	-0.600	16.600
120.00	-0.880	15.200
130.00	-1.090	13.000
140.00	-1.150	0.9600
150.00	-1.080	0.6200
160.00	-0.840	0.3100
170.00	-0.640	0.0500
180.00	-0.170	0.0200

s826_1603.dat

```
Re=3,000,000 (windward modified the flat Cl section near stall)
FROM Dayton Griffin, Sept 28'00, post stall combined with flat plate.
Foilchcked by Windward on 10-Oct-2000 at 10:37.

     1          Number of airfoil tables in this file
     0.00       Table ID parameter
    12.00       Stall angle (deg)
     0.00       No longer used, enter zero
     0.00       No longer used, enter zero
     0.00       No longer used, enter zero
    -6.61       Zero lift angle of attack (deg)
     6.16567    Cn slope for zero lift (dimensionless)
     2.0013     Cn at stall value for positive angle of attack
    -0.8000     Cn at stall value for negative angle of attack
    -4.0000     Angle of attack for minimum CD (deg)
     0.0067     Minimum CD value
```

AOA	Cl	Cd	AOA	Cl	Cd
-180.00	-0.170	0.0200	4.00	1.140	0.0082
-170.00	0.640	0.0500	5.00	1.250	0.0087
-160.00	0.840	0.3100	6.00	1.350	0.0104
-150.00	1.080	0.6200	7.00	1.440	0.0146
-140.00	1.150	0.9600	8.00	1.530	0.0184
-130.00	1.090	13.000	9.00	1.630	0.0200
-120.00	0.880	15.200	10.00	1.650	0.0219
-110.00	0.600	16.600	11.00	1.670	0.0239
-100.00	0.310	17.600	12.00	1.680	0.0262
-90.00	0.000	18.000	13.00	1.670	0.0288
-80.00	-0.310	17.600	14.00	1.650	0.0316
-70.00	-0.600	16.600	15.00	1.630	0.0520
-60.00	-0.880	15.200	30.00	1.080	0.6200
-50.00	-1.090	13.000	40.00	1.150	0.9600
-40.00	-1.150	0.9600	50.00	1.090	13.000
-30.00	-1.080	0.6200	60.00	0.880	15.200
-20.00	-0.840	0.3100	70.00	0.600	16.600
-10.00	-0.640	0.0144	80.00	0.310	17.600
-8.00	-0.480	0.0124	90.00	0.000	18.000
-6.00	0.060	0.0092	100.00	-0.310	17.600
-5.00	0.170	0.0082	110.00	-0.600	16.600
-4.00	0.280	0.0067	120.00	-0.880	15.200
-3.00	0.390	0.0068	130.00	-1.090	13.000
-2.00	0.500	0.0069	140.00	-1.150	0.9600
-1.00	0.600	0.0070	150.00	-1.080	0.6200
0.00	0.710	0.0072	160.00	-0.840	0.3100
1.00	0.820	0.0074	170.00	-0.640	0.0500
2.00	0.930	0.0076	180.00	-0.170	0.0200
3.00	1.040	0.0078			

A.2 Aerodynamics specifications

```
1.5 MW baseline aerodynamic parameters for FAST certification test #13.
SI              SysUnits         - System of units for used for input and
                                   output [must be SI for FAST]
                                   (unquoted string)
STEADY          StallMod         - Dynamic stall included [BEDDOES or
                                   STEADY] (unquoted string)
NO_CM           UseCm            - Use aerodynamic pitching moment model?
                                   [USE_CM or NO_CM] (unquoted string)
DYNIN           InfModel         - Inflow model [DYNIN or EQUIL]
                                   (unquoted string)
SWIRL           IndModel         - Induction-factor model [NONE or WAKE
                                   or SWIRL] (unquoted string)
0.005           AToler           - Induction-factor tolerance
                                   (convergence criteria) (-)
PRANDtl         TLModel          - Tip-loss model (EQUIL only) [PRANDtl,
                                   GTECH, or NONE] (unquoted string)
PRANDtl         HLModel          - Hub-loss model (EQUIL only) [PRANdtl
                                   or NONE] (unquoted string)
"wind\xxxxxxxxx.wnd"             - Name of file containing wind data
                                   (quoted string)
84.2876         HH               - Wind reference (hub) height
                                   [TowerHt+Twr2Shft+OverHang*SIN(ShftTi
                                   lt)] (m)
0.0             TwrShad          - Tower-shadow velocity deficit (-)
9999.9          ShadHWid         - Tower-shadow half width (m)
9999.9          T_Shad_Refpt     - Tower-shadow reference point (m)
1.225           Rho              - Air density (kg/m^3)
1.4639E-5       KinVisc          - Kinematic air viscosity [CURRENTLY
                                   IGNORED] (m^2/sec)
0.005           DTAero           - Time interval for aerodynamic
                                   calculations (sec)
4               NumFoil          - Number of airfoil files (-)
"Airfoils\cylinder.dat"          - Names of the airfoil files [NumFoil
"Airfoils\s818_2703.dat"           lines] (quoted strings)
"Airfoils\s825_2103.dat"
"Airfoils\s826_1603.dat"
15              BldNodes         - Number of blade nodes used for
                                   analysis (-)
RNodes    AeroTwst  DRNodes  Chord  NFoil  PrnElm
 2.85833  11.10     2.21667  1.949  1      NOPRINT
 5.07500  11.10     2.21667  2.269  2      NOPRINT
 7.29167  11.10     2.21667  2.589  2      PRINT
 9.50833  10.41     2.21667  2.743  2      NOPRINT
11.72500   8.38     2.21667  2.578  2      NOPRINT
13.94167   6.35     2.21667  2.412  2      NOPRINT
16.15833   4.33     2.21667  2.247  2      PRINT
18.37500   2.85     2.21667  2.082  3      NOPRINT
20.59167   2.22     2.21667  1.916  3      NOPRINT
22.80833   1.58     2.21667  1.751  3      NOPRINT
25.02500   0.95     2.21667  1.585  3      PRINT
27.24167   0.53     2.21667  1.427  3      NOPRINT
29.45833   0.38     2.21667  1.278  3      NOPRINT
31.67500   0.23     2.21667  1.129  4      NOPRINT
33.89167   0.08     2.21667  0.980  4      PRINT
```

A.3 Blade baseline

```
---------------------- FAST INDIVIDUAL BLADE FILE ----------------------
1.5 MW baseline blade model properties from "InputData1.5A08V07adm.xls"
(from C. Hansen) with bugs removed.

--------------------------- BLADE PARAMETERS --------------------------

21            NBlInpSt       - Number of blade input stations (-)
False         CalcBMode      - Calculate blade mode shapes internally
                               {T: ignore mode shapes from below, F:
                               use mode shapes from below} [CURRENTLY
                               IGNORED] (flag)
3.882         BldFlDmp(1)    - Blade flap mode #1 structural damping in
                               percent of critical (%)
3.882         BldFlDmp(2)    - Blade flap mode #2 structural damping in
                               percent of critical (%)
5.900         BldEdDmp(1)    - Blade edge mode #1 structural damping in
                               percent of critical (%)

------------------------ BLADE ADJUSTMENT FACTORS ----------------------

1.0           FlStTunr(1)    - Blade flapwise modal stiffness tuner, 1st
                               mode (-)
1.0           FlStTunr(2)    - Blade flapwise modal stiffness tuner, 2nd
                               mode (-)
1.0           AdjBlMs        - Factor to adjust blade mass density (-)
1.0           AdjFlSt        - Factor to adjust blade flap stiffness (-)
1.0           AdjEdSt        - Factor to adjust blade edge stiffness (-)

----------------------- DISTRIBUTED BLADE PROPERTIES ------------------
 BlFract     AeroCent    StrcTwst     BMassDen     FlpStff      EdgStff
                           (deg)        (kg/m)       (Nm^2)       (Nm^2)
   0.00000       0.250       11.10     1447.600  7.6815E+09  7.6815E+09
   0.02105       0.250       11.10      180.330  1.1699E+09  1.1699E+09
   0.05263       0.229       11.10      181.670  1.0206E+09  1.0923E+09
   0.10526       0.201       11.10      183.910  7.7188E+08  9.6297E+08
   0.15789       0.179       11.10      186.140  5.2314E+08  8.3366E+08
   0.21053       0.160       11.10      188.370  2.7440E+08  7.0435E+08
   0.26316       0.165        9.50      178.320  2.3457E+08  6.1465E+08
   0.31579       0.170        7.90      168.270  1.9474E+08  5.2496E+08
   0.36842       0.176        6.30      158.220  1.5490E+08  4.3526E+08
   0.42105       0.183        4.70      148.170  1.1507E+08  3.4557E+08
   0.47368       0.190        3.10      138.120  7.5230E+07  2.5587E+08
   0.52632       0.194        2.60      122.900  6.2490E+07  2.1787E+08
   0.57895       0.200        2.10      107.670  4.9750E+07  1.7986E+08
   0.63158       0.205        1.60       92.442  3.7010E+07  1.4186E+08
   0.68421       0.212        1.10       77.215  2.4270E+07  1.0385E+08
   0.73684       0.220        0.60       61.988  1.1530E+07  6.5850E+07
   0.78947       0.224        0.48       51.861  9.2700E+06  5.4250E+07
   0.84211       0.229        0.36       41.734  7.0100E+06  4.2660E+07
   0.89474       0.234        0.24       31.607  4.7500E+06  3.1060E+07
   0.94737       0.241        0.12       21.480  2.4900E+06  1.9470E+07
   1.00000       0.250        0.00       11.353  2.3000E+05  7.8700E+06
```

GJStff (Nm^2)	EAStff (N)	Alpha	FlpIner (kg m)	EdgIner (kg m)	PrecrvRef (m)
2.6552E+09	1.7153E+10	0	646.040	646.040	0
4.0880E+08	2.6408E+09	0	80.480	80.480	0
3.4381E+08	2.6113E+09	0	68.241	80.113	0
2.3550E+08	2.5621E+09	0	47.842	79.502	0
1.2719E+08	2.5129E+09	0	27.444	78.892	0
1.8870E+07	2.4636E+09	0	7.045	78.281	0
1.6800E+07	2.3328E+09	0	5.963	68.302	0
1.4720E+07	2.2020E+09	0	4.881	58.323	0
1.2640E+07	2.0712E+09	0	3.799	48.344	0
1.0560E+07	1.9404E+09	0	2.717	38.366	0
8.4800E+06	1.8096E+09	0	1.635	28.387	0
7.1200E+06	1.6053E+09	0	1.367	24.050	0
5.7600E+06	1.4011E+09	0	1.099	19.714	0
4.4000E+06	1.1968E+09	0	0.831	15.377	0
3.0400E+06	9.9260E+08	0	0.564	11.041	0
1.6800E+06	7.8830E+08	0	0.296	6.704	0
1.3800E+06	6.5430E+08	0	0.240	5.513	0
1.0800E+06	5.2040E+08	0	0.185	4.322	0
7.8000E+05	3.8640E+08	0	0.130	3.130	0
4.8000E+05	2.5240E+08	0	0.074	1.939	0
2.6552E+09	1.7153E+10	0	646.040	646.040	0

PreswpRef (m)	FlpcgOf (m)	EdgcgOf(m)	FlpEAOf(m)	EdgEAOf (m)
0	0	0.000	0	0.000
0	0	0.000	0	0.000
0	0	0.032	0	-0.005
0	0	0.086	0	-0.014
0	0	0.140	0	-0.023
0	0	0.194	0	-0.032
0	0	0.188	0	-0.020
0	0	0.182	0	-0.007
0	0	0.176	0	0.005
0	0	0.170	0	0.018
0	0	0.164	0	0.030
0	0	0.168	0	0.038
0	0	0.172	0	0.047
0	0	0.176	0	0.055
0	0	0.179	0	0.063
0	0	0.183	0	0.071
0	0	0.190	0	0.077
0	0	0.198	0	0.082
0	0	0.205	0	0.087
0	0	0.212	0	0.092
0	0	0.220	0	0.098

---------- BLADE MODE SHAPES ----------

0.0838	BldFl1Sh(2)	- Flap mode 1, coeff of x^2
1.6525	BldFl1Sh(3)	- , coeff of x^3
-1.5682	BldFl1Sh(4)	- , coeff of x^4
1.6947	BldFl1Sh(5)	- , coeff of x^5
-0.8628	BldFl1Sh(6)	- , coeff of x^6
-0.3008	BldFl2Sh(2)	- Flap mode 2, coeff of x^2
-1.9968	BldFl2Sh(3)	- , coeff of x^3
-4.6564	BldFl2Sh(4)	- , coeff of x^4
16.9661	BldFl2Sh(5)	- , coeff of x^5

```
-9.0121   BldFl2Sh(6) -            , coeff of x^6
 0.3165   BldEdgSh(2) - Edge mode 1, coeff of x^2
 3.2618   BldEdgSh(3) -            , coeff of x^3
-6.4005   BldEdgSh(4) -            , coeff of x^4
 6.0367   BldEdgSh(5) -            , coeff of x^5
-2.2146   BldEdgSh(6) -            , coeff of x^6
```

A.4 Linearization baseline

```
------------------------------------------------------------------------
-------------------- FAST LINEARIZATION CONTROL FILE -------------------
1.5 MW baseline linearization input properties.

-------------------- PERIODIC STEADY STATE SOLUTION --------------------
True          CalcStdy       - Calculate periodic steady state condition
                             {False: linearize about initial conditions}
                             (flag)
2             TrimCase       - Trim case {1: find nacelle yaw, 2: find
                               generator torque, 3: find collective
                               blade pitch} (switch) [used only when
                               CalcStdy=True and GenDOF=True]
9.01316E-04   DispTol        - Convergence tolerance for the 2-norm of
                               displacements in the periodic steady
                               state calculation (rad  ) [used only
                               when CalcStdy=True]
4.84390E-05   VelTol         - Convergence tolerance for the 2-norm of
                               velocities    in the periodic steady
                               state calculation (rad/s) [used only
                               when CalcStdy=True]


------------------------- MODEL LINEARIZATION -------------------------
360           NAzimStep      - Number of equally-spaced azimuth steps in
                             periodic linearized model (-)
1             MdlOrder       - Order of output linearized model {1: 1st
                               order A, B, Bd, C, D, Dd; 2: 2nd order
                               M, C, K, F, Fd, VelC, DspC, D, Dd}
                               (switch)

---------------------- INPUTS AND DISTURBANCES ----------------------
2             NInputs        - Number of control inputs [0 (none) or 1
                             to 4+NumBl] (-)
3,4           CntrlInpt      - List   of control inputs [1 to NInputs]
                               {1: nacelle yaw angle, 2: nacelle yaw
                               rate, 3: generator torque, 4: collective
                               blade pitch, 5: individual pitch of
                               blade 1, 6: individual pitch of blade 2,
                               7: individual pitch of blade 3
                               [unavailable for 2-bladed turbines]} (-)
                               [unused if NInputs=0]
2             NDisturbs      - Number of wind disturbances [0 (none) or
                             1 to 7] (-)
                               1,5      Disturbnc   - List   of input
                               wind disturbances [1 to NDisturbs] {1:
                               horizontal hub-height wind speed, 2:
                               horizontal wind direction, 3: vertical
                               wind speed, 4: horizontal wind shear, 5:
                               vertical power law wind shear, 6: linear
                               vertical wind shear, 7: horizontal hub-
                               height wind gust} (-) [unused if
                               NDisturbs=0]
```

A.5 FAST primary input file (.fst)

```
---------------------------------------------------------------------------
------------------------ FAST INPUT FILE ----------------------------------
Model WTG_v1: WindPACT 1.5 MW Baseline with 1 DOF and deterministic
wind field Juan José García Quirante
Model properties from "InputData1.5A08V07adm.xls" (from C. Hansen) with
bugs removed.  Compatible with FAST v6.0.

------------------------ SIMULATION CONTROL --------------------------
False      Echo          - Echo input data to "echo.out" (flag)
  1        ADAMSPrep     - ADAMS preprocessor mode {1: Run FAST, 2: use
                           FAST as a preprocessor to create an ADAMS
                           model, 3: do both} (switch)
  1        AnalMode      - Analysis mode {1: Run a time-marching
                           simulation, 2: create a periodic linearized
                           model} (switch)
  3        NumBl         - Number of blades (-)
600.0      TMax          - Total run time (s)
  0.005    DT            - Integration time step (s)

------------------------ TURBINE CONTROL -----------------------------
0          YCMode        - Yaw control mode {0: none, 1: user-defined
                           from routine UserYawCont, 2: user-defined
                           from Simulink} (switch)
9999.9     TYCOn         - Time to enable active yaw control (s) [unused
                           when YCMode=0]
2          PCMode        - Pitch control mode {0: none, 1: user-defined
                           from routine PitchCntrl, 2: user-defined
                           from Simulink} (switch)
0.0        TPCOn         - Time to enable active pitch control (s)
                           [unused when PCMode=0]
3          VSContrl      - Variable-speed control mode {0: none, 1:
                           simple VS, 2: user-defined from routine
                           UserVSCont, 3: user-defined from Simulink}
                           (switch)
1800.0     VS_RtGnSp     - Rated generator speed for simple variable-
                           speed generator control (HSS side) (rpm)
                           [used only when VSContrl=1]
8376.58    VS_RtTq       - Rated generator torque/constant generator
                           torque in Region 3 for simple variable-speed
                           generator control (HSS side) (N-m) [used
                           only when VSContrl=1]
0.002585   VS_Rgn2K      - Generator torque constant in Region 2 for
                           simple variable-speed generator control (HSS
                           side) (N-m/rpm^2) [used only when
                           VSContrl=1]
5          VS_SlPc       - Rated generator slip percentage in Region 2
                           1/2 for simple variable-speed generator
                           control (%) [used only when VSContrl=1]
1          GenModel      - Generator model {1: simple, 2: Thevenin, 3:
                           user-defined from routine UserGen} (switch)
                           [used only when VSContrl=0]
True       GenTiStr      - Method to start the generator {T: timed using
                           TimGenOn, F: generator speed using SpdGenOn}
                           (flag)
```

```
True        GenTiStp      - Method to stop the generator {T: timed using
                            TimGenOf, F: when generator power = 0}
                            (flag)
9999.9      SpdGenOn      - Generator speed to turn on the generator for
                            a startup (HSS speed) (rpm) [used only when
                            GenTiStr=False]
0.0         TimGenOn      - Time to turn on the generator for a startup
                            (s) [used only when GenTiStr=True]
9999.9      TimGenOf      - Time to turn off the generator (s) [used only
                            when GenTiStp=True]
1           HSSBrMode     - HSS brake model {1: simple, 2: user-defined
                            from routine UserHSSBr} (switch)
9999.9      THSSBrDp      - Time to initiate deployment of the HSS brake
                            (s)
9999.9      TiDynBrk      - Time to initiate deployment of the dynamic
                            generator brake [CURRENTLY IGNORED] (s)
9999.9      TTpBrDp(1)    - Time to initiate deployment of tip brake 1
                            (s)
9999.9      TTpBrDp(2)    - Time to initiate deployment of tip brake 2
                            (s)
9999.9      TTpBrDp(3)    - Time to initiate deployment of tip brake 3
                            (s) [unused for 2 blades]
9999.9      TBDepISp(1)   - Deployment-initiation speed for the tip brake
                            on blade 1 (rpm)
9999.9      TBDepISp(2)   - Deployment-initiation speed for the tip brake
                            on blade 2 (rpm)
9999.9      TBDepISp(3)   - Deployment-initiation speed for the tip brake
                            on blade 3 (rpm) [unused for 2 blades]
9999.9      TYawManS      - Time to start override yaw maneuver and end
                            standard yaw control (s)
9999.9      TYawManE      - Time at which override yaw maneuver reaches
                            final yaw angle (s)
0.0         NacYawF       - Final yaw angle for yaw maneuvers (degrees)
9999.9      TPitManS(1)   - Time to start override pitch maneuver for
                            blade 1 and end standard pitch control (s)
9999.9      TPitManS(2)   - Time to start override pitch maneuver for
                            blade 2 and end standard pitch control (s)
9999.9      TPitManS(3)   - Time to start override pitch maneuver for
                            blade 3 and end standard pitch control (s)
                            [unused for 2 blades]
9999.9      TPitManE(1)   - Time at which override pitch maneuver for
                            blade 1 reaches final pitch (s)
9999.9      TPitManE(2)   - Time at which override pitch maneuver for
                            blade 2 reaches final pitch (s)
9999.9      TPitManE(3)   - Time at which override pitch maneuver for
                            blade 3 reaches final pitch (s) [unused for
                            2 blades]
18.25       BlPitch(1)    - Blade 1 initial pitch (degrees)
18.25       BlPitch(2)    - Blade 2 initial pitch (degrees)
18.25       BlPitch(3)    - Blade 3 initial pitch (degrees) [unused for 2
                            blades]
0.0         B1PitchF(1)   - Blade 1 final pitch for pitch maneuvers
                            (degrees)
0.0         B1PitchF(2)   - Blade 2 final pitch for pitch maneuvers
                            (degrees)
0.0         B1PitchF(3)   - Blade 3 final pitch for pitch maneuvers
                            (degrees) [unused for 2 blades]

---------------------- ENVIRONMENTAL CONDITIONS -----------------------
```

```
   9.80665  Gravity     - Gravitational acceleration (m/s^2)

--------------------------- FEATURE FLAGS ----------------------------
False      FlapDOF1     - First flapwise blade mode DOF (flag)
False      FlapDOF2     - Second flapwise blade mode DOF (flag)
False      EdgeDOF      - First edgewise blade mode DOF (flag)
False      TeetDOF      - Rotor-teeter DOF (flag) [unused for 3 blades]
False      DrTrDOF      - Drivetrain rotational-flexibility DOF (flag)
True       GenDOF       - Generator DOF (flag)
False      YawDOF       - Yaw DOF (flag)
False      TwFADOF1     - First fore-aft tower bending-mode DOF (flag)
False      TwFADOF2     - Second fore-aft tower bending-mode DOF (flag)
False      TwSSDOF1     - First side-to-side tower bending-mode DOF
                          (flag)
False      TwSSDOF2     - Second side-to-side tower bending-mode DOF
                          (flag)
True       CompAero     - Compute aerodynamic forces (flag)
False      CompNoise    - Compute aerodynamic noise (flag)

----------------------- INITIAL CONDITIONS ---------------------------
0.0        OoPDefl      - Initial out-of-plane blade-tip displacement,
                          (meters)
0.0        IPDefl       - Initial in-plane blade-tip deflection,
                          (meters)
0.0        TeetDefl     - Initial or fixed teeter angle (degrees)
                          [unused for 3 blades]
0.0        Azimuth      - Initial azimuth angle for blade 1 (degrees)
20.01      RotSpeed     - Initial or fixed rotor speed (rpm)
0.0        NacYaw       - Initial or fixed nacelle-yaw angle (degrees)
0.0        TTDspFA      - Initial fore-aft tower-top displacement
                          (meters)
0.0        TTDspSS      - Initial side-to-side tower-top displacement
                          (meters)

---------------------- TURBINE CONFIGURATION -------------------------
35.0       TipRad       - The distance from the rotor apex to the blade
                          tip (meters)
1.75       HubRad       - The distance from the rotor apex to the blade
                          root (meters)
1          PSpnElN      - Number of the innermost blade element which
                          is still part of the pitchable portion of
                          the blade for partial-span pitch control [1
                          to BldNodes] [CURRENTLY IGNORED] (-)
0.0        UndSling     - Undersling length [distance from teeter pin
                          to the rotor apex] (meters) [unused for 3
                          blades]
0.0        HubCM        - Distance from rotor apex to hub mass
                          [positive downwind] (meters)
-3.3       OverHang     - Distance from yaw axis to rotor apex [3
                          blades] or teeter pin [2 blades] (meters)
-0.1449    NacCMxn      - Downwind distance from the tower-top to the
                          nacelle CM (meters)
0.0        NacCMyn      - Lateral  distance from the tower-top to the
                          nacelle CM (meters)
1.3890     NacCMzn      - Vertical distance from the tower-top to the
                          nacelle CM (meters)
82.39      TowerHt      - Height of tower above ground level [onshore]
                          or MSL [offshore] (meters)
1.61       Twr2Shft     - Vertical distance from the tower-top to the
```

```
                          rotor shaft (meters)
0.0       TwrRBHt      - Tower rigid base height (meters)
-0.0      ShftTilt     - Rotor shaft tilt angle (degrees)
0.0       Delta3       - Delta-3 angle for teetering rotors (degrees)
                          [unused for 3 blades]
0.0       PreCone(1)   - Blade 1 cone angle (degrees)
0.0       PreCone(2)   - Blade 2 cone angle (degrees)
0.0       PreCone(3)   - Blade 3 cone angle (degrees) [unused for 2
                          blades]
270.0     AzimB1Up     - Azimuth value to use for I/O when blade 1
                          points up (degrees)

------------------------- MASS AND INERTIA ---------------------------
0.0       YawBrMass    - Yaw bearing mass (kg)
51.170E3  NacMass      - Nacelle mass (kg)
15.148E3  HubMass      - Hub mass (kg)
0.0       TipMass(1)   - Tip-brake mass, blade 1 (kg)
0.0       TipMass(2)   - Tip-brake mass, blade 2 (kg)
0.0       TipMass(3)   - Tip-brake mass, blade 3 (kg) [unused for 2
                          blades]
49.130E3  NacYIner     - Nacelle inertia about yaw axis (kg m^2)
53.036    GenIner      - Generator inertia about HSS (kg m^2)
34.600E3  HubIner      - Hub inertia about rotor axis [3 blades] or
                          teeter axis [2 blades] (kg m^2)

---------------------------- DRIVETRAIN ------------------------------
100.0     GBoxEff      - Gearbox efficiency (%)
100.0     GenEff       - Generator efficiency [ignored by the Thevenin
                          and user-defined generator models] (%)
87.965    GBRatio      - Gearbox ratio (-)
False     GBRevers     - Gearbox reversal {T: if rotor and generator
                          rotate in opposite directions} (flag)
9999.9    HSSBrTqF     - Fully deployed HSS-brake torque (N-m)
9999.9    HSSBrDT      - Time for HSS-brake to reach full deployment
                          once initiated (sec) [used only when
                          HSSBrMode=1]
          DynBrkFi     - File containing a mech-gen-torque vs HSS-
                          speed curve for a dynamic brake [CURRENTLY
                          IGNORED] (quoted string)
5.6E9     DTTorSpr     - Drivetrain torsional spring (N-m/rad)
1.0E7     DTTorDmp     - Drivetrain torsional damper (N-m/s)

---------------------- SIMPLE INDUCTION GENERATOR ----------------------
5.0       SIG_SlPc     - Rated generator slip percentage (%) [used
                          only when VSContrl=0 and GenModel=1]
1800      SIG_SySp     - Synchronous (zero-torque) generator speed
                          (rpm) [used only when VSContrl=0 and
                          GenModel=1]
7957      SIG_RtTq     - Rated torque (N-m) [used only when VSContrl=0
                          and GenModel=1]
2.0       SIG_PORt     - Pull-out ratio (Tpullout/Trated) (-) [used
                          only when VSContrl=0 and GenModel=1]

---------------- THEVENIN-EQUIVALENT INDUCTION GENERATOR --------------
9999.9    TEC_Freq     - Line frequency [50 or 60] (Hz) [used only
                          when VSContrl=0 and GenModel=2]
9998      TEC_NPol     - Number of poles [even integer > 0] (-) [used
                          only when VSContrl=0 and GenModel=2]
9999.9    TEC_SRes     - Stator resistance (ohms) [used only when
```

```
                          VSContrl=0 and GenModel=2]
9999.9     TEC_RRes     - Rotor resistance (ohms) [used only when
                          VSContrl=0 and GenModel=2]
9999.9     TEC_VLL      - Line-to-line RMS voltage (volts) [used only
                          when VSContrl=0 and GenModel=2]
9999.9     TEC_SLR      - Stator leakage reactance (ohms) [used only
                          when VSContrl=0 and GenModel=2]
9999.9     TEC_RLR      - Rotor leakage reactance (ohms) [used only
                          when VSContrl=0 and GenModel=2]
9999.9     TEC_MR       - Magnetizing reactance (ohms) [used only when
                          VSContrl=0 and GenModel=2]

------------------------- PLATFORM MODEL -----------------------------
0          PtfmModel    - Platform model {0: none, 1: onshore, 2: fixed
                          bottom offshore, 3: floating offshore}
                          (switch)
           PtfmFile     - Name of file containing platform properties
                          (quoted string) [unused when PtfmModel=0]

------------------------------ TOWER ---------------------------------
10         TwrNodes     - Number of tower nodes used for analysis (-)
"TurbineData\Baseline   - Name of file containing tower properties
_Tower.dat"               (quoted string)

---------------------------- NACELLE-YAW -----------------------------
0.0        YawSpr       - Nacelle-yaw spring constant (N-m/rad)
0.0        YawDamp      - Nacelle-yaw damping constant (N-m/rad/s)
0.0        YawNeut      - Neutral yaw position--yaw spring force is
                          zero at this yaw (degrees)

------------------------------ FURLING -------------------------------
False      Furling      - Read in additional model properties for
                          furling turbine (flag)
           FurlFile     - Name of file containing furling properties
                          (quoted string) [unused when Furling=False]

---------------------------- ROTOR-TEETER ----------------------------
0          TeetMod      - Rotor-teeter spring/damper model {0: none, 1:
                          standard, 2: user-defined from routine
                          UserTeet} (switch) [unused for 3 blades]
0.0        TeetDmpP     - Rotor-teeter damper position (degrees) [used
                          only for 2 blades and when TeetMod=1]
0.0        TeetDmp      - Rotor-teeter damping constant (N-m/rad/s)
                          [used only for 2 blades and when TeetMod=1]
0.0        TeetCDmp     - Rotor-teeter rate-independent Coulomb-damping
                          moment (N-m) [used only for 2 blades and
                          when TeetMod=1]
0.0        TeetSStP     - Rotor-teeter soft-stop position (degrees)
                          [used only for 2 blades and when TeetMod=1]
0.0        TeetHStP     - Rotor-teeter hard-stop position (degrees)
                          [used only for 2 blades and when TeetMod=1]
0.0        TeetSSSp     - Rotor-teeter soft-stop linear-spring constant
                          (N-m/rad) [used only for 2 blades and when
                          TeetMod=1]
0.0        TeetHSSp     - Rotor-teeter hard-stop linear-spring constant
                          (N-m/rad) [used only for 2 blades and when
                          TeetMod=1]
```

```
------------------------------ TIP-BRAKE -----------------------------
0.0       TBDrConN     - Tip-brake drag constant during normal
                         operation, Cd*Area (m^2)
0.0       TBDrConD     - Tip-brake drag constant during fully-deployed
                         operation, Cd*Area (m^2)
0.0       TpBrDT       - Time for tip-brake to reach full deployment
                         once released (sec)

------------------------------ BLADE ---------------------------------
"TurbineData\Baseline_Blade.dat"  - Name of file containing properties
                                    for blade 1 (quoted string)
"TurbineData\Baseline_Blade.dat"  - Name of file containing properties
                                    for blade 2 (quoted string)
"TurbineData\Baseline_Blade.dat"  - Name of file containing properties
                                  for blade 3 (quoted string) [unused
                                  for 2 blades]


------------------------------ AERODYN -------------------------------
"aerodyn_non_linear_v1.ipt"  - Name of file containing AeroDyn input
                               parameters (quoted string)

------------------------------ NOISE ---------------------------------
"xxxxxxxx"                  - Name of file containing aerodynamic
                              noise input parameters (quoted string)
                              [used only when CompNoise=True]

------------------------------ ADAMS ---------------------------------
"xxxxxxxx"                  - Name of file containing ADAMS-specific
                              input parameters (quoted string)
                              [unused when ADAMSPrep=1]

---------------------- LINEARIZATION CONTROL -------------------------
"Baseline_Linear_v1_indiv.dat"  - Name of file containing FAST
                                  linearazation parameters (quoted
                                  string) [unused when AnalMode=1]

------------------------------ OUTPUT --------------------------------
True        SumPrint     - Print summary data to "<RootName>.fsm"
                           (flag)
True        TabDelim     - Generate a tab-delimited tabular output
                           file. (flag)
"ES10.3E2"  OutFmt       - Format used for tabular output except time.
                           Resulting field should be 10 characters.
                           (quoted string)  [not checked for
                           validity!]
0.0         TStart       - Time to begin tabular output (s)
10          DecFact      - Decimation factor for tabular output {1:
                           output every time step} (-)
1.0         SttsTime     - Amount of time between screen status
                           messages (sec)
0.0         NcIMUxn      - Downwind distance from the tower-top to the
                           nacelle IMU (meters)
0.0         NcIMUyn      - Lateral  distance from the tower-top to the
                           nacelle IMU (meters)
0.0         NcIMUzn      - Vertical distance from the tower-top to the
                           nacelle IMU (meters)
0.99        ShftGagL     - Distance from rotor apex [3 blades] or
                           teeter pin [2 blades] to shaft strain gages
```

```
                          [positive for upwind rotors] (meters)
2           NTwGages      - Number of tower nodes that have strain gages
                            for output [0 to 5] (-)
4,7         TwrGagNd      - List of tower nodes that have strain gages
                            [1 to TwrNodes] (-) [unused if NTwGages=0]
0           NBlGages      - Number of blade nodes that have strain gages
                            for output [0 to 5] (-)
            BldGagNd      - List of blade nodes that have strain gages
                            [1 to BldNodes] (-) [unused if NBlGages=0]
            OutList       - The next line(s) contains a list of output
                            parameters.  See OutList.txt for a listing
                            of available output channels, (-)

"WindVxi"          - Wind-speed, component x  (m/s)
"BldPitch2"        - Blade 2 pitch angle (deg)
"GenPwr"           - Generated power (kW)
"GenCp"            - Cp power coefficient
"GenTq"            - Electrical generator torque
"LSSTipVxa"        - Rotation speed of the rotor (rpm)
"LSSTipPxa"        - Azimuth angle (deg)
"LSSGagVxa"        - LSS strain gauge (gearbox side of the LSS) angular
                     speed (rpm)
"HSShftV"          - Generator angular speed (rpm)
"YawPzn"           - Yaw angle (deg)
"NacYawErr"        - ESTIMATE of yaw error (deg)(see remark in page 104)
"TipSpdRat"        - Blade tip speed ratio (lambda)
"RootMzc1"         - Pitching moment at the blade #1 root (kNm)
"RootMzb1"         - Same as RootMzc1
"RootMxb1"         - Edgewise moment at the blade #1 root (kNm)
"RootMyb1"         - Flapwise moment at the blade #1 root (kNm)
"RootFzb1"         - Axial force at the blade #1 root (kN)
"RootFxb1"         - Flapwise shear force at the blade #1 root (kN)
"RootFyb1"         - Edgewise shear force at the blade #1 root (kN)
"RootMzb2"         - Pitching moment at the blade #2 root (kNm)
"RootMzb3"         - Pitching moment at the blade #3 root (kNm)
"TipDxc1"          - Out-of-plane tip deflection of blade #1 (m)
"TipDyc1"          - In-plane tip deflection of blade #1 (m)
"TipDxb1"          - Flapwise tip deflection of blade #1 (m)
"TipDyb1"          - Edgewise tip deflection of blade #1 (m)
"LSShftFxa"        - Thrust force (kN)
"YawBrTDxp"        - Tower-top fore-aft (translational) deflection (m)
"RootMxb2"         - Edgewise moment at the blade #2 root (kNm)
"RootMyb2"         - Flapwise moment at the blade #2 root (kNm)
"RootMxb3"         - Edgewise moment at the blade #3 root (kNm)
"RootMyb3"         - Flapwise moment at the blade #3 root (kNm)
"RootMxc1"         - In-plane moment at blade #1 root (kNm)
"RootMyc1"         - Out-of-plane moment at blade #1 root (kNm)
"RootMxc2"         - In-plane moment at blade #2 root (kNm)
"RootMyc2"         - Out-of-plane moment at blade #2 root (kNm)
"RootMxc3"         - In-plane moment at blade #3 root (kNm)
"RootMyc3"         - Out-of-plane moment at blade #3 root (kNm)
"YawBrMzp"         - Tower top Yaw moment (kNm)
"YawBrMyp"         - Tower top Tilt moment (kNm)
"BldPitch1"        - Blade 1 pitch angle (deg)
"BldPitch3"        - Blade 3 pitch angle (deg)
"LSSTipMzs"        - Rotor shaft tip yaw moment (kNm)
"LSSTipMys"        - Rotor shaft tip tilt moment (kNm)
"TwrBsMzt"         - Tower base yaw moment (kNm)
"TwrBsMyt"         - Tower base tilt moment (kNm)
```

```
END of FAST input file (the word "END" must appear in the first 3
columns of this last line).
--------------------------------------------------------------------------
```

APPENDIX B

WIND FILES

B.1 Wind field #1

```
This summary file was generated by TurbSim (v1.21, 1-Feb-2007) on 20-
Sep-2007 at 01:21:34.


Runtime Options:

   2318573  Random seed #1
    RANLUX  Random Number Generator Type
         F  Output binary HH turbulence parameters?
         F  Output formatted turbulence parameters?
         F  Output AeroDyn HH files?
         F  Output AeroDyn FF files?
         T  Output BLADED FF files?
         F  Output tower data?
         F  Output formatted FF files?
         F  Output coherent turbulence time step file?
         T  Clockwise rotation when looking downwind?


Turbine/Model Specifications:

         6  Vertical grid-point matrix dimension
         6  Horizontal grid-point matrix dimension
```

```
     0.050  Time step [seconds]
   600.000  Analysis time [seconds]
   140.000  Usable output time [seconds]
    84.288  Hub height [m]
    80.000  Grid height [m]
    80.000  Grid width [m]
     0.000  Vertical flow angle [degrees]
     0.000  Horizontal flow angle [degrees]


Meteorological Boundary Conditions:

    SMOOTH  RISO Smooth Terrain spectral model
       N/A  IEC standard
       N/A  IEC turbulence characteristic
       N/A  IEC turbulence type
       IEC  Wind profile type
    84.288  Reference height [m]
    18.200  Reference wind speed [m/s]
       N/A  Jet height [m]
     0.143  Power law exponent
     0.010  Surface roughness length [m]


Non-IEC Meteorological boundary conditions:

    45.000  Site latitude [degrees]
     0.050  Gradient Richardson number
     0.777  Friction or shear velocity [m/s]
       N/A  Mixing layer depth [m]
    -0.103  u'w' cross-correlation coefficient
     0.000  u'v' cross-correlation coefficient
     0.000  v'w' cross-correlation coefficient
    18.200  U-component coherence decrement
    13.650  V-component coherence decrement
    18.200  W-component coherence decrement
     0.000  Coherence exponent


You have requested that the following file(s) be generated:

   TurbSim.wnd (AeroDyn/BLADED full-field wnd file)


Turbulence Simulation Scaling Parameter Summary:

   Turbulence model used                                =  RISO Smooth
Terrain
   Gradient Richardson number                       =    0.050
   Monin-Obukhov (M-O) z/L parameter                =    0.067
   Monin-Obukhov (M-O) length scale                 =  932.157 m
   Mean wind speed at hub height                    =   18.200 m/s

   Wind profile type                                 =  Power law on the
rotor disk/Logarithmic elsewhere
   Power law exponent                               =    0.143
   Mean shear across rotor disk                     =    0.033 (m/s)/m
   Assumed rotor diameter                           =   80.000 m
   Surface roughness length                         =    0.010 m
```

```
   Number of time steps in the FFT                  =    12000
   Number of time steps output                      =     2888


Mean Flow Angles:

   Vertical   =   0.0 degrees
   Horizontal =   0.0 degrees

Mean Wind Speed Profile:

  Height    Wind Speed   Horizontal Angle  U-comp   V-comp   W-comp
    (m)       (m/s)         (degrees)      (m/s)    (m/s)    (m/s)
  ------    ----------   ----------------  ------   ------   ------
   124.3       19.24            0.00        19.24     0.00     0.00
   108.3       18.86            0.00        18.86     0.00     0.00
    92.3       18.44            0.00        18.44     0.00     0.00
    84.3       18.20            0.00        18.20     0.00     0.00
    76.3       17.94            0.00        17.94     0.00     0.00
    60.3       17.35            0.00        17.35     0.00     0.00
    44.3       16.60            0.00        16.60     0.00     0.00


Harvested Random Seeds after Generation of the Random Numbers:

      6188250 K1
            0 K2


Hub-Height Simulated Turbulence Statistical Summary:

   Type of Wind     Min (m/s)    Mean (m/s)     Max (m/s)   Sigma (m/s)
TI (%)
   ------------     ---------    ----------     ---------   -----------
------
   Longitudinal         12.56         18.20         24.40         2.006
10.959
   Lateral               -5.99          0.00          5.75         1.483
8.106
   Vertical              -4.60          0.00          3.75         1.186
6.482
   Horizontal            12.56         18.26         24.48         1.995
10.925
   Total                 12.72         18.30         24.49         1.992
10.887


Turbulent Velocity Component Extremes:

   Comp  Min (m/s)  Max (m/s)
   ----  ---------  ---------
    u'       -5.64       6.20
    v'       -5.99       5.75
    w'       -4.60       3.75


Hub Friction Velocity (Ustar) = 0.92634 m/s
```

Mean Reynolds Stress Components:

sqrt(u'v') = -0.350 m/s
sqrt(u'w') = -0.926 m/s
sqrt(v'w') = -0.367 m/s

Instantaneous Reynolds-Stress Component Statistics:

Product	Min (m/s)^2	Max (m/s)^2	Mean (m/s)^2
u'v'	-19.68	15.13	-0.12
u'w'	-17.15	8.88	-0.86
v'w'	-12.61	10.33	-0.13

Maximum Instantaneous TKE = 22.20 (m/s)^2
Maximum Instantaneous CTKE = 12.07 (m/s)^2

Cross-Component Correlation Coefficients:

u'v' coef = -0.041
u'w' coef = -0.361
v'w' coef = -0.077

Grid Point Variance Summary:

Y-coord	-40.00	-24.00	-8.00	8.00	24.00	40.00
Height	Standard deviation at grid points for the u component:					
124.29	2.045	2.034	2.014	2.049	2.075	2.014
108.29	1.989	2.016	2.040	2.009	1.915	1.905
92.29	2.091	1.908	1.973	2.040	2.024	1.910
76.29	2.008	1.939	2.002	2.078	2.068	2.093
60.29	2.091	2.016	2.061	2.180	2.107	2.156
44.29	2.033	1.968	2.136	2.049	2.045	2.007
Height	Standard deviation at grid points for the v component:					
124.29	1.554	1.508	1.533	1.535	1.552	1.603
108.29	1.553	1.472	1.537	1.553	1.550	1.634
92.29	1.546	1.517	1.488	1.564	1.514	1.605
76.29	1.562	1.577	1.513	1.491	1.536	1.627
60.29	1.577	1.532	1.574	1.555	1.583	1.604
44.29	1.530	1.542	1.498	1.541	1.536	1.513
Height	Standard deviation at grid points for the w component:					
124.29	1.178	1.203	1.184	1.133	1.174	1.200
108.29	1.221	1.198	1.182	1.189	1.196	1.162
92.29	1.203	1.175	1.203	1.199	1.166	1.178
76.29	1.168	1.153	1.161	1.203	1.224	1.214
60.29	1.174	1.164	1.205	1.205	1.162	1.215
44.29	1.193	1.171	1.187	1.214	1.186	1.175

U-component statistics from the interpolated hub point:

```
   Mean =  18.1899 m/s
   TI   =   9.9007 %


Normalizing Parameters for Binary Data:

   UBar  =  18.2000 m/s
   TI(u) =  11.0197 %
   TI(v) =   8.1505 %
   TI(w) =   6.5179 %

   Height Offset =   0.0000 m
   Grid Base     =  44.2876 m

Nyquist frequency of turbulent wind field =        10.000 Hz
```

B.2 Wind field #3

```
This summary file was generated by TurbSim (v1.21, 1-Feb-2007) on 06-
Oct-2007 at 03:46:23.


Runtime Options:

  -2318573  Random seed #1
    RANLUX  Random Number Generator Type
         F  Output binary HH turbulence parameters?
         F  Output formatted turbulence parameters?
         F  Output AeroDyn HH files?
         F  Output AeroDyn FF files?
         T  Output BLADED FF files?
         F  Output tower data?
         F  Output formatted FF files?
         F  Output coherent turbulence time step file?
         T  Clockwise rotation when looking downwind?


Turbine/Model Specifications:

         6  Vertical grid-point matrix dimension
         6  Horizontal grid-point matrix dimension
     0.050  Time step [seconds]
   600.000  Analysis time [seconds]
   160.000  Usable output time [seconds]
    84.288  Hub height [m]
    84.000  Grid height [m]
    84.000  Grid width [m]
     0.000  Vertical flow angle [degrees]
     0.000  Horizontal flow angle [degrees]


Meteorological Boundary Conditions:

    IECKAI  IEC Kaimal spectral model
         1  IEC standard: IEC 61400-1 Ed. 2: 1999
         A  IEC turbulence characteristic
       NTM  IEC Normal Turbulence Model
       IEC  Wind profile type
    84.288  Reference height [m]
    10.000  Reference wind speed [m/s]
       N/A  Jet height [m]
     0.200  Power law exponent
     0.030  Surface roughness length [m]


You have requested that the following file(s) be generated:

   84m_10mps.wnd (AeroDyn/BLADED full-field wnd file)


Turbulence Simulation Scaling Parameter Summary:
```

```
   Turbulence model used                              =  IEC Kaimal
   Turbulence characteristic                          =  A
   IEC turbulence type                                          =   Normal
Turbulence Model
   IEC standard                                        =  IEC 61400-1 Ed.
2: 1999
   Mean wind speed at hub height                      =   10.000 m/s
   Char value of turbulence intensity at 15 m/s       =   18.000%
   Standard deviation slope                           =    2.000
   Characteristic value of standard deviation         =    2.100 m/s
   Turbulence scale                                   =   21.000 m
   U-component integral scale                         =  170.100 m
   Coherency scale                                    =   73.500 m
   Characteristic value of hub turbulence intensity   =   21.000%
   Gradient Richardson number                         =    0.000

   Wind profile type                                   =  Power law on the
rotor disk/Logarithmic elsewhere
   Power law exponent                                 =    0.200
   Mean shear across rotor disk                       =    0.025 (m/s)/m
   Assumed rotor diameter                             =   84.000 m
   Surface roughness length                           =    0.030 m

   Number of time steps in the FFT                    =    12000
   Number of time steps output                        =     3368


Mean Flow Angles:

   Vertical   =   0.0 degrees
   Horizontal =   0.0 degrees

Mean Wind Speed Profile:

  Height    Wind Speed   Horizontal Angle  U-comp   V-comp   W-comp
    (m)       (m/s)         (degrees)      (m/s)    (m/s)    (m/s)
  ------    ----------   ----------------  ------   ------   ------
   126.3       10.84            0.00        10.84     0.00     0.00
   109.5       10.54            0.00        10.54     0.00     0.00
    92.7       10.19            0.00        10.19     0.00     0.00
    84.3       10.00            0.00        10.00     0.00     0.00
    75.9        9.79            0.00         9.79     0.00     0.00
    59.1        9.31            0.00         9.31     0.00     0.00
    42.3        8.71            0.00         8.71     0.00     0.00


Harvested Random Seeds after Generation of the Random Numbers:

      6188250 K1
            0 K2


Hub-Height Simulated Turbulence Statistical Summary:

   Type of Wind     Min (m/s)    Mean (m/s)     Max (m/s)   Sigma (m/s)
TI (%)
   ------------     ---------    ----------     ---------   -----------
------
```

```
   Longitudinal          3.70         10.00         16.33         1.969
19.321
   Lateral              -5.45          0.00          5.62         1.647
16.157
   Vertical             -3.43          0.00          3.72         1.020
10.005
   Horizontal            4.37         10.14         16.33         1.943
19.160
   Total                 4.38         10.19         16.34         1.934
18.977


Turbulent Velocity Component Extremes:

   Comp  Min (m/s)  Max (m/s)
   ----  ---------  ---------
    u'       -6.30       6.33
    v'       -5.45       5.62
    w'       -3.43       3.72


Hub Friction Velocity (Ustar) = 0.31673 m/s


Mean Reynolds Stress Components:

      sqrt(u'v') = -0.476 m/s
      sqrt(u'w') =  0.317 m/s
      sqrt(v'w') =  0.200 m/s


Instantaneous Reynolds-Stress Component Statistics:

   Product  Min (m/s)^2  Max (m/s)^2  Mean (m/s)^2
   -------  -----------  -----------  ------------
     u'v'        -24.40        21.37         -0.23
     u'w'        -15.05        14.29          0.10
     v'w'        -10.80        14.38          0.04


Maximum Instantaneous  TKE =  24.96 (m/s)^2
Maximum Instantaneous CTKE =  12.21 (m/s)^2


Cross-Component Correlation Coefficients:

   u'v' coef = -0.070
   u'w' coef =  0.050
   v'w' coef =  0.024


Grid Point Variance Summary:

   Y-coord  -42.00  -25.20   -8.40    8.40   25.20   42.00

   Height   Standard deviation at grid points for the u component:
   126.29    2.051   2.124   2.014   2.218   2.048   2.058
   109.49    1.893   2.024   2.000   2.150   1.919   1.907
    92.69    1.913   1.830   1.968   2.116   2.118   1.750
```

```
    75.89    2.048   1.834   2.013   2.014   2.113   2.186
    59.09    2.098   2.037   1.993   2.205   2.055   2.285
    42.29    2.032   2.020   2.252   2.084   2.056   2.041

   Height   Standard deviation at grid points for the v component:
   126.29    1.647   1.647   1.647   1.647   1.647   1.647
   109.49    1.647   1.647   1.647   1.647   1.647   1.647
    92.69    1.647   1.647   1.647   1.647   1.647   1.647
    75.89    1.647   1.647   1.647   1.647   1.647   1.647
    59.09    1.647   1.647   1.647   1.647   1.647   1.647
    42.29    1.647   1.647   1.647   1.647   1.647   1.647

   Height   Standard deviation at grid points for the w component:
   126.29    1.020   1.020   1.020   1.020   1.020   1.020
   109.49    1.020   1.020   1.020   1.020   1.020   1.020
    92.69    1.020   1.020   1.020   1.020   1.020   1.020
    75.89    1.020   1.020   1.020   1.020   1.020   1.020
    59.09    1.020   1.020   1.020   1.020   1.020   1.020
    42.29    1.020   1.020   1.020   1.020   1.020   1.020


U-component statistics from the interpolated hub point:

   Mean =   9.9920 m/s
   TI   =  16.1546 %


Normalizing Parameters for Binary Data:

   UBar  =  10.0000 m/s
   TI(u) =  19.6933 %
   TI(v) =  16.4684 %
   TI(w) =  10.1981 %

   Height Offset =   0.0000 m
   Grid Base     =  42.2876 m

Nyquist frequency of turbulent wind field =        10.000 Hz
```

B.3 Wind field #5

```
This summary file was generated by TurbSim (v1.21, 1-Feb-2007) on 25-
Sep-2007 at 21:19:55.


Runtime Options:

   2318573  Random seed #1
    RANLUX  Random Number Generator Type
         F  Output binary HH turbulence parameters?
         F  Output formatted turbulence parameters?
         F  Output AeroDyn HH files?
         F  Output AeroDyn FF files?
         T  Output BLADED FF files?
         F  Output tower data?
         F  Output formatted FF files?
         F  Output coherent turbulence time step file?
         T  Clockwise rotation when looking downwind?


Turbine/Model Specifications:

         4  Vertical grid-point matrix dimension
         4  Horizontal grid-point matrix dimension
     0.050  Time step [seconds]
   650.000  Analysis time [seconds]
   600.000  Usable output time [seconds]
    84.288  Hub height [m]
    80.000  Grid height [m]
    80.000  Grid width [m]
     0.000  Vertical flow angle [degrees]
     0.000  Horizontal flow angle [degrees]


Meteorological Boundary Conditions:

    IECKAI  IEC Kaimal spectral model
         1  IEC standard: IEC 61400-1 Ed. 3: 2005
         B  IEC turbulence characteristic
       NTM  IEC Normal Turbulence Model
       IEC  Wind profile type
    84.288  Reference height [m]
    18.200  Reference wind speed [m/s]
       N/A  Jet height [m]
     0.200  Power law exponent
     0.030  Surface roughness length [m]


You have requested that the following file(s) be generated:

   wind_for_fatigue.wnd (AeroDyn/BLADED full-field wnd file)


Turbulence Simulation Scaling Parameter Summary:
```

```
   Turbulence model used                                =  IEC Kaimal
   Turbulence characteristic                            =  B
   IEC turbulence type                                          =   Normal
Turbulence Model
   IEC standard                                          =  IEC 61400-1 Ed.
3: 2005
   Mean wind speed at hub height                        =   18.200 m/s
   Expected value of turbulence intensity at 15 m/s =   14.000%
   Characteristic value of standard deviation       =    2.695 m/s
   Turbulence scale                                     =   42.000 m
   U-component integral scale                           =  340.200 m
   Coherency scale                                      =  340.200 m
   Characteristic value of hub turbulence intensity =   14.808%
   Gradient Richardson number                           =    0.000

   Wind profile type                                     =  Power law on the
rotor disk/Logarithmic elsewhere
   Power law exponent                                   =    0.200
   Mean shear across rotor disk                         =    0.046 (m/s)/m
   Assumed rotor diameter                               =   80.000 m
   Surface roughness length                             =    0.030 m

   Number of time steps in the FFT                      =    13000
   Number of time steps output                          =    12088


Mean Flow Angles:

   Vertical   =   0.0 degrees
   Horizontal =   0.0 degrees

Mean Wind Speed Profile:

  Height    Wind Speed   Horizontal Angle  U-comp   V-comp   W-comp
    (m)       (m/s)         (degrees)      (m/s)    (m/s)    (m/s)
  ------    ----------   ----------------  ------   ------   ------
   124.3       19.67            0.00        19.67     0.00     0.00
    97.6       18.74            0.00        18.74     0.00     0.00
    84.3       18.20            0.00        18.20     0.00     0.00
    71.0       17.58            0.00        17.58     0.00     0.00
    44.3       16.00            0.00        16.00     0.00     0.00


Harvested Random Seeds after Generation of the Random Numbers:

      3080088 K1
            0 K2


Hub-Height Simulated Turbulence Statistical Summary:

   Type of Wind     Min (m/s)    Mean (m/s)     Max (m/s)   Sigma (m/s)
TI (%)
   ------------     ---------    ----------     ---------   -----------
------
   Longitudinal          8.58         18.20         27.00         2.695
14.668
```

```
   Lateral              -6.57          0.00          6.35         2.115
11.509
   Vertical             -5.01          0.00          4.79         1.311
7.135
   Horizontal            8.64         18.32         27.00         2.683
14.643
   Total                 8.88         18.37         27.05         2.676
14.564


Turbulent Velocity Component Extremes:

   Comp  Min (m/s)  Max (m/s)
   ----  ---------  ---------
    u'       -9.62       8.80
    v'       -6.57       6.35
    w'       -5.01       4.79


Hub Friction Velocity (Ustar) = 0.24676 m/s


Mean Reynolds Stress Components:

      sqrt(u'v') = -0.350 m/s
      sqrt(u'w') =  0.247 m/s
      sqrt(v'w') = -0.255 m/s


Instantaneous Reynolds-Stress Component Statistics:

   Product  Min (m/s)^2  Max (m/s)^2  Mean (m/s)^2
   -------  -----------  -----------  ------------
     u'v'        -37.25        31.32         -0.12
     u'w'        -22.48        32.44          0.06
     v'w'        -18.56        18.74         -0.07


Maximum Instantaneous  TKE =  48.87 (m/s)^2
Maximum Instantaneous CTKE =  19.32 (m/s)^2


Cross-Component Correlation Coefficients:

   u'v' coef = -0.022
   u'w' coef =  0.017
   v'w' coef = -0.024


Grid Point Variance Summary:

   Y-coord  -40.00  -13.33   13.33   40.00

   Height   Standard deviation at grid points for the u component:
   124.29    2.505   2.530   2.730   2.844
    97.62    2.803   2.645   2.560   2.599
    70.95    2.545   2.515   2.784   2.525
    44.29    2.607   2.636   2.983   2.722
```

```
   Height   Standard deviation at grid points for the v component:
   124.29    2.115   2.115   2.115   2.115
    97.62    2.115   2.115   2.115   2.115
    70.95    2.115   2.115   2.115   2.115
    44.29    2.115   2.115   2.115   2.115

   Height   Standard deviation at grid points for the w component:
   124.29    1.311   1.311   1.311   1.311
    97.62    1.311   1.311   1.311   1.311
    70.95    1.311   1.311   1.311   1.311
    44.29    1.311   1.311   1.311   1.311


U-component statistics from the interpolated hub point:

   Mean =  18.1632 m/s
   TI   =  11.8655 %


Normalizing Parameters for Binary Data:

   UBar  =  18.2000 m/s
   TI(u) =  14.8068 %
   TI(v) =  11.6183 %
   TI(w) =   7.2027 %

   Height Offset =   0.0000 m
   Grid Base     =  44.2876 m

Nyquist frequency of turbulent wind field =        10.000 Hz
```

B.4 Constant hub-height wind speed with shear

```
! Wind file for Trivial turbine.
! Time  Wind    Wind    Vert.   Horiz.   Vert.   LinV   Gust
!       Speed   Dir     Speed   Shear    Shear   Shear  Speed
  0.0   25.0    0.0     0.0      0.0     0.2     0.0     0.0
  0.1   25.0    0.0     0.0      0.0     0.2     0.0     0.0
999.9   25.0    0.0     0.0      0.0     0.2     0.0     0.0
```

APPENDIX C

CONTENTS OF CD

E:\
- ▼Design codes
  - ▶ Airfoils
  - ▼ Models
    - ▼ With FAST non-linear model of the wind turbine
      - ▶ULQ power regulation + cyclic pitch controller
      - ▶CLQ power regulation + cyclic pitch controller
      - ▶ULQ power regulation + individual pitch controller
      - ▶CLQ power regulation + individual pitch controller
    - ▼ With Linear model of the wind turbine
      - ▶ULQ power regulation + cyclic pitch controller
      - ▶CLQ power regulation + cyclic pitch controller
      - ▶ULQ power regulation + individual pitch controller
      - ▶CLQ power regulation + individual pitch controller
    - ▶ Unsteady BEM code
  - ▼ Results
    - ▶ Power regulation
    - ▶ Load reduction
    - ▶ Aerodynamics
  - ▼ Turbine data
    - ▶ Blade baseline
    - ▶ Tower baseline

- ▶ Wind files
- ▶ Extra

▼ NREL software

- ▶ AeroDyn
- ▶ FAST
- ▶ TurbSim

▼ Report

- ▶ Report
- ▶ Bibliography (electronic version)